ACTA PROTOZOOLOGICA

NENCKI INSTITUTE OF EXPERIMENTAL BIOLOGY
WARSAW, POLAND
1998
VOLUME 37 NUMBER 4
ISSN 0065-1583

Polish Academy of Sciences
Nencki Institute of Experimental Biology
and
Polish Society of Cell Biology

ACTA PROTOZOOLOGICA

International Journal on Protistology

ACTA PROTOZOOLOGICA appears quarterly.

The price (including Air Mail postage) of subscription to ACTA PROTOZOOLOGICA at 1999 is: US $ 180.- by institutions and US $ 120.- by individual subscribers. Limited number of back volumes at reduced rate are available. TERMS OF PAYMENT: Cheque, money oder or payment to be made to the Nencki Institute of Experimental Biology. Account Number: 11101053-3522-2700-1-34 at Państwowy Bank Kredytowy XIII Oddz. Warszawa, Poland. WITH NOTE: ACTA PROTOZOOLOGICA! For matters regarding ACTA PROTOZOOLOGICA, contact Managing Editor, Nencki Institute of Experimental Biology, ul. Pasteura 3, 02-093 Warszawa, Poland; Fax: (4822) 8225342; E-mail: jurek@ameba.nencki.gov.pl (for more information see web page **http://www.nencki.gov.pl/public.htm**).

Front cover: *Polychaos dubium.* In: A. A. Schaeffer (1916) Notes on the specific and other characters of *Amoeba proteus* Pallas (Leidy), *A. discoides* spec. nov. and *A. dubia* spec. nov. *Arch. Protistenk.* **37:** 204 - 228

This publication is supported by the State Committee for Scientific Research

Desktop processing: Justyna Osmulska, Data Processing Laboratory of the Nencki Institute
Printed at the MARBIS, ul. Kombatantów 60, 05-070 Sulejówek, Poland

Acta Protozoologica (1998) 37: 191 - 199

ACTA
PROTOZOOLOGICA

Participation of Myosin I, Spectrin Analogue and Tyrosine-Phosphorylated Proteins at Early Stages of Phagocytosis in *Acanthamoeba castellanii*

Katarzyna KWIATKOWSKA and Andrzej SOBOTA

Department of Cell Biology, Nencki Institute of Experimental Biology, Warszawa, Poland

Summary. Uptake of particles during phagocytosis is driven by the actin-based cytoskeleton. We analyzed the localization of actin filaments, myosin I and II, spectrin analogue and phosphotyrosine-bearing proteins at various stages of yeast phagocytosis in *Acanthamoeba* in order to examine an involvement of these proteins in alterations of the cytoskeleton. Concentration of microfilaments at forming phagosomes was accompanied by accumulation of the spectrin-like protein and myosin I, but not myosin II. During phagosome maturation, these proteins were no longer detectable in the periphagosomal area. The onset of the phagocytosis was correlated with an intense and transient tyrosine-phosphorylation of 130, 120 and 60 kDa polypeptides which were also enriched at the sites of phagosome formation and disappeared at later stages of particle digestion. Inhibition of protein tyrosine kinase activity by genistein blocked particle uptake indicating the regulatory function played by the phosphorylated proteins in the process.

Key words: myosin I, phagocytosis, spectrin, tyrosine phosphorylation.

INTRODUCTION

Phagocytosis is an actin-dependent process of internalization of large particles, >0.5 μm in diameter, by cells. It is a common phenomenon in Eukaryota, although in higher organisms the ability of efficient particle uptake is attributed to specialized cells, so-called "professional" phagocytes, to which monocytes, neutrophils and macrophages belong (Rabinovitch 1995). These cells remove microorganisms, pollution debris and senescent cells of the host, as a key element of the immune defense system.

Address for correspondence: Andrzej Sobota, Department of Cell Biology, Nencki Institute of Experimental Biology, ul. Pasteura 3, 02-093 Warszawa, Poland; Fax: (4822) 8225342; E-mail: asobota@nencki.gov.pl

It has been established that the phagocytic abilities of the "professional" phagocytes are determined by the expression of specific plasma membrane receptors, which bind various ligands localized on the surface of the particles to be internalized. Among the receptors that promote phagocytosis are: mannose receptor, complement receptor C3 and Fcγ receptors (for review see: Brown 1994, Kwiatkowska and Sobota 1999). Clustering of the receptors is thought to occur upon ligand binding which triggers signal transduction events leading eventually to a local polymerization of actin (Griffin *et al.* 1975, Sheterline *et al.* 1984, Detmers *et al.* 1987, Greenberg *et al.* 1991). Microscopic studies revealed that the actin-based cytoskeleton provides scaffolding for pseudopods which embrace particles, firstly in phagocytic cups and, after closure, in nascent phagosomes (Axline and Reaven 1974,

Greenberg *et al.* 1990, Baines *et al.* 1992, Maniak *et al.* 1995, Allen and Aderem 1996). Direct implication of the active engagement of several actin-binding proteins like talin, coronin, ABP-120, myosin IB and IC in particle uptake came from the examination of phagocytosis-defective mutants of *Dictyostelium discoideum* which, as a haploid organism, provides a useful model system for gene targeting and anti-sense RNA studies (Maniak *et al.* 1995, Cox *et al.* 1996, Jung *et al.* 1996, Niewohner *et al.* 1997).

The last decade has witnessed extensive attempts to elucidate the signaling pathways leading from ligand-receptor interactions to actin rearrangements during phagocytosis, though these studies are almost exclusively confined to mammalian phagocytes. An increasing interest is especially focused on the role of protein tyrosine phosphorylation which controls phagocytosis mediated by Fcγ receptors and bacterial invasions of epithelial cells representing "nonprofessional" phagocytes (Dehio *et al.* 1995, Strzelecka *et al.* 1997a, Hauck *et al.* 1998). In contrast, data on the mechanisms which govern phagocytosis in protozoa are random, despite the fact that phagocytosis being a way of feeding for these organisms. In *Acanathamoeba castellanii*, two actin-binding proteins, myosin I and a α-spectrin immunoanalogue, were localized at sites of uptake of distinct particles (Baines *et al.* 1992, Kwiatkowska and Sobota 1997). Accordingly, microinjection of an anti-spectrin antibody inhibited phagocytosis in *Amoeba proteus* (Choi and Jeon 1992). On the other hand, our preliminary studies indicated that tyrosine phosphorylation of proteins may be important in phagocytosis of zymosan and latex beads in *Acanthamoeba castellanii* (Krawczyńska and Sobota 1996). In this report we examined the localization of myosin I and II, the spectrin immunanalogue and tyrosine phosphorylated proteins during phagocytosis of yeast in *Acanthamoeba castellanii* in order to test the involvement of these proteins in various stages of particle uptake.

MATERIALS AND METHODS

Cells

Acanthamoeba castellanii, Neff strain, was grown axenically in the dark, without aeration (Sobota *et al.* 1984). The phagocytic activity of *Acanthamoeba* was tested either in cells attached to cover slips (immunofluorescence studies) or in suspended culture (immunoblotting analysis and inhibitory studies). For the immunofluorescence observations, 4-day-old cultures were plated onto pre-cleaned coverslips at a 4×10^5/ml density and grown overnight as described earlier (Kwiatkowska and Sobota 1997). After rinsing with 100 mM NaCl, 2 mM $MgCl_2$, 20 mM Hepes, pH 7.0 (NaCl/$MgCl_2$/Hepes medium) the cells were chilled on ice and exposed to lipid-extracted baker yeast applied at ratio of about 20 yeast per amoeba in the ice-cold buffer. To promote the binding of the yeast particles to the cells, the incubation proceeded for 10 min at 0°C after which the excess of particles was washed out. Subsequently, the cells were warmed to 28°C for 3 min to induce the uptake of the bound yeast. The process was terminated by fixation of the cells with 3% formaldehyde for 30 min.

In experiments using suspended cells, 5-day-old cultures were shifted to NaCl/$MgCl_2$/Hepes medium (3×10^6 cells in 0.5 ml per sample) and supplemented with yeast-derived zymosan A particles (5 mg in 0.1 ml of medium per sample). Phagocytosis was carried out at room temperature. At various time points of the incubation the samples were mixed with 0.6 ml of ice-cold solution containing 6 mM pervanadate and 200 μM phenylarsine oxide, pelleted and processed for immunoblotting analysis. To examine the effect of genistein (GIBCO, Gaithersburg, MD) on phagocytic activity, the suspended cells were preincubated in NaCl/$MgCl_2$/Hepes medium containing various concentrations of the drug (10 min, room temperature). Subsequently, yeast particles were added to the suspension at a ratio of 20 yeast particles per amoeba. Phagocytosis was conducted for 10 min at room temperature in the constant presence of genistein. The cells were next washed twice with the NaCl/$MgCl_2$/Hepes medium and fixed with 3% formaldehyde in PBS for 10 min. The uptake of yeast was estimated by counting the number of amoeba cells with and without yeast particles under a Nikon microscope in the phase contrast mode.

Immunofluorescence microscopy

Microscopic observations were performed on cells attached to coverslips and undergoing phagocytosis of yeast for 3 min. The cells were fixed for 30 min with 3% formaldehyde in PHEM buffer (60 mM Pipes, 25 mM Hepes, 10 mM EGTA, 4 mM $MgCl_2$, pH 6.9; protease inhibitors: 2 mM PMSF, 100 μg/ml leupeptin, 10 μg/pepstatin A, 2 μg/ml aprotinin [Sigma, St. Louis, MO]) and processed as described previously (Kwiatkowska and Sobota 1997). Briefly, the cells were quenched with 50 mM NH_4Cl, permeabilized by acetone extraction on ice and incubated with 3% goat serum in PBS to block the unspecific binding of antibodies. To visualize the examined proteins, the cells were incubated sequentially for 1 h at room temperature with the appropriate primary antibody and anti-mouse or anti-rabbit antibody conjugated with Texas Red (Jackson ImmunoResearch, West Grove, PA). The procedure was modified in the case of phosphotyrosine staining: the cells were permeabilized for 5 min on ice with 0.1% Triton X-100 prepared in a buffer containing 75 mM NaCl and 25 mM Tris, pH 7.4. This buffer was also applied for the dilution of anti-phosphotyrosine antibody to facilitate antibody-antigen interactions. The samples were mounted in Mowiol containing 2.5% DABCO and examined under a Nikon microscope using fluorescence and phase contrast modes. Observations of the samples under the phase contrast allowed us the distinction of surface-attached particles from ingested ones. Photographs were taken using Kodak T-MAX 400 Asa film.

Mouse anti-myosin I M1.8 and anti-myosin II M2.37 antibodies were kindly provided by Dr. D. A. Kaiser (Johns Hopkins School of Medicine, Baltimore, MD) and applied at a 50 μg/ml concentration according to Yonemura and Pollard (1992). Mouse and rabbit anti-phosphotyrosine antibody (Transduction Laboratories, Lexington, KY) were diluted

1:200 whereas phalloidin-FITC (Sigma), a filamentous actin marker, was prepared at a 0.5 μg/ml concentration. An immunoanalogue of α-spectrin was identified with the use of rabbit anti-α-spectrin antibody which was obtained and purified as described elsewhere (Kwiatkowska and Sobota 1990, 1992). Texas Red-labeled secondary antibodies were diluted 1:100 in the presence of 0.02% NaN_3 and preadsorbed with formaldehyde-fixed and Triton X-100 permeabilized cells during a 1h incubation at room temperature. Control experiments in which the incubation with primary antibodies was omitted confirmed the lack of an unspecific reactivity for these purified antibodies with cells.

Immunoblotting analysis

For the analysis, pelleted samples were solubilized for 30 min on ice in 150 μl solution containing 1% Triton X-100, 0.5% Nonidet P-40, 100 mM NaCl, 2 mM EDTA, 0.5 mM Na_3VO_4, 5 mM DTT, 30 mM Hepes, pH 7.2, and protease inhibitors. Then, the mixture was centrifuged (10 000 g, 10 min, 4°C), the obtained supernatants were supplemented with equal volume of SDS-sample buffer (4 x concentrated) (Laemmli 1970) and boiled for 5 min. The proteins were separated on 8% SDS-polyacrylamide gels, transferred onto nitrocellulose (Towbin *et al.* 1979) and probed with mouse anti-phosphotyrosine antibody (Transduction Laboratories) as described earlier (Strzelecka *et al.* 1997b).

RESULTS

Myosin I and spectrin accompany actin filaments at forming phagosomes

An exposure of *Acanthamoeba castellanii* to lipid-extracted yeast at 28°C induced a robust uptake of the particles (Figs. 1, 2, 4). Preincubation of the cells with yeast for 10 min at 0°C greatly enhanced amoeba-yeast encounters, promoting binding of the particles to the cell surface. Thus, a subsequent 3 min of the incubation at 28°C allowed us to find cells containing several yeast particles; fully ingested particles, displaced deeper into the cell interior inside maturing phagosomes, frequently coexisted with particles undergoing internalization and enclosed into phagocytic cups and nascent phagosomes (Figs. 1A, B, asterisks and arrows, respectively). The two population of phagosomes could be distinguished by phalloidin-FITC staining: forming phagosomes displayed a prominent fluorescence indicating an accumulation of actin filaments around their membrane whereas maturing phagosomes were devoid of the label (Figs. 1A, B). Actin filaments were also enriched in a broad cortical band which often delineated the whole cell periphery and reflected an unpolarized, non-motile profile of avidly phagocytizing cells (Fig. 1A).

Localizations of two motor proteins, myosin I and II, and spectrin-like protein, which cross-links actin filaments, were next examined due to their possible involvement in actin reorganization during particle uptake. Myosin I was found to be concentrated in a distinct line closely apposing the membrane of forming phagosomes (Figs. 1D, F, arrows). This prominent labeling of myosin I at phagocytic cups corresponded with actin filament staining, indicating co-localization of the two proteins (Figs. 1E,F, arrows). As with actin, myosin I was no longer observed around maturing phagosomes (Fig. 1D, asterisks). In cell regions which were uninvolved in particle uptake, the distribution of myosin I was more diffuse and partially correlated with actin filament localization, whereas a moderate labeling of the nucleus by the anti-myosin antibody resulted from its cross-reactivity with nuclear actin binding protein (Hagen *et al.* 1986) (Figs. 1E, F). In contrast to myosin I, no clear accumulation of myosin II was detected at sites of the yeast engulfment (Fig. 1C, arrowheads). The protein remained rather uniformly distributed throughout the cytoplasm in both phagocytizing and resting cells (Fig. 1C). These observations also indicate that the local enrichment of myosin I, seen in Figs. 1D, F (arrows), was not evoked by the enlarged optical thickness of the periphagosomal area.

Distribution of the α-spectrin immunoanalogue during yeast phagocytosis showed a heterogeneity resembling that of actin filaments and myosin I (Fig. 2). The protein was accumulated around phagocytic cups where it co-localized with actin (Figs. 2C, D, arrows), although, in contrast to myosin I labeling, the adjoining cytoplasm also revealed spectrin enrichment (Figs. 2A, C, arrows). Decoration of the membrane vicinity of maturing phagosomes by the anti-α-spectrin antibody was weaker and varied, ranging from a distinct ring of fluorescence to a lack of staining (Figs. 2A, B, double arrow and asterisk, respectively). Only a fraction of the cellular α-spectrin immunoanalogue was translocated toward sites of the yeast phagocytosis manifesting the local character of cytoskeletal rearrangements during this process.

Protein tyrosine phosphorylation controls the onset of phagocytosis

Cytoskeletal reorganization during phagocytosis in "professional" phagocytes of vertebrates requires an activation of protein tyrosine kinases (Greenberg *et al.* 1996). To examine if a similar phenomenon takes place in protozoan cells, we studied tyrosine phosphorylation of proteins in *Acanthamoeba*. The onset of phagocytosis of yeast-derived zymosan particles in *Acanthamoeba* was correlated with an intense tyrosine phosphorylation of three major proteins, as revealed by immunoblotting analysis of whole cell lysates (Fig. 3A, arrowheads).

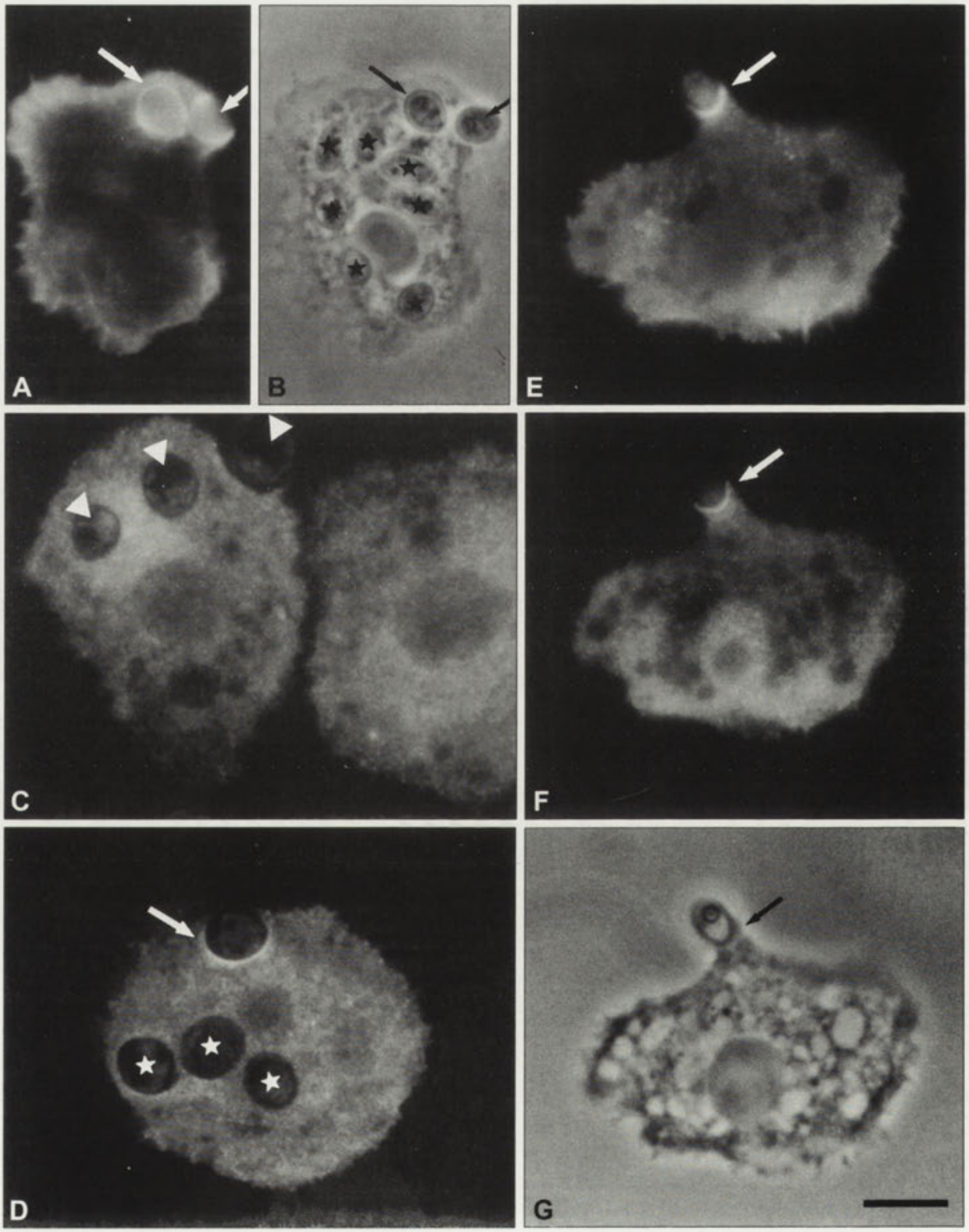

Fig. 1. Actin filaments and myosin I, but not myosin II, accumulate at forming phagosomes. The cells were fixed after 3 min of yeast uptake and were processed for immunofluorescence microscopy to visualize: A, E - actin filaments, C - myosin II, D, F - myosin I. B, G - phase contrast images corresponding to A and E-F, respectively. Note the accumulation of actin filaments and myosin I at phagocytic cups and nascent phagosomes (arrows) and their lack at maturing phagosomes (asterisks). Both forming and maturing phagosomes are devoid of myosin II label (arrowheads). Scale bar - 10 μm

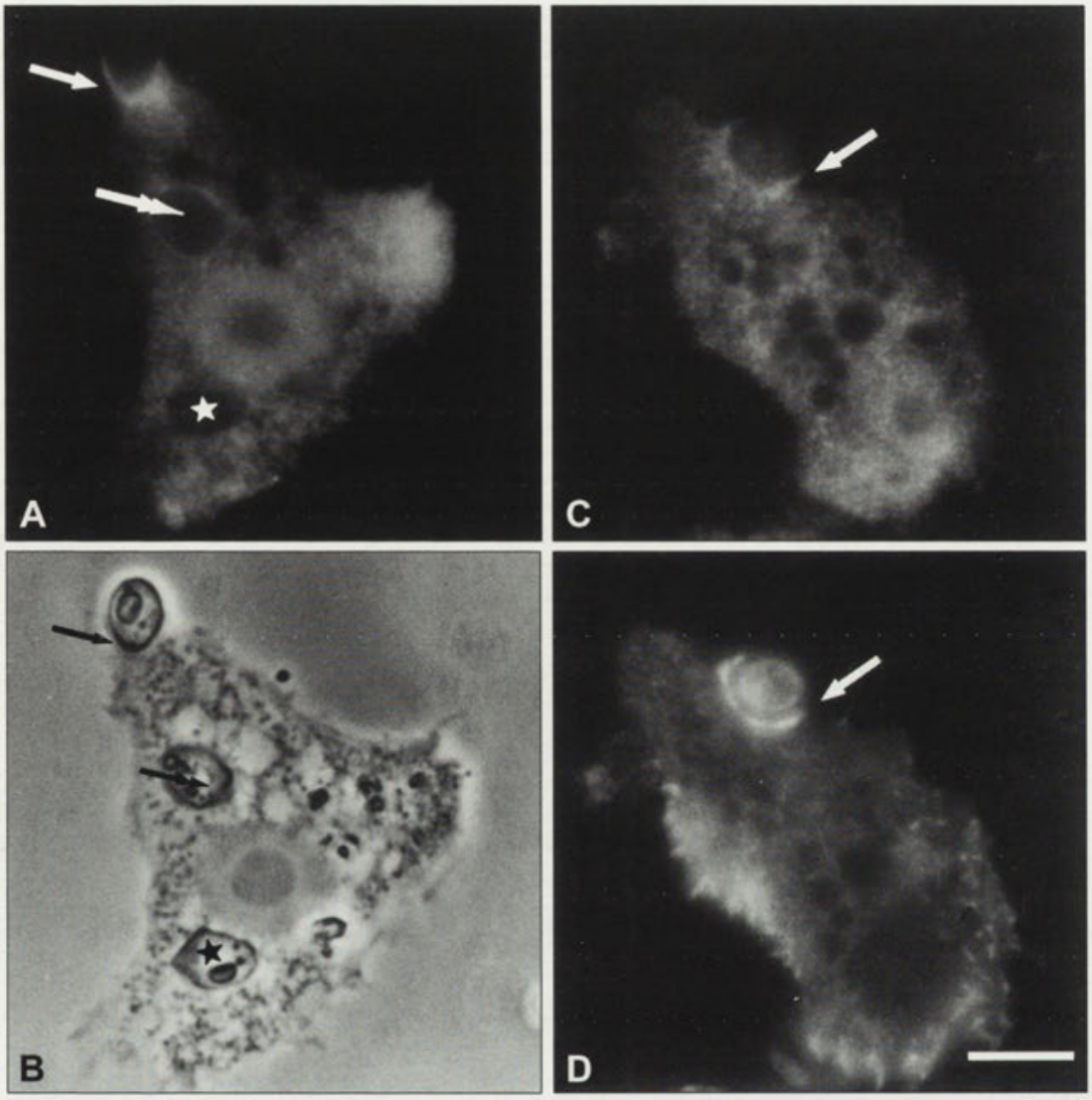

Fig. 2. The immunoanalogue of α-spectrin is present at early stages of yeast phagocytosis. A - spectrin localization, B - phase contrast image of A. The spectrin analogue is concentrated at phagocytic cups and some phagosomes (arrow and double arrows, respectively) while vanished at others (asterisks). C, D - cells double labeled to visualize spectrin (C) and actin filaments (D) revealed the coexistence of these proteins at phagocytic cups (arrows). Scale bar - 10 μm

Based on the electrophoretic mobilities of these polypeptides their molecular masses were estimated at 130, 120 and 60 kDa. The rise in tyrosine phosphorylation was already significant 1 min after phagocytosis had begun and was especially well pronounced for the 130 kDa polypeptide, the phosphorylation of which was undetectable in unstimulated cells (Fig. 3A, compare lanes 1 and 2). The enhanced tyrosine phosphorylation of proteins was transient and declined after 15 min, simultaneously with particle uptake (Fig. 3A, lane 5).

The phosphotyrosine-bearing proteins were gathered in *Acanthamoeba* at sites of particle engulfment (Fig. 4). The proteins were abundant at the membrane of forming phagosomes and in the neighboring cytoplasm (Figs. 4A, B, arrows); they vanished at later stages of phagosome maturation (Figs. 4A, B, asterisks). Similar images were obtained when either polyclonal or monoclonal anti-phosphotyrosine antibodies were applied, although the latter produced more punctuate pattern of the phosphotyrosine staining (not shown).

Genistein, a broad-spectrum inhibitor of protein tyrosine kinases (Akiyama *et al.* 1987), blocked the yeast phagocytosis by *Acanthamoeba* in a dose dependent manner (Fig. 3B). The 50 μM concentration of genistein

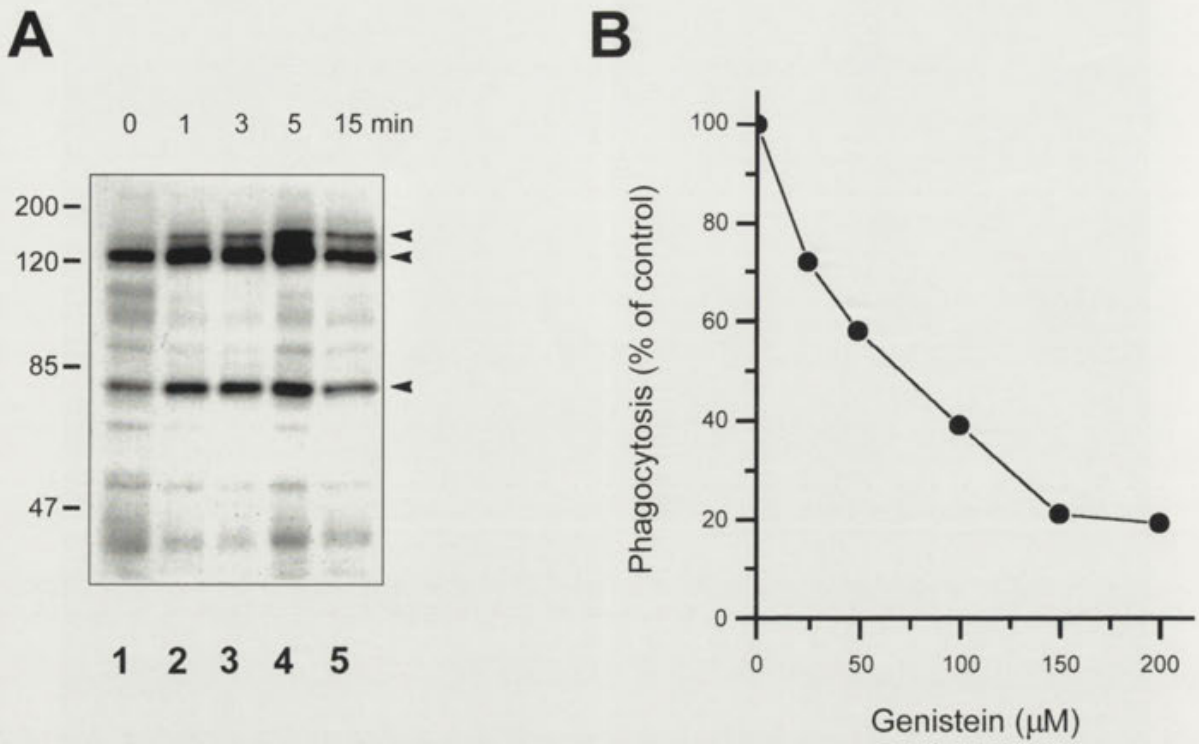

Fig. 3. Tyrosine phosphorylation of proteins controls phagocytosis in *Acanthamoeba*. A - time course of protein tyrosine hyperphosphorylation during phagocytosis of zymosan particles analyzed by immunoblotting of whole cell lysates with monoclonal anti-phosphotyrosine antibody. Lane 1: control cells, unexposed to the particles; lanes 2-5: cells after 1 min (lane 2), 3 min (lane 3), 5 min (lane 4) and 15 min (lane 5) after the uptake of particles. Arrowheads point to polypeptides undergoing tyrosine phosphorylation during phagocytosis. On the left, molecular mass standards are shown in kDa. B - a dose dependent inhibition of yeast phagocytosis by genistein. After 10 min of the particle uptake, a percent of cell containing internalized yeast was calculated and expressed assuming that the percent of phagocytizing cells which were unexposed to the drug equals 100. Data from one representative experiment are shown

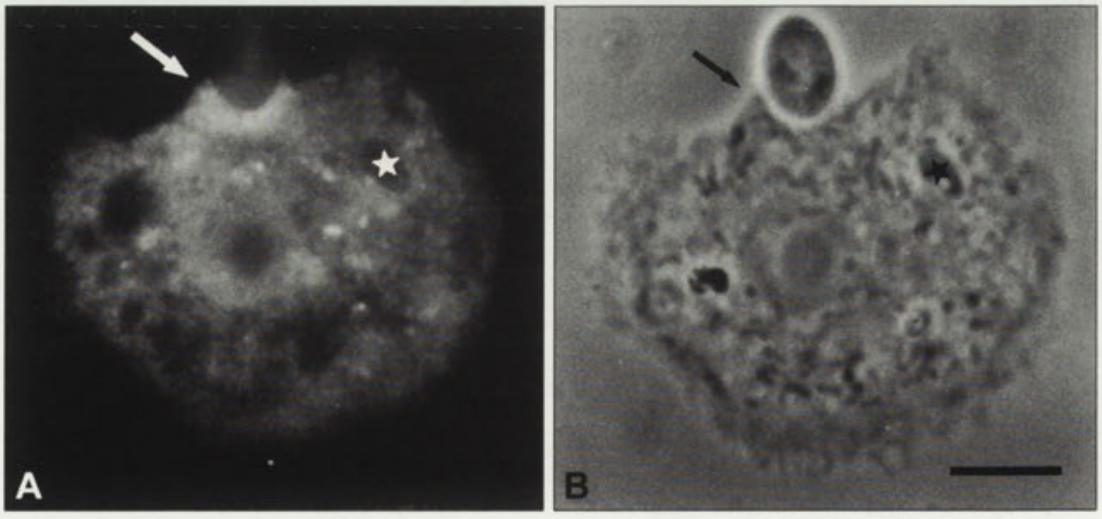

Fig. 4. Accumulation of tyrosine-phosphorylated proteins during yeast uptake (A). B - phase contrast image of A. Cells treated with polyclonal anti-phosphotyrosine antibody display the presence of the phosphotyrosine-containing proteins at sites of the particle uptake (arrows) and lack of their concentration around fully ingested particles (asterisks). Scale bar - 10 μm

diminished particle uptake by nearly 50%, i.e., with an efficiency comparable to that in "professional" phagocytes (Greenberg et al. 1993). These data showed that tyrosine phosphorylation of proteins is required for phagocytosis to occur in *Acanthamoeba*.

DISCUSSION

In the present report we demonstrate that actin filaments, myosin I, spectrin-like protein and tyrosine-phosphorylated proteins are accumulated simultaneously at forming phagosomes during uptake of yeast in *Acanthamoeba castellanii*, indicating that possible cooperation of these proteins is required for the process to proceed. Phagocytosis of the particles was likely to be promoted by an amoeba plasma membrane receptor which recognizes and binds mannose-rich residues of the yeast cell wall (Allen and Dawidowicz 1990). Sequential ligand-receptor interactions could force the plasma membrane to spread to a limited extend around bound particles, as suggested recently by Lowry *et al.* (1998). However, it has been well established that extension of the pseudopods which embrace bound particles and eventually close up into nascent phagosomes requires an actin filament engagement. The onset of phagocytosis is correlated with actin polymerization whereas cytochalasin B, an actin depolymerizing agent, inhibits particle uptake (Zigmond and Hirsch 1972, Axline and Reaven 1974, Sheterline *et al.* 1984, Greenberg *et al.* 1991). The newly polymerized actin filaments are concentrated at sites of the particle engulfment, as also seen in *Acanthamoeba* (Figs. 1A, B).

Actin-dependent mechanisms, which govern the protrusion of pseudopods during phagocytosis, are likely to reflect those operating at the leading edge of crawling cells. It has been proposed, for example, that actomyosin contraction participates in moving cell margins forward (Heath and Holifiled 1991). Accordingly, myosin II was localized at the sites of particle uptake in macrophages by early immunofluorescence observations (Painter and McIntosh 1979, Stendhal *et al.* 1980), although, opposite results were obtained in *Dictyostelium* (Yumura *et al.* 1984). Most importantly, *Dictyostelium* mutants devoid of native myosin II displayed unimpaired phagocytic abilities while being defective in other actin-dependent events like cytokinesis and capping of cell surface receptors (De Lozanne and Spudich 1987, Fukui *et al.* 1990). The obtained indication on the lack of myosin II involvement in phagocytosis was further underscored by a finding that no phosphorylation of myosin II light chain took place during phagocytosis in macrophages (De Lanerolle *et al.* 1993). Our observations which revealed no detectable accumulation of myosin II at forming or maturing phagosomes in *Acanthamoeba* are in line with these data (Fig. 1C). Possible limitations of the immunofluorescence sensitivity should be kept in mind when estimating this lack of myosin II staining. Nevertheless, in contrast to myosin II, the concentration of myosin I around forming phagosomes was easily detected (Figs. 1D, F).

Three isoforms of myosin I: IA, IB and IC have been identified in *Acanthamoeba*. They all share a similar structure comprising a N-terminal conserved motor domain and C-terminal tail homology domains which mediate the binding of membrane/acid phospholipids and contain the second, ATP-insensitive actin binding site (for review see Hasson and Mooseker 1995). Despite this similarity, myosins IA-C display different subcellular localizations in *Acanthamoeba* (Baines and Korn 1990, Baines *et al.* 1992). Myosin IA, IB, and possibly IC, are recognized by the MI.8 antibody used in this study (Yonemura and Pollard 1992). We assume, however, that myosin IB mainly accounted for the prominent staining of submembraneous layer of phagocytic cups since antibody MI.7, which does not bind to myosin IB, produced only moderate and less distinct labeling of this cell region (not shown). This supposition is in agreement with report of Baines *et al.* (1992) about the myosin IB concentration at early stages of phagocytosis in *Acanthamoeba*. Myosin I, visualized by MI.8 antibody, co-localized with abundant actin filaments at forming phagosomes and disappeared concomitantly with actin during phagosome maturation (Fig. 1). Given the structure of *Acanthamoeba* myosin I and its co-localization with microfilaments, it seems possible that myosin I can participate in the extension of the pseudopods during particle engulfment, enabling either movement of the pseudopod membrane relative to actin filaments and/or sliding of actin filaments relative to each other, as considered earlier (Stossel 1993). The actin-actin interactions mediated by myosin I can be especially important in phagocytosis since out of five *Dictyostelium* myosin I isoforms, myosin IB and IC having this property were required for efficient particle uptake and myosin IB was found to concentrate at sites of the particle ingestion in these cells (Fukui *et al.* 1989, Jung *et al.* 1996).

An ability to generate tension within the actin gel by myosin I can be regulated in at least two ways, as proposed by Baines *et al.* (1995). The first mechanism operates at the level of serine/threonine phosphorylation of myosin I which is required for maximal Mg^{2+}-ATPase activity of the

enzyme (Albanesi *et al.* 1983). The second one concerns actin filaments: three-dimensional organization of the microfilaments, maintained by actin-binding proteins, can control the susceptibility of filaments to the contraction. Confirming the first supposition, myosin IB, concentrated at forming phagosomes in *Acanthamoeba,* was found to be phosphorylated (Baines *et al.* 1995). On the other hand, we found that actin and myosin I accumulated at phagosomes are accompanied by the spectrin-like protein (Fig. 2 in this paper, Kwiatkowska and Sobota 1997). Proteins of the spectrin family are heterotetramers which cross-link actin filaments (for review see Bennett 1990). The structure of the *Acanthamoeba* spectrin-like protein is not completely elucidated. Nevertheless, biochemical studies and co-localization with actin filaments points to its actin-binding abilities (Pollard 1984, Kwiatkowska and Sobota 1990, 1997). Therefore, is seems possible that an interplay between spectrin, actin and myosin I can participate in the regulation of microfilament alterations that are required for pseudopod extensions during uptake of particles.

The onset of yeast phagocytosis in *Acanthamoeba* is controlled by tyrosine phosphorylation of proteins, as indicated by the inhibitory effect of a tyrosine kinase activity blocker and accumulation of hyperphosphorylated proteins at the sites of particle ingestion (Figs. 3, 4). This is one of a few phenomena known to be correlated with changes in the phosphotyrosine content of proteins in lower Eukaryota (Schweiger *et al.* 1992, Gauthier *et al.* 1997, Venkataraman *et al.* 1997). On the other hand, being dependent on tyrosine kinase activity, phagocytosis in *Acanthamoeba* surprisingly resembles that mediated by Fcγ receptors in "professional" phagocytes of mammals (Greenberg *et al.* 1993, Strzelecka *et al.* 1997b). Among proteins known to undergo tyrosine hyperphosphorylation during Fcγ receptor-mediated phagocytosis are the Fcγ receptors, tyrosine kinases of Src and Syk families, several signaling molecules, like Vav and Shc, phospholipase Cγ as well as paxilin, a component of the actin-based cytoskeleton (Kiener *et al.* 1993, Darby *et al.* 1994, Greenberg *et al.* 1994, Crowley *et al.* 1997). Phosphorylation of tyrosine residues up-regulates the activity of the enzymes mentioned above. Simultaneously, it converts the phosphorylated molecules into docking sites for Src homology 2 (SH2) domain-containing proteins. Therefore, phosphotyrosine residues are involved in assembling the proteins in an active complex at the sites of particle binding. Further studies will reveal the identity of proteins which are phosphorylated at tyrosine residues during phagocytosis in *Acanthamoeba* and elucidate their role in the process.

Acknowledgments. We thank Dr. D. A. Kaiser for providing anti-myosin I and anti-myosin II antibodies. We also thank Kazimiera Mrozińska for excellent technical assistance. This work was supported by a grant from the State Committee for Scientific Research KBN 0082/P2/94/07 and by a grant from the State Committee for Scientific Research to the Nencki Institute of Experimental Biology.

REFERENCES

Akiyama T., Ishida J., Nakagawa S., Ogawara H., Watanabe S. Itoh N., Shibuya M., Fukami. Y. (1987) Genistein, a specific inhibitor of tyrosine-specific protein kinase. *J. Biol. Chem.* **262:** 5592-5595

Albanesi J.P., Hammer J.A. III, Korn E. D. (1983) The interaction of F-actin with phosphorylated and unphosphorylated myosins IA and IB from *Acanthamoeba castellanii*. *J. Biol. Chem.* **258:** 10176-10181

Allen L.-H. P., Aderem A. (1996) Molecular definition of distinct cytoskeletal structures involved in complement- and Fc receptor-mediated phagocytosis in macrophages. *J. Exp. Med.* **184:** 627-637

Allen P. G., Dawidowicz E. A. (1990) Phagocytosis in *Acanthamoeba*: I. A mannose receptor is responsible for the binding and phagocytosis of yeast. *J. Cell. Physiol.* **145:** 508-513

Axline S. G., Reaven E. P. (1974) Inhibition of phagocytosis and plasma membrane mobility of the cultivated macrophage by cytochalasin B. *J. Cell Biol.* **62:** 647-659

Baines I. C., Korn E. D. (1990) Localization of myosin IC myosin II in *Acanthamoeba castellanii* by indirect immunofluorescence and immunogold electron microscopy. *J. Cell. Biol.* **111:** 1895-1904

Baines I. C., Brzeska H., Korn E.D. (1992) Differential localization of *Acanthamoeba* myosin I isoforms. *J. Cell Biol.* **119:** 1193-1203

Baines I. C., Corigliano-Murphy A., Korn E.D. (1995) Quantification and localization of phosphorylated myosin I isoforms in *Acanthamoeba casellanii*. *J. Cell Biol.* **130:** 591-603

Bennett V. (1990) Spectrin-based membrane skeleton: A multipotentional adaptor between plasma membrane and cytoplasm. *Physiol. Rev.* **70:** 1029-1065

Brown E. J. (1994) Phagocytosis. *BioEssays* **17:** 109-117.

Choi E.Y., Jeon K.W. (1992) Role of spectrin in *Amoeba proteus*, as studied by microinjection of anti-spectrin monoclonal antibodies. *Exp. Cell Res.* **199:** 174-178

Cox D., Wessel D., Soll D. R., Hartwig J., Condeelis J. (1996) Re-expression of ABP-120 rescues cytoskeletal, motility, and phagocytic defects of ABP-120$^-$ *Dictyostelium* mutants. *Molec. Biol. Cell* **7:** 803-823

Crowley M. T., Costello P. S., Fitzer-Attas C. J., Turner M., Meng F., Lowell C., Tybulewicz V. L. J., DeFranco A. L. (1997) A critical role for Syk in signal transduction and phagocytosis mediated by Fcγ receptor on macrophages. *J.Exp. Med.* **186:** 1027-1039

Darby C., Geahlen R. L., Schreiber A. D. (1994) Stimulation of macrophage Fcγ RIIIA activates the receptor-associated protein tyrosine kinase syk and induces phosphorylation of multiple proteins including p95Vav and p62/GAP-associated protein. *J. Immnol.* **152:** 5429-5437

Dehio C., Prevost M.-C., Sansonetti P. J. (1995) Invasion of epithelial cells by *Shigella flexneri* induces tyrosine phosphorylation of cortactin by a pp60$^{c\text{-}src}$-mediated signalling pathway. *EMBO J.* **14:** 2471-2482

De Lanerolle P., Gorgas G., Li X., Schluns K. (1993) Myosin light chain phosphorylation does not increase during yeast phagocytosis by macrophages. *J. Biol. Chem.* **268:** 16883-16886

De Lozanne A., Spudich J. A. (1987) Disruption of the *Dictyostelium* myosin heavy chain gene by homologous recombination. *Science* **236:** 1086-1091

Detmers P. A., Wright S.D., Olsen E., Kimbal., Cohn Z. A. (1987) Aggregation of complement receptor on human neutrophils in the absence of ligand. *J. Cell Biol.* **105:** 1137-1145

Fukui Y., Lynch T. J., Brzeska H., Korn E. D. (1989) Myosin I is located at the leading edges of locomoting *Dictyostelium* amoebae. *Nature* **341:** 328-331

Fukui Y., De Lozanne A., Spudich J. A. (1990) Structure and function of the cytoskeleton of a *Dictyostelium* myosin-defective mutant. *J. Cell Biol.* **110:** 367-378

Gauthier M. L., Lydan M. A., O'Day D. H., Cotter D. A. (1997) Endogenous autoinhibitors regulate changes in actin tyrosine phosphorylation during *Dictyostelium* spore germination. *Cell. Signal.* **9:** 79-83

Greenberg S., Burridge K., Silverstein S. C. (1990) Colocalization of F-actin and talin during Fc receptor-mediated phagocytosis in mouse macrophages. *J. Exp. Med.* **172:** 1853-1856

Greenberg S., Khoury J. E., Di Virgillio F., Kaplan E. M., Silverstein S. C. (1991) Ca^{2+}-independent F-actin assembly and disassembly during Fc receptor-mediated phagocytosis in mouse macrophages. *J. Cell Biol.* **113:** 757-767

Greenberg S., Chang P., Silverstein S. (1993) Tyrosine phosphorylation is required for Fc receptor-mediated phagocytosis in mouse macrophages. *J. Exp. Med.* **177:** 529-534

Greenberg S., Chang P., Silverstein S. C. (1994) Tyrosine phosphorylation of the α subunit of Fcγ receptors, $p72^{syk}$, and paxillin during Fc receptor-mediated phagocytosis in macrophages. *J. Biol.Chem.* **269:** 3897-3902

Greenberg S., Chang P., Wang D.-C., Xavier R., Seed B. (1996) Clustered syk tyrosine kinase domains trigger phagocytosis. *Proc. Natl. Acad. Sci. USA.* **93:**1103-1107

Griffin F. M., Griffin J A., Leider J. E., Silverstein S. C. (1975) Studies on the mechanisms of phagocytosis. I. Requirement for circumferential attachment of particle-bound ligands to specific receptors on the macrophage membrane. *J. Exp. Med.* **86:** 955-966

Hagen S. J., Kiehart D. P., Kaiser D. A., Pollard T. D. (1986) Characterization of monoclonal antibodies to *Acanthamoeba* myosin-I that cross-react with both myosin II and low-molecular mass nuclear proteins. *J. Cell Biol.* **103:** 2121-2128

Hasson T., Mooseker M. S. (1995) Molecular motors, membrane movements and physiology: Emerging roles for myosins. *Cur. Opin. Cell Biol.* **7:** 587-594

Hauck C. R., Meyer T. F. Lang F., Gulbins E. (1998) CD66-mediated phagocytosis of Opa_{CC} *Neisseria gonorrhoeae* requires a Src-like tyrosine kinase- and Rac1- dependent signalling pathway. *EMBO J.* **17:** 443-454

Heath J. P., Holifield B. F. (1991) Cell locomotion: New research tests old ideas on membrane and cytoskeletal flow. *Cell Motil. Cytoskeleton* **18:** 245-257

Jung G., Xufeng W., Hammer J.A. III (1996) *Dictyostelium* mutants lacking multiple classic myosin I isoforms reveal combination of shared and distinct functions. *J. Cell Biol.* **133:** 305-323

Kiener P. A, Rankin B. M., Burkhardt A. L., Schievent G. L., Gilliland L. K., Rowley R. B., Bolen J. B., Ledbetter J. A. (1993) Cross-linking of Fcγ receptor I (Fcγ RI) and receptor II (Fcγ RII) on monocytic cells activates a signal transduction pathway common to both Fc receptors that involves the stimulation of p72 syk protein tyrosine kinase. *J. Biol. Chem.* **268:** 24442-24448

Krawczyńska W., Sobota A. (1996) Participation of 125 kDa tyrosine-phosphorylated protein in phagocytosis of *Acanthamoeba* cells. *Folia Histochem. Cytochem.* **34 Suppl:** 11-12

Kwiatkowska K., Sobota A. (1990) Alpha-spectrin immunoanalog in *Acanthamoeba* cells. *Histochemistry* **94:** 87-93

Kwiatkowska K., Sobota A. (1992) 240-kDa immunoanalogue of vertebrate α-spectrin occurs in *Paramecium* cells. *Cell Motil. Cytoskeleton* **23:** 111-121.

Kwiatkowska K., Sobota A. (1997) Local accumulation of α spectrin-related protein under plasma membrane during capping phagocytosis in *Acanthamoeba*. *Cell Motil. Cytoskeleton* **36:** 253-265

Kwiatkowska K., Sobota A. (1999) Signaling pathways in phagocytosis. *BioEssays* (in press)

Laemmli U. K. (1970) Cleavage of structural proteins during the assembly of the head of bacteriophage T4. *Nature* **277:** 680-685

Lowry M. B., Duchemin A. M., Robinson J. M., Anderson C. L. (1998) Functional separation of pseudopod extension and particle internalization during Fcγ receptor-mediated phagocytosis. *J. Exp. Med.* **187:** 161-176

Maniak M., Rauchenberger R., Albrecht R., Murphy J., Gerisch G. (1995) Coronin involved in phagocytosis: Dynamic particle-induced relocalization visualized by a green fluorescent protein tag. *Cell* **83:** 915-924

Niewohner J., Weber I, Maniak M., Muller-Taubenberger A., Gerisch G. (1997) Talin-null cells of *Dictyostelium* are strongly defective in adhesion to particle and substrate surfaces and slightly impaired in cytokinesis. *J. Cell Biol.* **138:** 349-361

Painter R. G., McIntosh A. I. (1979) The regional association of actin and myosin with sites of particle phagocytosis. *J. Supramolec. Struc.* **12:** 369-384

Pollard T. D. (1984) Purification of a high molecular weight actin filament gelation protein from *Acanthamoeba* that shares antigenic determinants with vertebrate spectrin. *J. Cell Biol.* **99:** 1970-1980

Rabinovitch M. (1995) Professional and non-professional phagocytes: An introduction. *Trend. Cell Biol.* **5:** 85-87

Schweiger A., Mihalache O., Ecke M., Gerisch G. (1992) Stage-specific tyrosine phosphorylation of actin in *Dictyostelium discoideum* cells. *J. Cell Sci.* **102:** 601-609

Sheterline P., Rickard J. E., Richards R. C. (1984) Fc receptor-directed phagocytic stimuli induce transient actin assembly at an early stage of phagocytosis in neutrophil leukocytes. *Eur. J. Cell Biol.* **34:** 80-87

Sobota A., Burovina I.V., Pogorelov A.G., Solus A. A. (1984) Correlation between potassium and phosphorus content and their distribution in *Acanthamoeba castellanii. Histochemistry* **81:** 201-204

Stendahl O. I., Hartwig J. H., Brotschi E. A., Stossel T. P. (1980) Distribution of actin-binding protein and myosin in macrophages during spreading and phagocytosis. *J.Cell Biol.* **84:** 215-224

Stossel T.P. (1993) On the crawling of animal cells. *Science* **260:** 1089-1094

Strzelecka A., Kwiatkowska K., Sobota A. (1997a) Tyrosine phosphorylation and Fcγ receptor-mediated phagocytosis. *FEBS Lett.* **400:** 11-14

Strzelecka A., Pyrzyńska B., Kwiatkowska K., Sobota A. (1997b) Syk kinase, tyrosine-phosphorylated proteins and actin filaments accumulate at forming phagosomes during Fcγ receptor-mediated phagocytosis. *Cell Motil. Cytoskeleton* **38:** 287-296

Towbin H., Staehelin T., Gordon J. (1979) Electrophoretic transfer of proteins from polyacrylamide gels to nitrocellulose sheets: Procedure and some applications. *Proc. Natl. Acad. Sci. USA* **76:** 4350-4354

Venkataraman C., Haack B. J., Bondada S., Kwaik Y.A. (1997) Identification of a Gal/GalNAc lectin in the protozoan *Hartmannella vermiformis* as a potential receptor for attachment and invasion by the legionnaires disease bacterium. *J. Exp. Med.***186:** 537-547

Yonemura S., Pollard T. D. (1992) The localization of myosin I and myosin II in *Acanthamoeba* by fluorescence microscopy. *J. Cell Sci.* **102:** 629-642

Yumura S., Mori H., Fukui Y. (1984) Localization of actin and myosin for the study of ameboid movement in *Dictyostelium* using improved immunofluorescence. *J. Cell Biol.* **99:** 894-899

Zigmond S. H., Hirsch J. G. (1972) Effect of cytochalasin B on polymorphonuclear leucocyte locomotion, phagocytosis and glycolysis. *Exp. Cell Res.* **73:** 383-393

Received on 31st July, 1998; accepted on 14th October, 1998

Acta Protozoologica (1998) 37: 201 - 208

ACTA
PROTOZOOLOGICA

Effect of Ceramide-Analogues on the Actin Cytoskeleton of *Tetrahymena pyriformis* GL. A Confocal Microscopic Analysis

Péter KOVÁCS and György CSABA

Department of Genetics, Cell and Immunobiology, Semmelweis University of Medicine, Budapest, Hungary

Summary. Using monoclonal antibody to actin (MAB) and phalloidin, F- and G-actin were demonstrated separately in the unicellular *Tetrahymena*. MAB labeled mucocysts, basal body cage complexes, the surface of food vacuoles and the surface of the nucleus. A bright fluorescent globular structure was seen attached to the nucleus. Some labels were present along the oral field. Phalloidin labeled these structures similarly, except the bright nucleus-attached globular structure. However, phalloidin labeled contractile vacuoles in some cases. C_2-ceramide treatment weakened MAB labeling in general and abolished the fluorescence of the bright nucleus-associated area. Nevertheless basal body cage complexes remained unchanged. Under the effect of this cell permeable ceramide analogue, extremely large vacuoles appeared at the bottom of the cells, and the bright phalloidin labeling of the epiplasmic area (basal body cage complexes, mucocysts) disappeared. Non-hydroxy fatty-acid ceramide influenced the cytoskeleton similarly. There was no detectable alteration after treatment with hydroxy fatty-acid ceramide and sphingosine-1-phosphate. The experiments call attention to the ceramide regulation of cytoskeleton in *Tetrahymena* and to the possibility of differences in this regulation depending on the cellular localization and forms (G and F) of actin.

Key words: actin, apoptosis, C_2-ceramide, cytoskeleton, *Tetrahymena*.

INTRODUCTION

The presence of actin was demonstrated in all types of eukaryote cells from protists to mammals. The rapid conversion of actin between monomeric (G) and filamentous (F) forms plays a crucial role in cell motility, intracellular movements, cell division and the maintenance of cell shape (Cooper 1991). Stimulus-mediated alterations in the actin assembly and disassembly accompany cell surface changes in peripheral cytoplasm. Some experimental results suggest that depolymerization of F-actin may also be a necessary component of the process of apoptosis including overall cyto-architectural changes (Laster and McKenzie 1996). Actin assembly and disassembly, crosslinking of actin filaments are affected by intracellular agents such as actin-binding proteins and second messengers (Stossel 1989). These agents are synthesized and (or) activated frequently after the activation of membrane receptors. Phosphoinositides have been reported to be important in the regulation of actin polymerization (Cooper 1991), by binding to actin-binding proteins such as gelsolin resulting in an increase of the

Address for correspondence: György Csaba, Department of Genetics, Cell and Immunobiology, Semmelweis University of Medicine, Nagyvárad tér. 4, POB 370, H-1445 Budapest, Hungary; E-mail: csagyor@net.sote.hu

nucleation sites and a stimulation of actin polymerization (Cunningham *et al.* 1991).

The membrane skeleton in ciliated Protozoa, called the "epiplasm", is well developed and serves to anchor basal bodies and cell surface structures (Pitelka 1969). Actin filaments were found close to the inner alveolar membrane or the epiplasmic filamentous meshwork, and may be involved in the positioning of some organelles, such as mucocysts, kinetosomes and mitochondria, at the cell surface (Méténier 1984). In *Paramecium* ciliary basal bodies become clearly visible by labeling of cells with F-actin specific phalloidin, and also the surface of food vacuoles and the borders of the buccal cavity were labeled by phalloidin; while no labeling was observed in association with the osmoregulatory system (Kersken *et al.* 1986). Whereas Hirono *et al.* (1990) have shown that actin of *Tetrahymena pyriformis* does not interact with phalloidin; *Tetrahymena* actin has both properties similar (muscle myosin binds to it) and dissimilar (muscle tropomyosin does not, while muscle α-actinin hardly bind to it) to that of skeletal muscle actin. In *Amoeba proteus* actin is distributed around the nucleus, in cortical layer delineating the granuloplasm from the peripheral hyaloplasm, and - in contrast with *Paramecium* - around the contractile vacuole (Stocker *et al.* 1983). In *Tetrahymena* ciliary 14S (inner-arm) dynein fraction is in association with actin revealed by polyclonal antibody against *Tetrahymena* actin (Muto *et al.* 1994). Actin has been identified in the *Tetrahymena paravorax* typically decorated with heavy meromyosin (Méténier 1984). During cytokinesis beneath the division furrow the actin filaments are in coexistence with profilin in *Tetrahymena*, implying the possible involvement of profilin in assembly and disassembly of contractile ring microfilaments in the process of cytokinesis (Edamatsu *et al.* 1992).

The basal body-cage complex is a fibrillar chamber which surrounds each basal body in the ciliate cytoskeleton. In *Tetrahymena* the cage contains actin filaments as well as myosin and the formation of actin filament bundles in the cage complex requires one or more actin-binding proteins (Garcés *et al.* 1995). Pinching off food vacuoles at the cytostome, fusion of vesicles at the food vacuole surface and transport of food vacuoles within the cell appear to involve actin filaments (Méténier 1984). These processes are inhibited by cytochalasin. Treatments that inhibit the activity of actin interfere with expulsion of excess water by the contractile vacuole, leading to overfilling of this organelle and cell lysis (Cohen *et al.* 1984).

Tetrahymena has receptor - hormone - second messenger systems, which work similar to vertebrate ones (Csaba 1980, 1985, 1994; Kovács 1986). Receptor activated cyclic-AMP (Csaba *et al.* 1976, Kuno *et al.* 1979), cyclic-GMP (Kőhidai *et al.* 1992), calmodulin-dependent guanylate cyclase (Kovács *et al.* 1989), inositol phosphates (Kovács and Csaba 1990) have a very important role in the regulation of protozoan cell functions. The sphingomyelin metabolite ceramide has been shown to play an important role in such fundamental biological processes as cell proliferation, oncogenesis and apoptosis (for reviews see Hannun and Bell 1989). We previously found that the cell permeable ceramide analog N-acetyl-sphingosine (C_2-ceramide) has a spectacular effect on the synthesis and breakdown of inositol phospholipids; on the growth rate, chromatin condensation, DNA fragmentation and morphological features of unicellular *Tetrahymena pyriformis* (Kovács *et al.* 1997). It may be supposed that some of these phenomena are connected with the array and function of the actin cytoskeleton, considering that in fibroblasts ongoing sphingolipid synthesis is required for the assembly of both new membrane and of the underlying cytoskeleton (Meivar-Levy *et al.* 1997). In an effort to examine the similar relationship between ceramide and actin cytoskeleton, we tested the effects of C_2-ceramide and other ceramide analogues (sphingosine-1-phosphate; hydroxy- and non-hydroxy fatty-acid ceramides) on the arrangement of the actin cytoskeleton of *Tetrahymena.*

MATERIALS AND METHODS

Mouse monoclonal antibody to actin was obtained from Boehringer (Mannheim, Germany). FITC-phalloidin; N-acetyl-sphingosine (C_2-ceramide); sphingosine-1-phosphate; hydroxy fatty-acid ceramide; non-hydroxy fatty-acid ceramide; goat antimouse IgG FITC conjugate were purchased from Sigma (St Louis, MO, USA). Yeast extract and tryptone were obtained from Difco (Michigan, USA). All other chemicals used were of analytical grade available from commercial sources.

Tetrahymena cultures

In the experiments *Tetrahymena pyriformis* GL strain was tested in the logarithmic phase of growth. The cells were cultured axenically at 28° C in 0.1 % yeast extract containing 1 % tryptone medium. Before the experiments the cells were washed with fresh culture medium, and were resuspended at a concentration of 10^5 cells/ml.

Treatments with the ceramide analogues

Tetrahymena cultures were treated with: C_2-ceramide (10 and 50 μM), sphingosine-1-phosphate (0.5 and 1.0 μM), hydroxy fatty-acid ceramide (100 and 250 μM), non-hydroxy fatty-acid ceramide (100 and 250 μM). Non-treated cells served as controls.

Samples were taken after 10 and 60 min. The cells were fixed with 4 % paraformaldehyde, in phosphate buffered saline (PBS, pH 7.2) for 5 min, and they were washed twice in wash buffer [0.1 % BSA (bovine

serum albumin); 20 mM Tris-HCl; 0.9 % NaCl; 0.05 % Tween 20, pH 8.2].

Immunocytochemical labeling of cells by anti-actin antibody

After washing with wash buffer to block nonspecific binding of antibodies the cells were treated with blocking buffer (1 % BSA in PBS) for 30 min at room temperature. Aliquots from cell suspensions (50 µl) were transferred into Eppendorf microfuge tubes, and 50 µl primary antibody were added [mouse anti-actin antibody, 10 µg/ml; diluted in antibody buffer (1 % BSA in wash buffer)] for 45 min at room temperature.

Negative controls were carried out with 50 µl PBS containing 10 mg/ml BSA in place of the primary antibody.

After four times washing with wash buffer for remove excess primary antibody, the cells were incubated in secondary antibody (goat anti-mouse IgG, dilution 1 : 200) conjugated with FITC (fluorescein isothyocyanate), for 30 min at room temperature. After four times washing in wash buffer the cells were mounted onto microscopic slides.

Labeling of cells with FITC-phalloidin

To localize F-actin, treated, fixed and washed cells (see above) were incubated with 0.1 µM FITC-phalloidin diluted in antibody buffer for 45 min at room temperature. After incubation the four times washed cells (with wash buffer) were mounted onto microscopic slides.

Fluorescence microscopy

The labeled and mounted cells were analyzed in a Bio-Rad MRC 1024 laser scanning confocal microscope equipped a krypton/argon mixed gas laser as a light source. Excitation carried out with the 480 nm line from the laser.

RESULTS

The mouse monoclonal antibody against actin binds to the cortical epiplasm of *Tetrahymena*. This labeling can be considered as specific binding, as in immunoblot analysis the MAB showed an immunocomplex with the crude extract of *Tetrahymena* at a migration position corresponding to ~ 45 kDa (data not shown). The elements surrounding mucocysts as well as the ciliary basal bodies (basal body cage complex) show bright fluorescence. The surface of food vacuoles also show strong labeling, similarly to the surface of nucleus. In most cells, to the intensively fluorescent nuclear surface a large globular area of bright fluorescence is associated. Some labeling occurs on the cytostome and along the buccal cavity (Fig. 1).

Treatments with C_2-ceramide (both 10 and 50 µM) for 60 min resulted in spectacular alterations in the pattern of fluorescence. The fluorescence of the nuclear surface became discontinuous: some parts of surface show no fluorescence, and the nuclear envelope-associated area-brightly fluorescent in the controls - was missing. A large area in the central part of the cytoplasm was unlabeled, whereas the cortical structures showed similar labeling pattern as the controls (Fig. 2). This unlabeled area is free from cytoplasmic organelles revealed by transmission images of same cells. The shorter (10 min) treatments seemed to be ineffective.

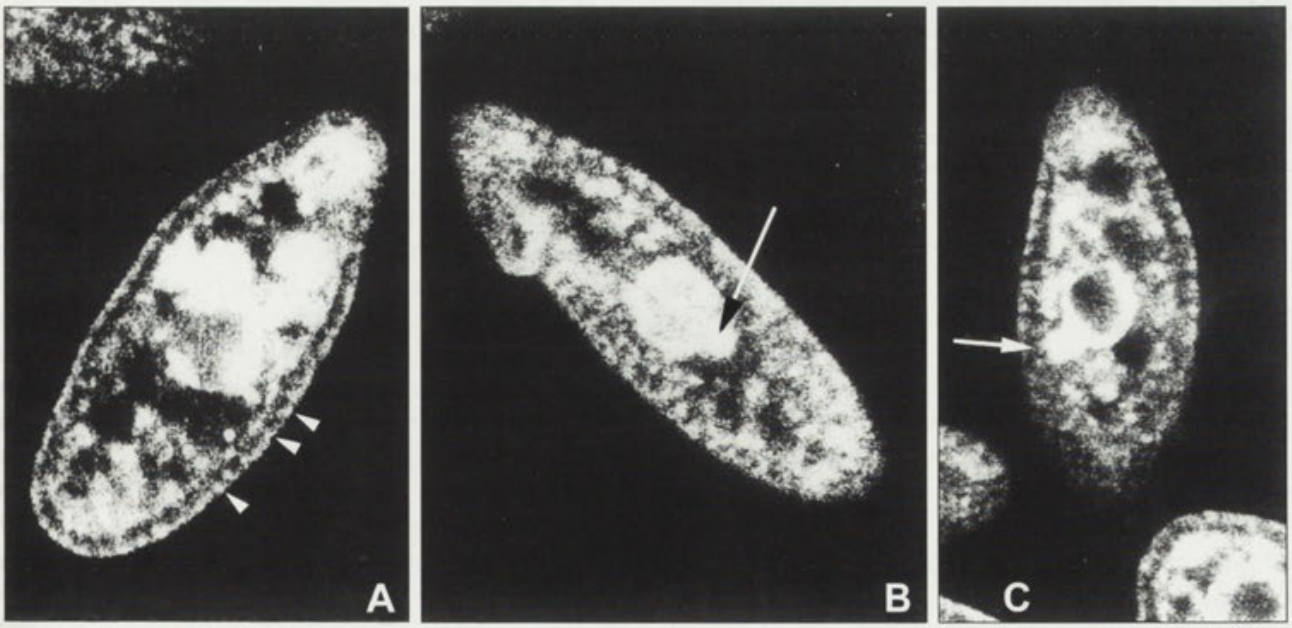

Fig. 1. Control (untreated) *Tetrahymena* cells labeled with mouse monoclonal anti-actin antibody and goat anti-mouse IgG - FITC conjugate. A - elements surrounding mucocysts and cilary basal bodies show bright fluorescence (arrowheads); B,C - strong fluorescent area associated to the nucleus (arrows). CLMS pictures in a median focal plane (A,C) and plane on the surface of nucleus (B) thickness of optical sections: 1 µm. x 1400

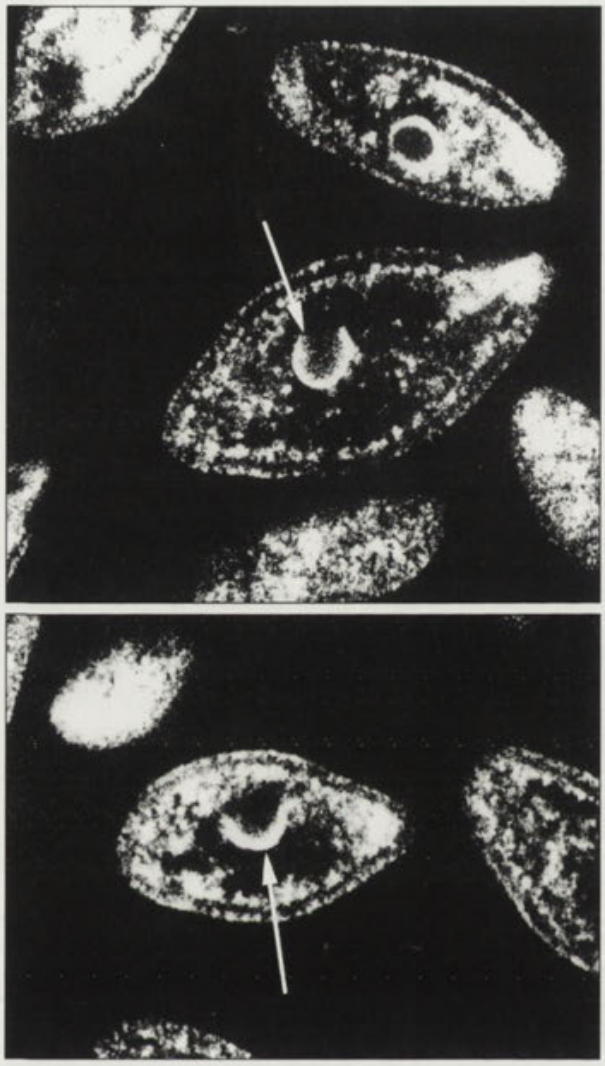

Fig. 2. C_2- ceramide treated (50 μM, 60 min) *Tetrahymena* cells. CLSM pictures in a median focal plane, 1 μm thick optical sections. Discontinuous nuclear surface labeling with anti-actin antibody (arrows). x 1200

The F-actin specific phalloidin binds to the cortical epiplasm of *Tetrahymena* similar to that of the antibody against actin. The mucocysts show a very strong fluorescence, and the microtubular rootlets associated with basal bodies are intensively labeled. In some cases also the surface of contractile vacuoles show intense fluorescence (Fig. 3).

Treatment with 50 μM C_2- ceramide resulted in the appearance of large vacuoles in the posterior cytoplasm - already after 10 min. The effect of lower concentration (10 μM) C_2-ceramide appeared later (60 min). After the C_2-ceramide treatments (10 μM - 60 min; 50 μM - 10 and 60 min) the bright labeling of epiplasmic area disappeared. Many cells were completely rounded (Fig. 4).

Hydroxy fatty-acid ceramide caused no detectable alterations in the phalloidin labeling, whereas non-hydroxy fatty-acid ceramide provoked similar changes in the labeling pattern as the C_2- ceramide (Fig. 5).

Sphingosine-1-phosphate treatment did not cause visible changes in the fluorescence.

DISCUSSION

The involvement of sphingomyelin-metabolite ceramide as a mediator (effector) of some cellular functions in *Tetrahymena* emerged in our earlier experiments (Kovács *et al.* 1997). In these experiments treatments with cell-permeable ceramide analogue C_2 -ceramide (N-acetyl-sphingosine) caused alterations in the synthetic activity of inositol phospholipids, condensation of chromatin, nucleosomal fragmentation and provoked morphological changes (eg. rounding-off). In the rounding-off of the cells the alteration (disassembly, reassembly) of cytoskeletal system has a very important role.

In the epiplasmic layer of ciliata (e.g. *Tetrahymena, Paramecium*) contains actin in association with alveolar membrane, mucocysts, mitochondria, kinetosomes (Méténier 1984); with the basal body cage complex (Garcés *et al.* 1995) and at the division furrow (Edamatsu *et al.* 1992).

The assembly (nucleating, severing, filament-end blocking) and disassembly of actin filaments are closely connected with the turnover of plasma membrane phospholipids, mainly with inositol phospholipids (Stossel 1989). In *Tetrahymena* C_2 -ceramide treatment caused a significant alteration in the uptake of ^{32}P into the phospholipids and also an inhibition in the turnover of inositol phospholipids (Kovács *et al.* 1997). It can be supposed that - at least in part - this effect helped to provoke the rounding-off of the cells, which is a consequence of the destruction of the microfilamentary system. The another characteristic effect of C_2-ceramide treatments: the disappearance of cortical phalloidin labeling, refers likewise to the effect of the disturbed actin-assembly. Further effect of C_2 -ceramide on actin function is demonstrated by the enlargement of contractile vacuoles revealed by large organelle-free area at the posterior part of cytoplasm. The overfilling (enlargement) of contractile vacuoles may be responsible - besides the fact that this drug acts on the skeleton of cells - for rounding-off of the cells. This latter

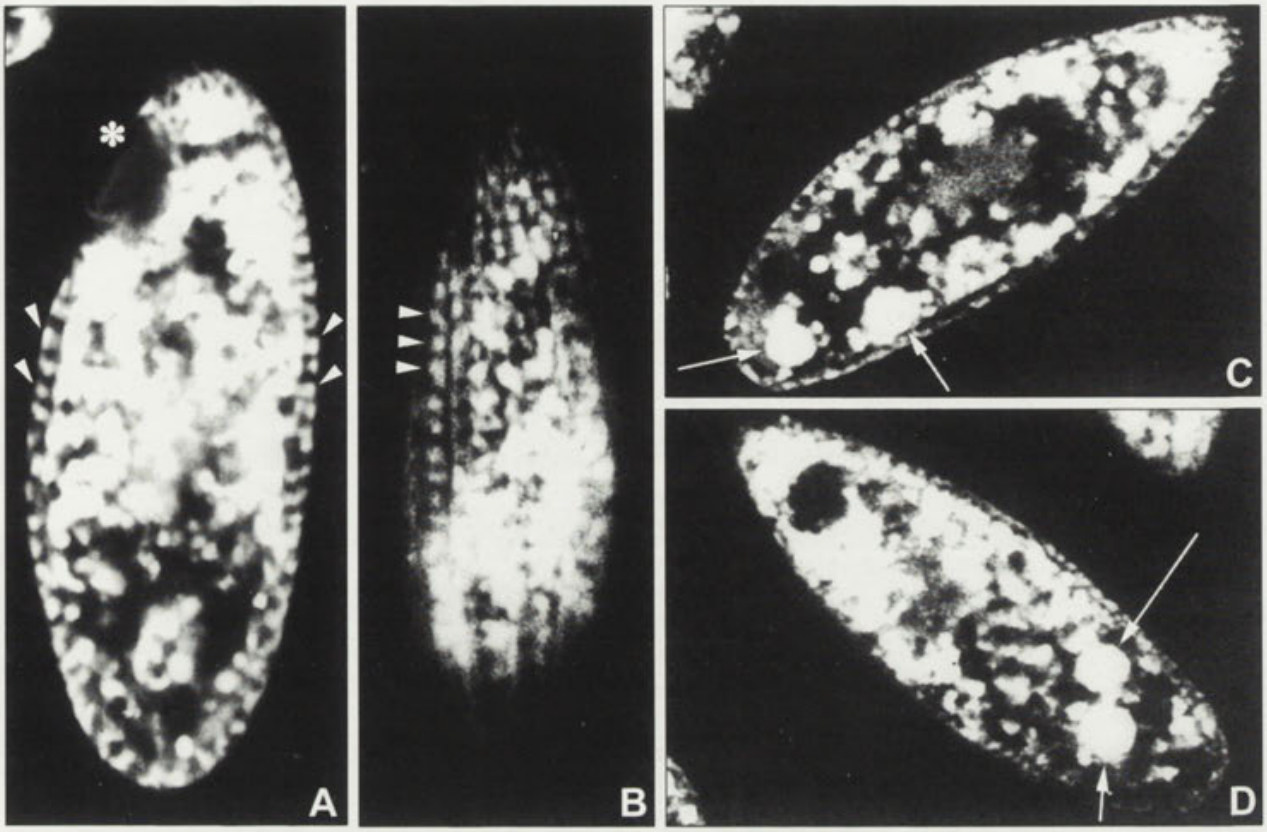

Fig. 3. Control (untreated) *Tetrahymena* cells labeled with FITC-phalloidin. A - median focal plane (1 μm thick optical section); asterisk - cytopharingeal area, fluorescent area associated with mucocysts (arrowheads); B - same cell as in (A) focused at the surface of cell; C,D - median focal plane of the cells. Strong fluorescent labeling of the contractile vacuoles (arrows). x 1300

phenomenon also indicates that in the *Tetrahymena* the function of osmoregulatory system depends on the normal function of actin filaments which are sometimes well visible on the surface of these extended contractile vacuoles.

Phalloidin exclusively demonstrates F-actin. The monoclonal antibody (MAB) used by us was a pan-anti-actin. This means that it was produced against an epitope in a highly conserved region of actin. It reacts to all six isoforms of vertebrate actins and also to invertebrate actins. Having this property, it can demonstrate G- and F-actin alike and many other isoforms which could be present in *Tetrahymena*. This is why the pictures produced by the MAB and phalloidin are disparate.

A characteristic feature shown by MAB is the strong labeling of the nuclear envelope and the globular structure attached to it. Considering that fluorescent phalloidin did not stain these structures, they must be other than F-actin. Contractile vacuoles were not labeled by anti-actin antibody; however they were well visible by phalloidin, which means that they are covered with F-actin. Cortical structures were labeled by both fluorescent material, containing mixed actin (F- and G-actin) skeletal elements.

The actin-disturbing effect of C_2-ceramide is also indicated by the disappearance of continuous nuclear envelope-labeling, and the disappearance of bright fluorescent area associated to the nuclear envelope. Though it would be difficult to declare exactly, this bright area can be a centrosome like microtubule-organizing center (MTOC). In *Tetrahymena* microtubule associated proteins (for example dynein) are in association with actin (Muto *et al.* 1994), and this region in *Tetrahymena* is associated also with myosin (Garcés *et al.* 1995). An actin homologue associated with the centrosome, centractin, was shown to be located at the focal point of MTOC playing a crucial role in the cell division process (Clark and Meier 1992). Perinuclear actin connected with the cortical layer in *Amoeba proteus* was also observed suggesting its important role in the nuclear movements (Pomorski and Grębecka 1995). In the dinoflagellates *Crypthecodinium*

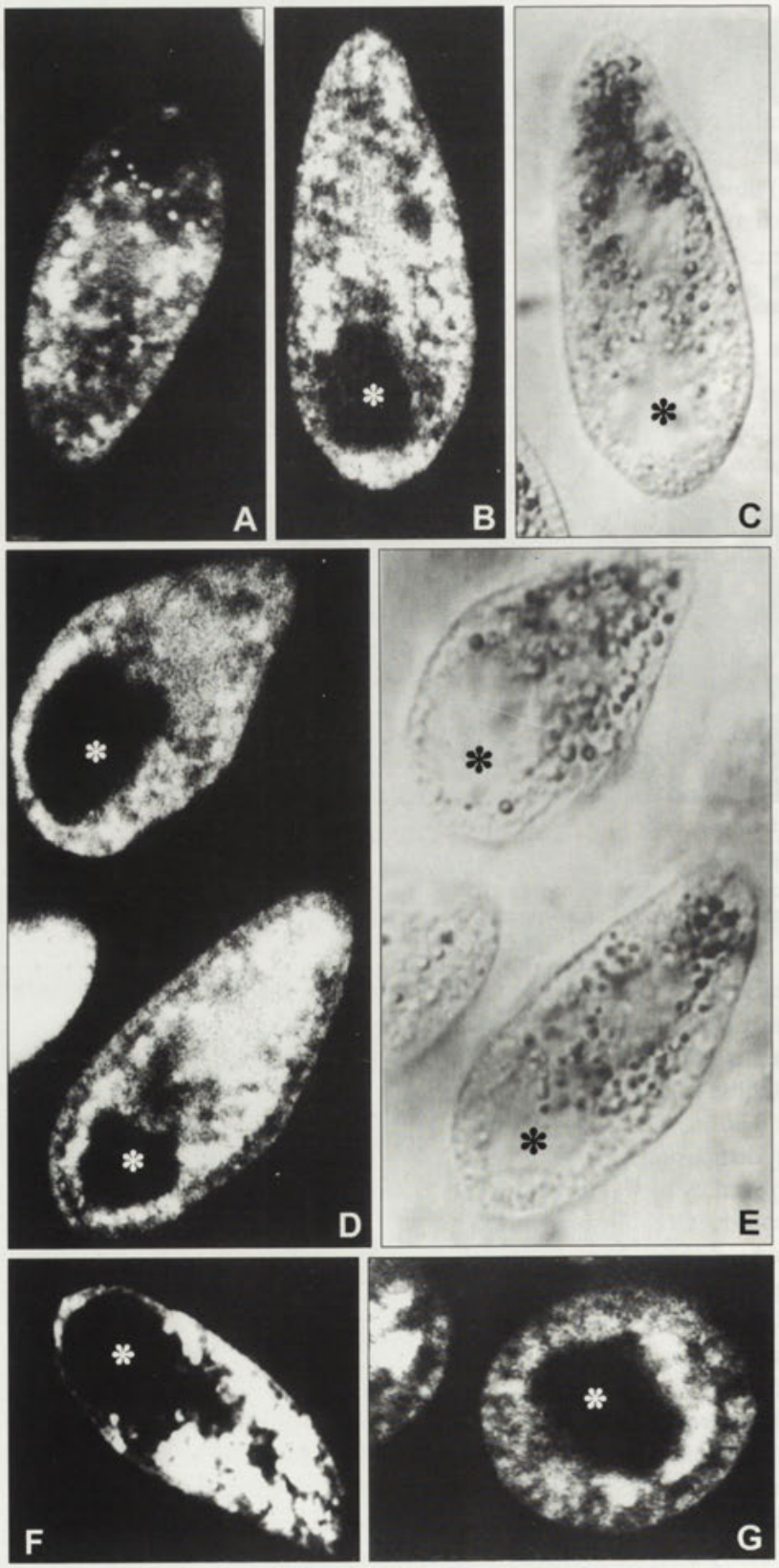

Fig. 4. CLSM pictures of C_2- ceramide treated *Tetrahymena* cells labeled with FITC-phalloidin. A - 50 μM C_2- ceramide for 10 min; B,D - 10 μM C_2 - ceramide for 60 min; C,E - same cells as in (B,D) transmissions pictures; asterisk - large, organelle-free area; F - 50 μM C_2- ceramide for 60 min - no labeled cortical structures; G - 50 μM C_2 - ceramide for 60 min - rounded cell. x 1200

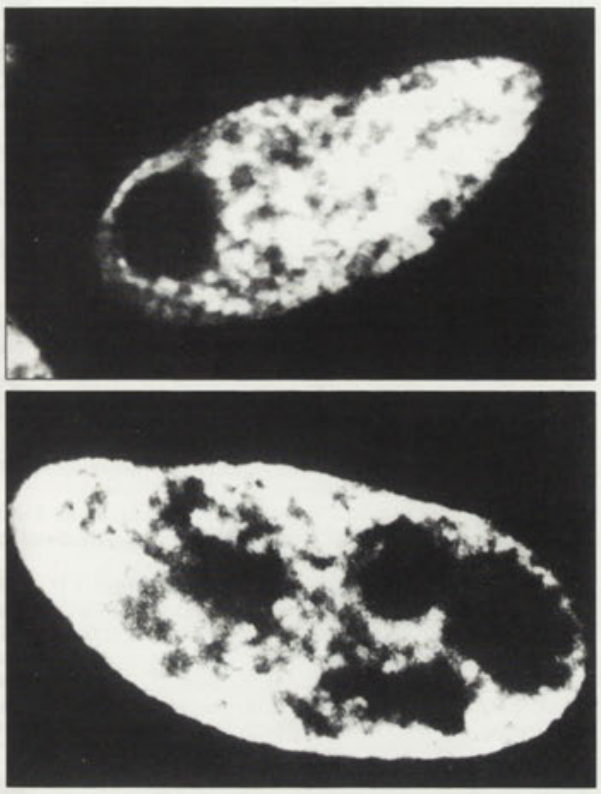

Fig. 5. Non-hydroxy fatty-acid ceramide treated (250 μM; 60 min) *Tetrahymena* cells labeled with FITC-phalloidin. x 1300

cohnii and *Prorocentrum micans* the centrosome like regions are labeled by anti-actin antibody and phalloidin (Soyer-Sobilard *et al.* 1996) , moreover in this region a human centrosomal protein (CTR 210) was demonstrated, which protein is conserved from dinoflagellates to human cells (Perret *et al.* 1995). The disappearance of the bright fluorescent area associated to the nuclear envelope under the effect of C_2-ceramide runs parallel with the actin-denudation of nuclear envelope, however it seems to be difficult to explain the biological importance of this phenomenon.

After C_2-ceramide treatment the cortical areas (basal body cage complexes, mucocysts) remain intact, if it was studied with anti-actin antibody and they disappeared by observing with phalloidin staining. This means that ceramide deteriorates F-actin, however other actins keep the structure. An other possibility for assembly and disassembly of actin filaments is the effect of small actin-binding protein cofilin; this protein binds to G-actin and F-actin filaments *in vitro*, and stimulates depolymerization of actin filaments (Lappalainen and Drubin 1997). Every eukaryotic cell type examined contains at least one member of actin-binding protein as cofilin, however there are no data on the presence of it in *Tetrahymena.*

With the observations mentioned above the functional effects of ceramide got a morphological basis. It is known from our earlier experiments that in the presence of C_2-ceramide the growth activity of *Tetrahymena* populations is totally inhibited (Kovács *et al.* 1997). This inhibition can be a consequence of disturbed actin assembly in the division furrow or in MTOC-s.

The ceramides (e.g. C_2-ceramide) are able to induce apoptosis in different kind of cells (Laster and McKenzie 1996). In our earlier experiments C_2-ceramide caused apoptotic-like effects (chromatin condensation; nucleosomal degradation; morphological alterations; total inhibition of mitotic activity) in *Tetrahymena* (Kovács *et al.* 1997). On the basis of our present experiments the participation of the disturbed actin cytoskeletal system in this process can be imagined. Several recent studies have implicated proteases as important triggers of apoptosis. Some caspase substrates have been identified which influence cell morphology such as gelsolin (Kothakota *et al.* 1997), and PAK2 (Rudel and Bokoch 1997). Thus far, substrates that are cleaved during apoptosis have been elusive. It is presumable that also in the case of membrane blebbing during apoptosis is the consequence of the proteolysis of cytoskeletal proteins. This means that the rounding off and the cytoskeletal reorganization (destruction?) of *Tetrahymena* could be similar phenomena.

The non-hydroxy fatty-acid ceramide caused similar alterations as C_2-ceramide, indicating that this molecule can penetrate the plasma membrane of the *Tetrahymena*, while the more hydrophylic hydroxy fatty-acid ceramide can not penetrate. It was found that free ceramides of erythrocytes contained mainly non-hydroxy fatty acids, and the hydroxy fatty acids not exceeding 1 % (Bouhours and Bouhours 1984). Interestingly, the treatments with C_2-ceramide and non-hydroxy fatty-acid ceramide resulted in a very strong induction of the extrusion of mucocyst material, while hydroxy fatty-acid ceramide and sphingosine-1-phosphate produced no such alterations (Kovács *et al.* 1998). These effects could be in keeping with the influence on the actin skeleton.

Summarizing the results: the experiments demonstrate that F-actin as well as other actins are present in *Tetrahymena*. Ceramide influences the actin cytoskeleton. F-actin and other actins react to ceramide differently. This

means that ceramide can regulate actin assembly and disassembly at a low level of phylogeny influencing many cellular functions connected to the changes of cytoskeleton. The results broadened our knowledge on the spectrum of signaling mechanisms in Protozoa.

Acknowledgment. This work was supported by the National Research Found (OTKA) T-024064, Hungary.

REFERENCES

Bouhours J.F. and Bouhours D. (1984) Identification of free ceramide in human erythrocyte membrane. *J. Lipid Res.* **25:** 613-619

Clark S.W., Meyer D.L (1992) Centractin is an actin homologue associated with the centrosome. *Nature* **359:** 246-250

Cohen J., Garreau-Loubresse N., Beisson J. (1984) Actin microfilaments in *Paramecium*: localization and role in intracellular movements. *Cell. Motil.* **4:** 443-468

Cooper J.A. (1991) The roles of actin polymerization in cell motility. *Annu. Rev. Physiol.* **53:** 585-605

Csaba G. (1980) Phylogeny and ontogeny of hormone receptors: the selection theory of receptor formation and hormonal imprinting. *Biol. Rev.* **55:** 47-63

Csaba G. (1985) The unicellular *Tetrahymena* as a model cell for receptor research. *Int. Rev. Cytol.* **95:** 327-377

Csaba G. (1994) Phylogeny and ontogeny of chemical signaling: origin and development of hormone receptors. *Int. Rev. Cytol.* **155:** 1-48

Csaba G., Nagy S.U., Lantos T. (1976) Are biogenic amines acting on Tetrahymena through a cyclic AMP mechanism? *Acta Biol. Med. Germ.* **35:** 259-261

Cunningham C.C., Stossel T.P., Kwiatkowski D.J. (1991) Enhanced motility in NIH 3T3 fibroblasts that overexpress gelsolin. *Science* **251:** 1233-1236

Edamatsu M., Hirono M., Watanabe Y. (1992) *Tetrahymena* profilin is localized in the division furrow. *J. Biochem. (Tokyo)* **112:** 637-642

Garcés J.A., Hoey J.G., Gavin R.H. (1995) Putative myosin heavy and light chains in *Tetrahymena*: co-localization to the basal body-cage complex and association of the heavy chain with skeletal muscle actin filaments *in vitro*. *J. Cell Sci.* **108:** 869-881

Hannun Y.A. , Bell R.M. (1989) Functions of sphingolipids and sphingolipid breakdown products in cellular regulation. *Science* **243:** 500-507

Hirono M., Tanaka R., Watanabe Y. (1990) *Tetrahymena* actin: copolymerization with skeletal muscle actin and interactions with muscle actin-binding proteins. *J. Biochem. (Tokyo)* **107:** 32-36

Kersken H., Vilmart-Seuwen J., Momayezi M., Plattner H. (1986) Filamentous actin in *Paramecium* cells: mapping by phalloidin affinity labeling in *vivo* and in *vitro*. *J. Histochem. Cytochem.* **34:** 443-454

Kothakota S., Azuma T., Reinhard C., Klippel A., Tang J., Chu K., McGarry T.J., Kirschner M.W., Koths K., Kwiatkowski D.J., Williams L.T. (1997) Caspase-3-generated fragment of gelsolin: effector of morphological change in apoptosis. *Science* **278:** 294-298

Kovács P. (1986) The mechanism of receptor development as implied by hormonal imprinting studies on unicellular organisms. *Experientia* **42:** 770-775

Kovács P., Csaba G. (1990) Involvement of phosphoinositol (PI) system in the mechanism of hormonal imprinting. *Biochem. Biophys. Res. Commun.* **170:** 119-126

Kovács P., Csaba G., Nagao S., Nozawa Y. (1989) The regulatory role of calmodulin-dependent guanylate cyclase in association with hormonal imprinting in *Tetrahymena*. *Microbios* **59:** 123-128

Kovács P., Hegyesi H., Kőhidai L., Csaba G. (1997) Effect of C_2-ceramide on the phosphoinositol metabolism and apoptosis-related morphological changes in *Tetrahymena*. *Comp. Biochem. Physiol.* (in press)

Kovács P., Csaba G., Müller W.E.G. (1998) The effects of ceramide and their analogues on the secretion of the mucocysts content of Tetrahymena. *Cell Mol. Biol.* (in press)

Kőhidai L., Bársony J., Roth J., Marx S.J. (1992) Rapid effects of insulin on cyclic GMP location in an intact protozoan. *Experientia* **48:** 476-481

Kuno T., Yoshida N., Tanaka C. (1979) Immunocytochemical localisation of cyclic AMP and cyclic GMP in synchronously dividing *Tetrahymena*. *Acta Histochem. Cytochem.* **12:** 563-569

Lappalainen P., Drubin D.G. (1997) Cofilin promotes rapid actin filament turnover *in vivo*. *Nature* **388:** 78-82

Laster S.M., McKenzie J.M.J. (1996) Bleb formation and F-actin distribution during mitosis and tumor necrosis factor-induced apoptosis. *Microsc. Res. Tech.* **34:** 272-280

Meivar-Levy I., Sabanay H., Bershadsky A.D., Futerman A.H. (1997) The role of sphingolipids in the maintenance of fibroblast morphology. The inhibition of protrusional activity, cell spreading, and cytokinesis induced by fumonisin B1 can be reversed by ganglioside GM3. *J. Biol. Chem.* **272:** 1558-1564

Méténier G. (1984) Actin in *Tetrahymena paravorax*: Ultrastructural localization of HMM-binding filaments in glicerinated cells. *J. Protozool.* **31:** 205-215

Muto E., Edamatsu M., Hirono M., Kamiya R. (1994) Immunological detection of actin in the 14S ciliary dynein of *Tetrahymena*. *FEBS Lett.* **343:** 173-177

Perret E., Moudjou M., Géraud M.L., Derancourt J., Soyer-Gobilard M.O., Bornens M. (1995) Identification of an HSP-70-related protein associated with the centrosome from dinoflagellates to human cells. *J. Cell Sci.* **108:** 711-725

Pitelka D.R. (1969) Fibrillar systems in protozoa. In: Research in Protozoology (Ed. T.T. Chen). Pergamon Press, Oxford. **3:** 279-338

Pomorski P., Grębecka L. (1995) Nuclear movements and nuclear actin in bilobed nuclei of *Amoeba proteus*. *Eur. J. Protistol.* **31:** 260-267

Rudel T., Bokoch G.M. (1997) Membrane and morphological changes in apoptotic cells regulated by caspase-mediated activation of PAK2. *Science* **276:** 1571-1574

Soyer-Sobilard M.O., Ausseil J., Géraud M.L. (1996) Nuclear and cytoplasmic actin in dinoflagellates. *Biol. Cell.* **87:** 17-35

Stocker W., Naib-Majani W., Wohlfarth-Bottermann K.E., Osborn M., Weber K. (1983) Pinocytosis and locomotion of amoebae. XIX. Immunocytochemical demonstration of actin and myosin in *Amoeba proteus*. *Eur. J. Cell Biol.* **29:** 171-178

Stossel T.P. (1989) From signal to pseudopod. *J. Biol. Chem.* **264:** 18261-18264

Received on 15th June, 1998; accepted on 29th July, 1998

Acta Protozoologica (1998) 37: 209 - 213

ACTA
PROTOZOOLOGICA

Identification of Protein Homologous to Inositol Trisphosphate Receptor in Ciliate *Blepharisma*

Hanna FABCZAK, Mirosława WALERCZYK and Stanisław FABCZAK

Department of Cell Biology, Nencki Institute of Experimental Biology, Warszawa, Poland

Summary. The protozoan ciliate *Blepharisma japonicum* is thought to utilize an enzymatic cascade in light signal transduction and inositol trisphosphate seems to be one of the messengers that causes the cells' electrical and behavioural responses. We have examined the presence and localization of putative inositol trisphosphate receptor ($InsP_3R$) in the cell by means of confocal microscopy and immunoblotting to further elucidate the possible involvement of the phosphoinositide signaling pathway in phototransduction of ciliate cells. The immunohistochemical examination indicated that the $InsP_3$-binding sites are expressed in abundance exclusively in the cortex layer of the cell and are spread over the entire cell body. The localization of $InsP_3R$, primarily in the cortex of *Blepharisma,* was also revealed by immunoblot analysis which clearly showed the existence of $InsP_3R$-like proteins of molecular mass above 200 kDa in the cell cortex fraction. This is the first demonstration of the existence of $InsP_3R$ in ciliated protozoa and its morphological localization within the cell. The results presented, along with our earlier data, support further the possibility of participation of the phosphoinositide second messenger system in light signal transduction in *Blepharisma* cells.

Key words: *Blepharisma japonicum,* ciliate, inositol trisphosphate, inositol trisphosphate receptor, light signal transduction, photophobic response.

INTRODUCTION

The protozoan ciliate *Blepharisma japonicum* exhibits its distinct light avoiding motile behaviour (Kraml and Marwan 1983, Matsuoka 1983, Fabczak *et al.* 1993). Its sensitivity to light is ascribed to an endogenous pigment, blepharismin (Gioffre *et al.* 1993, Matsuoka *et al.* 1997), which is enclosed in small granules (photoreceptive units) and distributed within the cell cortex layer over the entire cell body (Kraml and Marwan 1983, Matsuoka 1983). The observed light-dependent behaviour, known as the step-up photophobic response, consists of a transient ciliary reversal followed by renewed forward movement in a changed direction. The photophobic response (ciliary reversal) is preceded by a gradual, depolarizing receptor potential. This generates, in turn, an action potential (Fabczak *et al.* 1993). In dark-adapted cells, light also induces a rapid and significant increase in the basal level of inositol trisphosphate (Fabczak *et al.* 1998). Both the photophobic responses and light-induced alterations of internal inositol trisphosphate levels in these ciliates are suppressed by externally applied neomycin, heparin and Li^+ (Fabczak *et al.* 1996, 1998), agents known to modify phosphoinositide turnover in various cell receptor systems (Prentki *et al.* 1986, Berridge 1987, Joseph and Samanta

Address for correspondence: Hanna Fabczak, Department of Cell Biology, Nencki Institute of Experimental Biology, ul. Pasteura 3, 02-093 Warszawa, Poland; Fax: (4822) 8225342; E-mail: hannafab@nencki.gov.pl

1993, Ehrlich *et al.* 1994). These results suggest that inositol trisphosphate may be involved as a second messenger in the mechanism of light transduction in *Blepharisma* cell and thus in the activity of their ciliary locomotor system.

We demonstrate in the present study the existence of an $InsP_3R$-like protein and $InsP_3R$ sites localized within the cell cortex layer. These data support the hypothesis that inositol trisphosphate plays a crucial role in light signal transduction in *Blepharisma* cells.

MATERIALS AND METHODS

Cells

Stock cultures of the heterotrichous ciliate *Blepharisma japonicum* were maintained as previously described (Fabczak *et al.* 1996). The cell samples chosen were washed in an excess of fresh culture medium without nutritional components, incubated in this medium in the darkness for about 12 h (control conditions) and subsequently used for the described experiments.

Detection of $InsP_3R$-like protein

Cell cortex fractions for the detection of protein homologous to $InsP_3R$ were obtained according to the method reported elsewhere (Stelly *et al.* 1991). A total cell lysate prepared from macrophage-like cells, line J774A.1 (ATTC) was used as a positive control for the detection of $InsP_3R$ protein. Samples were resolved on 8% SDS-polyacrylamide gels (Laemmli 1970) using a Mini-Protean II Electrophoresis System (Bio-Rad). The proteins were transferred from the gel to nitrocellulose by electroblotting for 1 h at 100 V in a transfer buffer containing 192 mM glycine, 20% methanol and 25 mM Tris, pH 8.3 with a Trans-Blot System (Towbin *et al.* 1979). After transfer, the blot was blocked with a solution of 5% dry skim milk in TBS (150 mM NaCl, 10 mM Tris, pH 8.0). Overnight incubation with a polyclonal antibody raised against Ins(1,4,5)P_3R (Calbiochem) (1:1000 dilution in TBS with 1% BSA) at 4°C was followed by three 10 min washings with TBS containing 0.05% Tween 20 (TBS/Tween). The blot was then incubated for 1 h with horseradish peroxidase conjugated goat anti-rabbit IgG (Calbiochem) (1:10 000 dilution in TBS with 0.2% BSA) at room temperature. The blot was washed several times for 5 min each in TBS/Tween followed by one 5 min wash in TBS alone. The immunocomplexes were developed using an enhanced horseradish peroxidase/luminol chemiluminescence reaction according to the manufacturer's instructions. After incubation with luminol reagents, the blot was exposed to X-ray film (Roentgen XS-1, Foton).

Immunolocalization of $InsP_3R$ sites

Cells suspended in PHEM buffer (60 mM Pipes, 25 mM Hepes, 10 mM EGTA, 2mM $MgCl_2$, pH 6.9, and protease inhibitors: 1 mM PMSF, 10 µg/ml leupeptin, 2 µg/ml aprotinin) were fixed in 70% (final concentration) ethanol at -70°C for 30 min. After fixation, the cells were permeabilized with 0.05% Triton X-100 in PHEM buffer and were then incubated for 1 h with 2% BSA in TBS to block nonspecific binding antibodies. Next, the samples were incubated with anti-$InsP_3R$ antibody for 1 h (1:30 dilution in TBS containing 1% BSA). Then, the incubated cell samples were extensively washed with TBS and exposed to goat anti-rabbit IgG conjugated with FITC (1:300 dilution in TBS with 1% BSA). The cells were again washed several times in TBS and mounted in Mowiol containing 2.5% DABCO. Nonspecific fluorescence determined by incubation without primary antiserum was negligible. The samples were analyzed using a laser scanning confocal microscope (Nikon).

RESULTS AND DISCUSSION

In the present study, immunochemistry and immunoblotting were employed to identify and determine the localization of $InsP_3R$ in the ciliate *Blepharisma*. Immunohistochemical examination revealed prominent cell cortex fluorescence indicating that $InsP_3R$ sites are distributed exclusively within the cortex layer (Fig. 1). $InsP_3R$ is spread almost uniformly over the cell body, excluding any regionalization of its expression. Significant $InsP_3R$ immunoreactivity did not extend beneath the cortex layer into the underlying region of the cell (Figs. 1 B, C). Cells only containing secondary antibody (control) show no immunolabeling (Fig. 1 A). Immunoblot analysis of *Blepharisma* cells with rabbit polyclonal antibody raised against $InsP_3R$ revealed a major protein band of molecular weight above 200 kDa (Fig. 2, lanes 4, 6), similar to the protein labeled from mouse macrophage-like cell lysate (Fig. 2, lane 8), evidencing that the antibody acts selectively against $InsP_3R$ in the ciliate cells. The $InsP_3R$-like protein was found either in the homogenate of whole cells, (Fig. 2, lane 6) or only the cell cortex fraction (Fig. 2, lane 4). The second, less pronounced, band of about 100 kDa might reflect proteolytic degradation as shown in rats by others (Restrepo *et al.* 1992). It is established that $InsP_3R$ proteins in various tissues of different species all have a molecular weight above 200 kDa on SDS-PAGE (Fadool and Ache 1992, Parys *et al.* 1992, Yoshikawa *et al.* 1992, Cunningham *et al.* 1993, Yoshida and Imai 1997). In control blots (Fig. 2, lanes 5, 7, 9) with identical protein loads and incubated with the secondary antibody only, no immunolabeling is found confirming a specificity of labelling. Coomassie blue R-250 stained gels (Fig. 2, lanes 1, 2, 3) also show that there is a rather low density of proteins in the region labeled by anti-$InsP_3R$, excluding the possibility that the staining is due to non-specific labeling.

Our findings provide the first evidence that the $InsP_3R$ is present in ciliated protozoa, in particular in *Blepharisma*

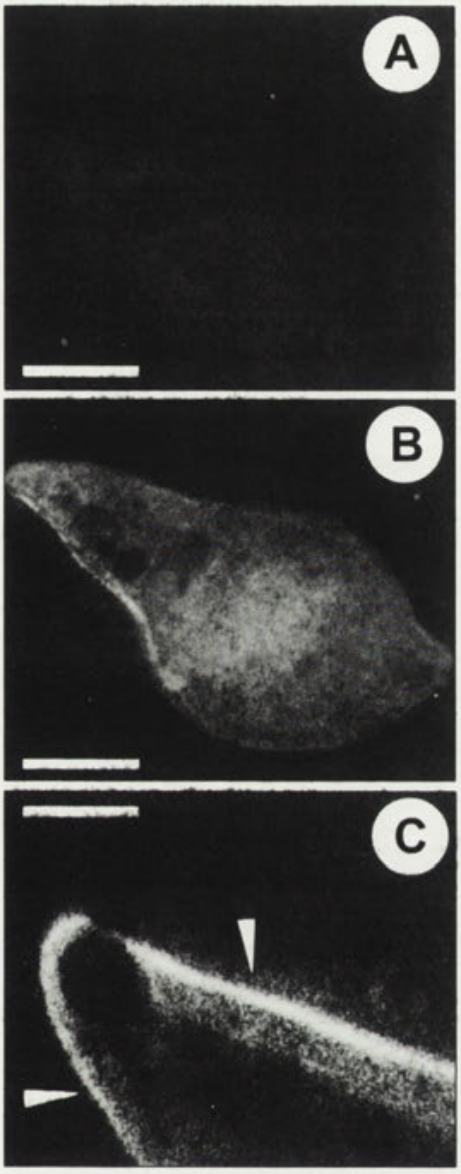

Fig. 1. Localization of $InsP_3R$ in *Blepharisma* viewed on a confocal laser scanning microscope. A - control cell with TBS containing 1% BSA in place of the primary antibody. B and C - cells labelled with rabbit polyclonal anti-$InsP_3R$ and goat anti-rabbit IgG-FITC conjugate. An optical section of the anterior part of the cell confirms that the distribution of $InsP_3R$ is restricted to the cell cortex layer (arrowheads in C). Scale bars - A and B - 20 μm; C - 60 μm

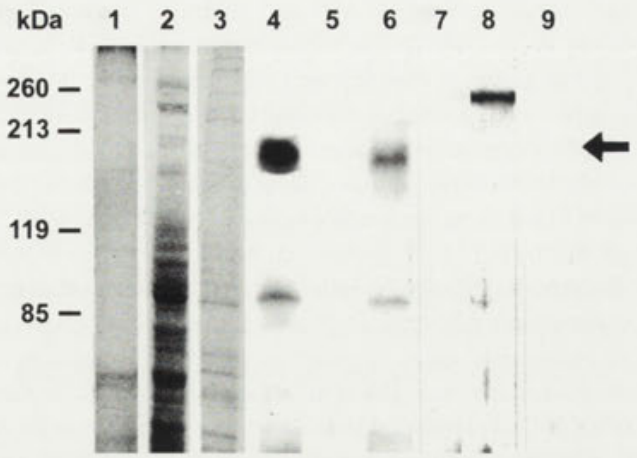

Fig. 2. Immunoblot of rabbit polyclonal anti-$InsP_3R$ reactivity with proteins from *Blepharisma* cells. Lanes 1 - 3: part of the electrophoresed proteins stained with coomasie blue R-250; lanes 4 - 9: proteins electrophoretically transferred to nitrocellulose filter paper; lanes 1, 4, 5: cortex fractions of *Blepharisma* cells (40 μg proteins/lane); lanes 2, 6, 7: homogenate of *Blepharisma* cells (120 μg proteins/lane); lanes: 3, 8, 9: mouse macrophage-like cell lysate, line J774A.1 (15 μg proteins/lane); lanes 5, 7, 9: control immunolabeling carried out with secondary antibody only. Peptide antibodies recognize bands above 200 kDa only in samples incubated with primary and secondary antibodies (lanes 4, 6, and 8)

cells, where $InsP_3R$ is distributed in the cortex layer. The presence of $InsP_3R$ within the cell cortex seems to be reasonable considering the structure and function of the cortex in ciliates. The cortical region in *Blepharisma* possesses, besides large granules containing the pigment blepharismin (Gioffre *et al.* 1993, Matsuoka *et al.* 1997) that is possibly responsible for cell photomotile responses (Giese 1973), numerous small, high electron-dense vesicles which constitute Ca^{2+} and phosphorus compartments (Ishida *et al.* 1991, Gobbi *et al.* 1994). The cell membrane of most ciliates is underlain by a vast network of membrane vesicles known as cortical alveoli (Allen 1971; Tsuchiya and Takahashi 1976; Satir and Wassig 1982; Stelly *et al.* 1991, 1995). The presence of such vesicles is not limited to ciliates; they are observed in many other organisms as well, such as *Amoeba* (Stockem and Klein 1979) and squid giant axons (Oschman *et al.* 1974). The detailed physiological role of these vesicular structures in ciliates is unknown. However, their close location to the plasma membrane suggests some recemblance to the sarcoplasmic reticulum and they may correspond to intracellular Ca^{2+} storage sites (Stelly *et al.* 1991, 1995; Erxleben and Plattner 1994).

For signal transduction involving phosphoinositide systems, an initial release of intracellular Ca^{2+} coupled with an increase in the internal inositol trisphosphate level is usually followed by a phase of Ca^{2+} entry from extracellular space (Berridge 1987, 1989). The mechanism by which inositol trisphosphate elicits an electrophysiological responses in these systems is not precisely elucidated. It has been suggested that inositol trisphosphate is responsible for Ca^{2+} movement across plasma membranes or it

may act directly at the plasma membrane (Irvine 1990, Khan *et al.* 1992). The localization of $InsP_3R$ in the cortical region of *Blepharisma*, together with the recently established light-dependent alteration of internal inositol trisphosphate levels (Fabczak *et al.* 1998) and existance of phosphatidylinositol 4, 5-bisphosphate within the cell cortex (not shown), clearly imply that $InsP_3R$ may participate in the light signal transduction chain of these ciliates. The reported changes in inositol trisphosphate level in this cell may activate receptor-associated ion channels in the alveolar membrane and cause an initial Ca^{2+} release from the vesicular stores. The resultant increase in the cytoplasmic Ca^{2+} level may influence then the ciliary membrane conductance, causing an action potential generation, followed by the observed ciliary reversal during the photophobic response in this ciliate (Fabczak *et al.* 1993). It is likely moreover, that elevated inositol trisphosphate levels can directly act on the receptor channels in the ciliary and/or plasma membrane, permitting Ca^{2+} entry from the external environment and depolarization of the cell membrane in a concentration-dependent manner, similar to other cells (Faddol and Ache 1992, Khan *et al.* 1992, Feng and Kraus-Friedmann 1993, Kraus-Friedmann 1994). The precise function of $InsP_3R$ in the light signal transduction in *Blepharisma* cells however, needs to be clarified.

Acknowledgement. This work was supported in part by grant KBN-6-P203-046-04 and statutory grant to the Nencki Institute of Experimental Biology from the Committee for Scientific Research.

RERERENCES

Allen R. D. (1971) Fine structure of membranous and microfibrillar systems in the cortex of *Paramecium caudatum*. *J. Cell Biol.* **49:** 1-20

Berrige M. J. (1987) Inositol trisphosphate and diacylglycerol: two interacting second messengers. *Ann. Rev. Biochem.* **56:** 159-193

Berrige M. J. (1989) Inositol phosphates and cell signalling. *Nature* **341:** 197-205

Cunningham A. M., Ryugo D. K., Sharp A. H., Reed R. R., Snyder S. H., Ronnett G. V. (1993) Neuronal inositol 1,4,5-trisphosphate receptor localized to the plasma membrane of olfactory cilia. *Neurosci.* **57:** 339-352

Ehrlich B. E., Kaftan E., Bezprozvannaya S., Bezprozvanny I. (1994) The pharmacology of intracellular Ca^{2+}-release channels. *Trends Pharmacol. Sci.* **15:** 145-149

Erxleben C., Plattner H. (1994) Ca^{2+} release from subplasmalemmal store as a primary event during exocytosis in *Paramecium* cells. *J. Cell Biol.* **127:** 935-945

Fabczak S., Fabczak H., Song P.-S. (1993) Photosensory transduction in ciliates. III. The temporal relation between membrane potentials and photomotile responses in *Blepharisma japonicum*. *Photochem. Photobiol.* **57:** 872-876

Fabczak H., Walerczyk M., Fabczak S., Groszyńska B. (1996) $InsP_3$-modulated photophobic responses in *Blepharisma* (short communication). *Acta Protozool.* **35:** 251-255

Fabczak H., Walerczyk M., Groszyńska B., Fabczak S. (1998) Light induces inositol trisphosphate elevation in *Blepharisma japonicum*. *Photochem. Photobiol.* (in press)

Faddool D. A., Ache B. W. (1992) Plasma membrane inositol 1,4,5-trisphosphate-activated channels mediate signal transduction in lobster olfactory receptor neurons. *Neuron* **9:** 907-918

Feng L., Kraus-Friedmann N. (1993) Association of the hepatic IP_3 receptor with the plasma membrane: relevance to mode of action. *Am. J. Physiol. (Cell Physiol.)* **34:** C1588-C1596

Giese A. C. (1973) *Blepharisma*. The Biology of a Light-Sensitive Protozoan. Stanford Univ. Press, Stanford

Gioffre D., Ghetti F., Lenci F., Paradiso C., Dai R., Song P.-S. (1993) Isolation and characterization of the presumed photoreceptor protein of *Blepharisma japonicum*. *Photochem. Photobiol.* **58:** 275-279

Gobbi L., Albertini G., Lucarini G., Carboni V., Marangoni R., Colombetti G. (1994) Identification of calcium and phosphorus binding sites in the heterotrich ciliate *Blepharisma japonicum*. *Micron* **25:** 135-139

Irvine R. F. (1990) Quantal Ca^{2+} release and the control of Ca^{2+} entry by inositol phosphates- a possible mechanism. *Fed. Eur. Biochem. Soc. Lett.* **263:** 5-9

Ishida M., Shigenaka Y., Suzaki T. (1991) Studies on the mechanism of cell elongation in *Blepharisma japonicum*. *Eur. J. Protistol.* **26:** 365-369

Joseph S. K., Samanta S. (1993) Detergent solubility of the inositol trisphosphate receptor in rat brain membranes: evidence for association of the receptor with ankyrin. *J. Biol. Chem.* **268:** 6477-6486

Khan A. A., Steiner J. P., Snyder S. H. (1992) Plasma membrane inositol 1,4,5-trisphosphate receptor of lymphocytes: selective enrichment in sialic acid and unique binding specifity. *Proc. Natl. Acad. Sci. USA.* **89:** 2849-2853

Khan A. A., Steiner J. P., Klein M. G., Schneider M. F., Snyder S. H. (1992) IP_3 receptor: localization to plasma membrane of T cells and cocapping with the T cell receptor. *Science* **257:** 815-818

Kraml M., Marwan W. (1983) Photomovement responses in the heterotrichous ciliate *Blepharisma japonicum*. *Photochem. Photobiol.* **37:** 313-319

Kraus-Friedmann N. (1994) Signal transduction and calcium: a suggested role for the cytoskeleton in inositol 1,4,5-trisphosphate action. *Cell Motil. Cytoskel.* **28:** 279-284

Laemmli U. K. (1970) Cleavage of structural proteins during the assembly of the head of bacteriophage T4. *Nature* **277:** 680-685

Matsuoka T. (1983) Negative phototaxis in *Blepharisma japonicum*. *J. Protozool.* **30:** 337-340

Matsuoka T., Sato M., Maeda M., Naoki H., Tanaka T., Kotsuki H. (1997) Localization of blepharismin photosensors and identification of a photoreceptor complex mediating the step-up photophobic response of the unicellular organism, *Blepharisma*. *Photochem. Photobiol.* **65:** 915-921

Oschman J. L., Hall T. A., Peters P. D. (1974) Association of calcium with membranes of squid giant axon. Ultrastructure and microprobe analysis. *J. Cell Biol.* **61:** 156-165

Parys J. B., Sernett S. W., DeLisle S., Snyder P. M., Welsh M. J., Campbell K. P. (1992) Isolation, characterization, and localization of the inositol 1,4,5-trisphosphate receptor protein in *Xenopus laevis* oocytes. *J. Biol. Chem.* **264:** 18776-18782

Prentki M., Deeney J.T., Matchinsky F. M., Joseph S. K. (1986) Neomycin: a specific drug to study the inositol phospholipid signalling system? *FEBS Lett.* **197:** 285-288

Restrepo D., Teeter J. H., Honda E., Boyle A. G., Maracek J. F., Prestwich G. D., Kalinoski D. J. (1992) Evidence for an $InsP_3$-gated channel protein in isolated rat olfactory cilia. *Am. J. Physiol.* **263:** 667-673

Satir B. H., Wassig S. L. (1982) Alveolar sacs of *Tetrahymena*: ultrastructural characteristics and similarities to subsurface cisterns of muscle and nerve. *J. Cell Sci.* **55:** 13-33

Stelly N., Mauger J.-P., Claret M., Adoutte A. (1991) Cortical alveoli of *Paramecium*: a vast submembranous calcium storage component. *J. Biol. Chem.* **113:** 103-112

Stelly N., Halpern S., Nicolas G., Fragu P., Adoutte A. (1995) Direct visualization of a vast cotrical calcium compartment in *Paramecium* by secondary ion mass spectrometry (SIMS) microscopy: possible involvement in exocytosis. *J. Cell Sci.* **108:** 1895-1909

Stockem W., Klein H. P. (1979) Pinocytosis and locomotion in amoebae. XV. Demonstration of Ca^{2+}-binding sites during induced pinocytosis in *Amoeba proteus*. *Protoplasma* **100:** 33-43

Towbin H., Staehelin T., Gordon J. (1979) Electrophoresis transfer of proteins from polyacrylamide gels to nitrocellulose sheets: Procedure and some applications. *Proc. Natl. Acad. Sci. USA* **76:** 4350-4354

Tsuchiya T., Takahashi K. (1976) Localization of possible calcium-binding sites in the cilia of *Paramecium caudatum*. *J. Protozool.* **23:** 523-526

Yoshida Y., Imai S. (1997) Structure and function of inositol 1,4,5-trisphosphate receptor. *Jap. J. Pharmacol.* **74:** 125-137

Yoshikawa S., Tanimura T., Miyawaki A., Nakamura M., Yuzaki M., Furuichi T., Mikoshiba K. (1992) Molecular cloning and characterization of the inositol 1,4,5-trisphosphate receptor in *Drosophila melanogaster*. *J. Biol. Chem.* **267:** 16613-16619

Received on 12th July, 1998; accepted on 12th October, 1998

Acta Protozoologica (1998) 37: 215 - 219

ACTA
PROTOZOOLOGICA

PCR Amplification of *Paramecium* DNA Using the β-Adrenergic-Specific Primers

Jolanta WIEJAK, Anna PŁATEK, Liliana SURMACZ and Elżbieta WYROBA

Department of Cell Biology, Nencki Institute of Experimental Biology, Warszawa, Poland

Summary. In continuation to our previous cytophysiological studies on the effect of β-adrenergic ligands on *Paramecium* we present here a new evidence based on molecular investigation of isolated DNA. Specific oligonucleotides designed to hydrophobic transmembrane regions TM 3 and TM 6 of the β_2-adrenergic receptor have been applied for hybridization analysis and PCR. In PCR analysis the DNA species of ~530 bp were generated which subsequently hybridized to another β-adrenergic-specific molecular probe located within the amplified region suggesting that the amplified region comprises one of the essential sequence motifs of the β_2-adrenergic receptor.

Key words: β-adrenergic receptor, digoxigenin-labeled oligonucleotides, DNA, nucleic acid hybridization, *Paramecium aurelia*, PCR.

INTRODUCTION

Since our previous experiments indicated a regulative role of β-adrenergic ligands on *Paramecium* membrane properties (Wyroba 1986, 1987, 1989, 1991), the PCR and DNA hybridization analysis was undertaken in order to look for this G-protein-coupled receptor (Wyroba and Surmacz 1996, 1997; Surmacz *et al.* 1997).

The set of the β-adrenergic-specific degenerated oligonucleotides has been used as: the molecular probes for Southern hybridization, and the primers in PCR amplification of DNA isolated from a ciliate *Paramecium*. Another oligonucleotide probe - located within the amplified region - has been next constructed to analyze the PCR products.

The primers were designed to the conservative sequences of the β_2-receptor (Dixon *et al.* 1986, Lefkowitz *et al.* 1986, Dohlman *et al.* 1987, Kobilka *et al.* 1987 a, b) within the transmembrane region TM 3 (forward primer - No 4) including Asp 113 involved in binding of agonists and antagonists (Strader *et al.* 1987, 1989) and TM 6 (backward primer - No 9) corresponding to the "gene-specific universal mammalian primers" (Venta *et al.* 1996).

MATERIALS AND METHODS

Cells

Paramecium aurelia cells (299s strain) were cultivated in axenic medium at 27°C (Soldo and Wagtendonk 1967). 5-day-old cultures were

Address for correspondence: Elżbieta Wyroba, Department of Cell Biology, Nencki Institute of Experimental Biology, ul. Pasteura 3, 02-093 Warszawa, Poland; Fax: (4822) 8225342; E-mail: wyroba@nencki.gov.pl

collected by centrifugation at 600 x g and washed twice in sterile buffer composed of: 5 mM Tris-HCl, 10 mM $MgCl_2$, 1 mM KCl, pH 7.0.

Molecular probes and Southern hybridization analysis

The isolation of DNA, digestion with restriction enzymes and hybridization analysis were carried out as described previously (Subramanian *et al.* 1994, Wyroba *et al.* 1995, Surmacz *et al.* 1997). Non-radioactive detection system using 3'-Digoxigenin-labeled oligonucleotides (Wyroba *et al.* 1995) with chemiluminescent substrate CDP-Star (Boehringer Mannheim) was applied (Surmacz *et al.* 1997). The molecular probes for hybridization of restriction enzyme digest of *Paramecium* DNA were constructed to the characteristic regions of the β_2-adrenergic receptor:

1) probe No 4: 29 mer - 3rd hydrophobic region (TM 3) including Asp 113 involved in binding of agonists and antagonists (Strader *et al.* 1987, 1989) of the sequence given in Surmacz *et al.* 1997;

2) probe No 9: 24 mer - 6th hydrophobic region (TM 6): 5'-TAACCAACATAAT(A)GTGAAT(A)GTTCC - corresponds (within 18 nucleotides stretch) to the probe No 7 (Wyroba *et al.* 1998) which is the one of "gene specific mammalian tagged sites" (Venta *et al.* 1996);

3) the third internal β-adrenergic-specific oligonucleotide (Probe No 1), 45 mer: 5'-AGAAGATCA(T)TCA(T)AAATTCTGTTT (G)AAAGAACATAAAGCT(A)TTA(G)AAA - designed to the sequence from the 3rd cytoplasmic loop was located in the region involved in G-protein interaction, including Ser 262 - the phosphorylation site by protein kinase A in the process of receptor desensitization (Clark *et al.* 1989, Okamoto *et al.* 1991). This oligonucleotide was used as a specific probe for Southern blot analysis of PCR amplified products.

The molecular probes were synthesized according to the protozoan codon usage (Caron and Meyer 1985, Martindale 1989).

PCR

PCR was performed using *Paramecium* DNA as a template, purity of which was checked by horizontal electrophoresis (at 50 V for 2 h) on 0.8 % agarose gel.

The chemicals used were: Taq polymerase (Perkin-Elmer, Gibco BRL, Fisher Biotech), deoxynucleotides (Promega, Gibco BRL) and $MgCl_2$ (Promega, Gibco BRL).

PCR setting was as follows: denaturation at 95°C for 30 s, annealing at 55°C for 30 s and extension at 72°C for 1 min - x 34 cycles with additional extension at 72°C for 10 min before cooling down to 4°C (PTC-150HB MiniCycler, MJ Research, Inc.).

Forward primer was the probe No 4 and the backward primer was the probe No 9 described above. The PCR products have been analyzed by horizontal electrophoresis on 1.8 % agarose after staining with

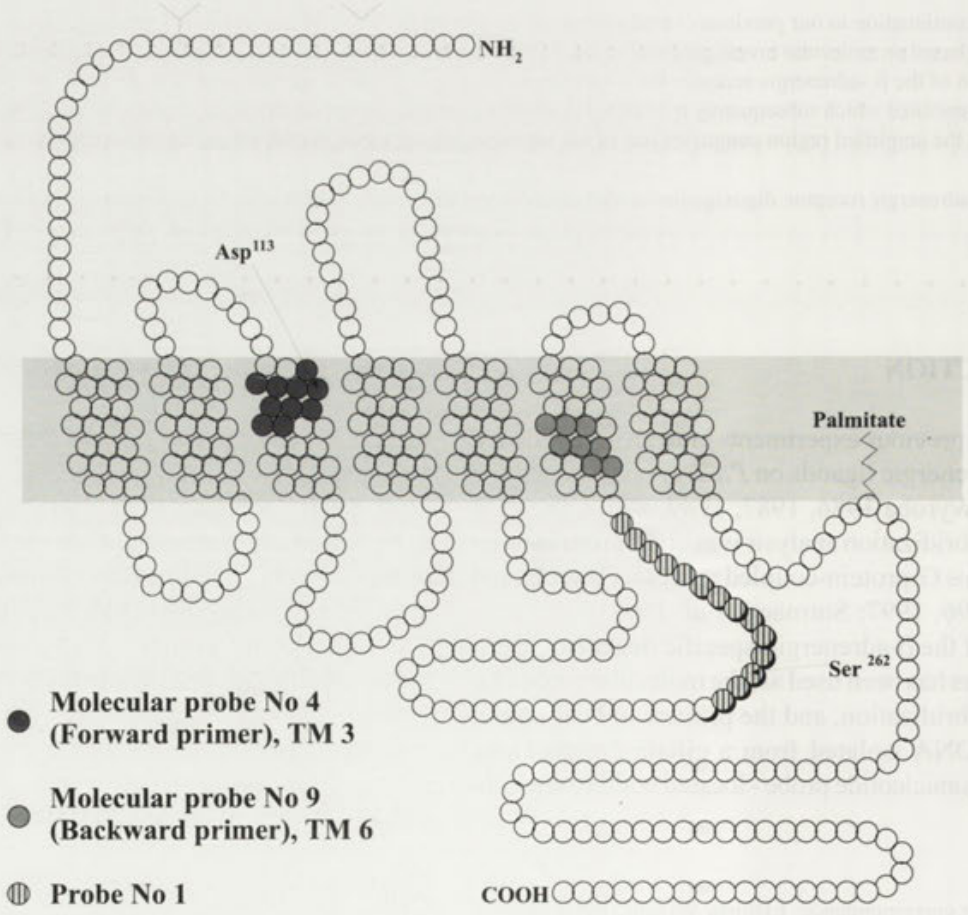

Fig. 1. Location of β-adrenergic specific molecular probes No 1, No 4 and No 9 designed as described in Materials and Methods. Membrane topography of β_2-adrenergic receptor is shown (the scheme modified from Lefkowitz *et al.* 1986, Dohlman *et al.* 1987, Kobilka *et al.* 1987a).

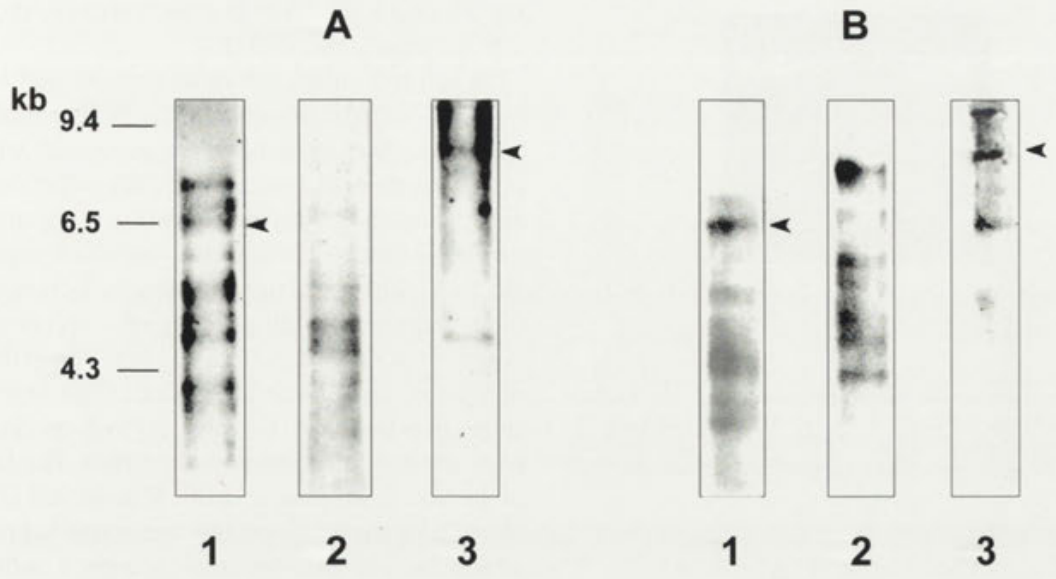

Fig. 2. Comparison of the Southern hybridization pattern of *Paramecium* DNA obtained with the two β-adrenergic-specific oligonucleotides: No 4 (A) and No 9 (B). The restriction enzymes were the following: lane 1 *Eco* RI; lane 2 *Hind* III; lane 3 *Pst* I. The DNA species of ~6.5 kb detected with both probes in *Eco* RI digests (lane 1) and of 8.5 kb (lane 3) in *Pst* I digests are shown with arrowheads

ethidium bromide and then capillary transferred to the nylon membrane (Zeta-Probe, BioRad) (Wyroba *et al.* 1995). The blots were further examined by Southern hybridization analysis with the probe No 1.

RESULTS

In this paper we present the results obtained with the two oligonucleotide probes: No 4 - directed to the region of ligand binding to the beta-adrenergic receptor, and No 9, being one of the universal PCR primer for β_2-adrenergic receptor (Venta *et al.* 1996). Location of these molecular probes in TM 3 and TM 6 of the β_2-receptor, respectively, is shown in the Fig. 1.

First, we compared the hybridization pattern of *Paramecium* DNA cut with the restriction enzymes and next tested the same oligonucleotides as the primers for PCR amplification. Fig. 2 illustrates a comparison of the Southern hybridization pattern when these molecular probes were applied: the DNA species of 6.5 kb (detected by Surmacz *et al.* 1997) have been found hybridizing to both the molecular probes in *Eco* RI restriction digest of *Paramecium* DNA (lane 1 in Figs. 2 A and 2 B). On the other hand, in *Pst* I digests the species of ~ 8.5 kb were detected with the probe No 4 and probe No 9 (lane 3 in Figs. 2 A and 2 B, respectively).

On the basis of the obtained result we decided to perform PCR amplification using the same set of the oligonucleotides (i.e. No 4 and No 9) as the primers and the isolated DNA as a template. The purity of the template was confirmed by agarose-gel electrophoresis as shown in Fig. 3 - the high molecular DNA from different preparations was used. The products of PCR amplification are shown in Fig. 4 A, of which two prominent ones are the DNA species of ~ 530 bp and of ~ 460 bp.

To characterize the PCR-amplified DNA species a next hybridization analysis was performed with the probe constructed to the internal β-adrenergic region (Probe No 1, Wyroba and Surmacz 1997) involved in G-protein interaction. The molecular probe constructed to this aim (No 1) is located within the region which was PCR amplified (see Fig. 1). Fig. 4B indicates that the DNA species observed in hybridization analysis were those of ~530 bp, which corresponds to the predicted molecular size of the PCR product. The DNA species of the lower molecular size did not hybridize to the probe No 1 and may be considered as the aborted PCR products.

DISCUSSION

The β-adrenergic-specific molecular probes designed to TM 3 (No 4) and TM 6 (No 9) regions of the β_2-receptor reveal at least two DNA species of the same molecular size in hybridization analysis of *Paramecium*

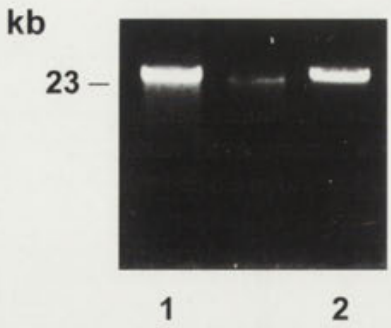

Fig. 3. Isolated *Paramecium* DNA after purification. Two samples from different experiments are shown: lane 1 - sample 1 (2.5 μg), lane 2 - sample 2 (2.5 μg) after agarose electrophoresis and ethidium bromide staining. These DNA preparations were used as templates for PCR amplification

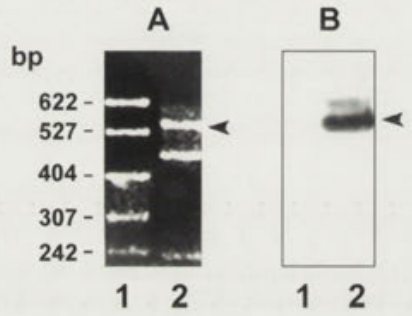

Fig. 4. Polymerase chain reaction (PCR) amplification of *Paramecium* DNA using β-adrenergic-specific primers No 4 and No 9. Location of the primers is shown in Fig.1. **A.** Electrophoresis of PCR products - ethidium stained 1.8% agarose gel, lane 1 - molecular marker pBR 322 DNA - *Msp* I Digest; lane 2 - PCR amplified products; **B.** Southern blot analysis of PCR products (shown in **A**) using the oligonucleotide molecular probe No 1. This probe is constructed to the β-adrenergic receptor sequence located within the amplified region. Arrowhead indicates the DNA species of ~530 bp, which is the predicted molecular size of the amplified product

DNA: 6.5 kb in *Eco* RI digest and 8.5 kb in *Pst* I. It should be pointed out that these DNA species have been previously described by us when the hybridization analysis was performed with the oligonucleotide probes located in other regions of the β_2-adrenergic receptor, i. e. in the adjacent transmembrane regions TM 3 and TM 4 (Surmacz *et al.* 1997).

Our next approach was to apply PCR analysis to amplify β-adrenergic homologous sequences from *Paramecium* DNA. The PCR analysis seems to be an useful tool in this case since β-adrenergic receptor is intronless (Kobilka *et al.* 1987b), whereas the *Paramecium* genes sequenced so far either do not posses introns (Kink *et al.* 1990) or they are very short (Dupuis 1992, Russel *et al.* 1994).

When the molecular probes mentioned above (i. e. No 4 and No 9) were applied as the PCR primers, the DNA species of the ~530 bp were generated which is the predicted molecular size. The PCR products were further analyzed by Southern hybridization using another oligonucleotide located within the amplified region - probe No 1 - which was designed to the third cytoplasmic loop of the receptor including the region of its interaction with G-proteins (Zhao *et al.* 1998). This region of the molecule may be of great importance since G-proteins by themselves may be involved in phagocytosis process (Didenko *et al.* 1996, Ogier-Denis *et al.* 1996). The fact that the probe No 1 hybridized to the PCR generated DNA species of ~530 bp may suggest that the amplified region comprises one of the essential sequence motifs of the β_2-adrenergic receptor.

Acknowledgments. This work was supported by the State Committee for Scientific Research (KBN) grant No 6P04A 05910 and the statutable funds to the Nencki Institute of Experimental Biology.

REFERENCES

Caron C. F., Meyer E. (1985) Does *Paramecium primaurelia* use a different genetic code in its macronucleus? *Nature* **314:** 185-188

Clark R. B., Friedman J., Dixon R. A. F., Strader C. D. (1989) Identification of a specific site required for rapid heterologous desensitization of the β-adrenergic receptor by cAMP-dependent protein kinase. *Molec. Pharmacol.* **36:** 343-348

Didenko L. W., Buchwalow I. B., Schulze W., Augsten K., Susa M., Unger E. (1996) Localization of G-proteins in macrophages and *E. coli* during phagocytosis. *Acta Histochem.* **98:** 399-409

Dixon R. A. F., Kobilka B. K., Strader D. J., Benovic J. L., Dohlman H. G., Frielle T., Bolanowski M. A., Bennet C. D., Rands E., Diehl R. E., Mumford R. A., Slater E. E., Sigal I. S., Caron M. G., Lefkowitz R. J., Strader C. D. (1986) Cloning of the gene and cDNA for mammalian β-adrenergic receptor and homology with rhodopsin. *Nature* **321:** 75-79

Dohlman H. G., Bouvier M., Benovic J. L., Caron M. G., Lefkowitz R. J. (1987) The multiple membrane spanning topography of the β_2-adrenergic receptor. *J. Biol. Chem.* **262:** 14282-14288

Dupuis P. (1992) The β-tubulin genes of *Paramecium* are interrupted by two 27 bp introns. *EMBO J.* **11:** 3713-3719

Kink J. A., Maley M. E., Preston R. R., Ling K-Y., Wallen-Friedman M. A., Saimi Y., Kung C. (1990) Mutations in *Paramecium* calmodulin indicate functional differences between the C- and the N- terminal lobes *in vivo*. *Cell* **62:** 165-174

Kobilka B. K., Dixon R. A. F., Frielle T., Dohlman H. G., Bolanowski M. A., Sigal I. S., Yang-Feng T. L., Francke U., Caron M. G., Lefkowitz R. J. (1987a) cDNA for the human β_2-adrenergic receptor: A protein with multiple membrane-spanning domains and encoded by a gene whose chromosomal location is shared with that of the receptor for platelet-derived growth factor. *Proc. Natl. Acad. Sci. USA* **84:** 46-50

Kobilka B. K., Frielle T., Dohlman H. G., Bolanowski M. A., Dixon R. A. F., Keller P., Caron M. G., Lefkowitz R. J. (1987b) Delineation of the intronless nature of the genes for the human and hamster β_2-adrenergic receptor and their putative promoter regions. *J. Biol. Chem.* **262:** 7321-7327

Lefkowitz R. J., Benovic J. L., Kobilka B. K, Caron M. G (1986) β-adrenergic receptors and rhodopsin: shedding new light on an old subject. *TIPS* **7:** 444-448

Martindale D. W. (1989) Codon usage in *Tetrahymena* and other ciliates. *J. Protozool.* **36:** 29-34

Ogier-Denis E., Houri J. J., Bauvy C., Codogno P. (1996) Guanine nucleotide exchange on heterotrimeric G i3 protein controls autophagic sequestration in HT-29 cells. *J. Biol. Chem.* **271:** 28593-28600

Okamoto T., Murayama Y., Hayashi Y., Inagaki M., Ogate E., Nishimoto I. (1991) Identification of a G_s activator region of the β_2-adrenergic receptor that is autoregulated via protein kinase A - dependent phosphorylation. *Cell* **67:** 723-730

Russell C. B., Fraga D., Hinrichsen R. D. (1994) Extremely short 20 to 30 nucleotides introns are the standard length in *Paramecium tetraurelia*. *Nucleic Acids Res.* **22:** 1221-1225

Soldo A. T., van Wagtendonk W. J. (1967) A method for the mass collection of axenically cultivated *Paramecium aurelia*. *J. Protozool.* **14:** 497-498

Strader C. D., Sigal I. S., Register R. B., Candelore M. R., Rands E., Dixon R. A. F. (1987) Identification of residues required for ligand binding to the β-adrenergic receptor. *Proc. Natl. Acad. Sci. USA* **84:** 4384-4388

Strader C. D., Sigal I. S., Dixon R. A. F. (1989) Structural basis of β-adrenergic receptor function. *FASEB J.* **3:** 1825-1835

Subramanian S. V., Wyroba E., Andersen A. P., Satir B. H. (1994) Cloning and sequencing of parafusin, a calcium-dependent exocytosis-related phosphoglycoprotein. *Proc. Natl. Acad. Sci. USA* **91:** 9832-9836

Surmacz L., Krawczyk K., Wyroba E. (1997) Different β-adrenergic-specific molecular probes reveal the same DNA species in *Paramecium* hybridization analysis. *Cell. Mol. Biol. Letters* **2:** 379-387

Venta P. J., Brouillette J. A., Yuzbasiyan-Gurkan V., Brewer G. J. (1996) Gene-specific universal mammalian sequence-tagged sites: application to the canine genome. *Biochem. Genetics* **34:** 321-341

Wyroba E. (1986) Effect of β-receptor antagonist dichloroisoproterenol on *Paramecium* endocytosis. *Acta Protozool.* **25:** 167-174

Wyroba E. (1987) Stimulation of *Paramecium* phagocytosis by phorbol ester and forskolin. *Cell Biol. Rep.* **11:** 657-664

Wyroba E. (1989) Beta-adrenergic stimulation of phagocytosis in the unicellular eukaryote *Paramecium aurelia*. *Cell. Biol. Int. Rep.* **13:** 667-678

Wyroba E. (1991) Quantitation of fluid phase uptake in the cells blocked in phagocytic activity. *Cell. Biol. Int. Rep.* **15:** 1207-1216

Wyroba E., Surmacz L. (1996) Beta-adrenergic receptor: Structure and essential sequence motifs. *Postępy Biologii Komórki* **23:** 601-614 (in Polish).

Wyroba E., Surmacz L. (1997) Genomic Southern blot analysis of *Paramecium* using β-adrenergic specific probes. *FASEB J.* **11:** A920, 370

Wyroba E., Widding Hoyer A., Storgaard P. S., Satir H. B. (1995) Mammalian homologue of the calcium-sensitive phosphoglycoprotein, parafusin. *Eur. J. Cell Biol.* **68:** 419-426

Wyroba E., Wiejak J., Płatek A., Surmacz L. (1998) PCR amplification of *Paramecium* genomic DNA with the β-adrenergic specific primers. *25th FEBS Meeting, Copenhagen,* 182

Zhao M. M., Gaivin R. J., Perez D. M. (1998) The third extracellular loop of the β_2-adrenergic receptor can modulate receptor/G protein affinity. *Mol. Pharmacol.* **53:** 524-529

Received on 12th August, 1998; accepted on 12th October, 1998

Acta Protozoologica (1998) 37: 221 - 225

ACTA
PROTOZOOLOGICA

Toxic Effect of Chemical Disinfection of Wastewater on Freshwater Ciliates

Paolo MADONI, Gessica GORBI and Elena TAJÉ

Department of Environmental Sciences, University of Parma, Parma, Italy

Summary. The toxic effect of chemical disinfection of sewage treatment plants was tested on freshwater ciliates inhabiting the receiving water bodies. For this purpose, the effluent from an activated-sludge plant was treated with sodium hypochlorite (NaClO), chlorine dioxide (ClO_2) and peracetic acid (PAA) for 15 min and the treated effluent was inoculated for 24 h with the ciliates *Dexiostoma campylum, Euplotes patella* and *Spirostomum teres.* The effluent treated with ClO_2 was highly toxic to *S. teres* but resulted only slightly toxic to the other two ciliate species. The effluent treated with NaClO produced a moderate toxic effect only on *E. patella.* The effluent treated with peracetic acid caused mortality only to *E. patella.* Since the poly-isosaprobic ciliate *D. campylum* - the smallest of the ciliate species tested - showed the lowest sensitivity, this can lead to the hypothesis that toxicity of the treated effluents may be related to both saprobity and size of the ciliates.

Key words: activated sludge, ciliates, disinfectants, toxicology, wastewater treatment.

INTRODUCTION

Municipal sewage usually contains a high amount of germs originated from i.e. human excreta. Although conventional treatment plants remove up to 3 log units of enteric bacteria, effluents from sewage treatment processes often contain high numbers of faecal coliforms and enterococci which makes it necessary to disinfect the final discharge.

Chlorination was the preferred method of disinfection for water and wastewater until the recognition that some natural organic substances, such as phenols, humic and fulvic acids, may act as precursors for formation of trihalomethanes (THMs) and other disinfection by-products (DBP), later suspected of being potentially toxic. As a result, the Cl-disinfection has fallen under close scrutiny and alternative methods based either on chemical or physical effects (e.g. peracetic acid, H_2O_2, UV etc.) are actively searched for (Lykins *et al.* 1986, Morris 1993, Carmineo *et al.* 1994). In particular, studies concerning the effects of DBP upon the localised flora and fauna of the receiving water are still scarce.

In this work we analysed the influence of three chemical disinfectants such as, sodium hypochlorite (NaClO), chlorine dioxide (ClO_2) and peracetic acid (PAA) - and their DBP - upon the microbiota that usually inhabit the receiving watercourse. Among freshwater protista we selected three species of Ciliophora

Address for correspondence: Paolo Madoni, Dipartimento di Scienze Ambientali, Universitŕ di Parma, viale delle Scienze, 43100 Parma, Italy; Fax: 0039-521-905402; E-mail: madoni@dsa.unipr.it

(*Dexiostoma campylum, Spirostomum teres* and *Euplotes patella*) as representative of filter-feeding organisms belonging to the detritus food-chain.

In spite of the important role played by the ciliated protozoa in the ecology of aquatic ecosystems, little is known about the lethal effects of toxicants upon these microorganisms. Only a few papers describe the lethal effects of toxic chemicals on marine (Dini 1981, Stebbinga *et al.* 1990) and freshwater ciliates (Cairns *et al.* 1980, Le Du *et al.* 1990, Fernandez-Leborans and Novillo 1996). Moreover, some investigations were concerned with tests on ciliates from activated-sludge plants (Madoni *et al.* 1992, 1994, 1996; Gracia *et al.* 1994).

MATERIALS AND METHODS

Experimental procedure

All toxicological experiments were performed using samples of final effluent from the activated-sludge plant in Roncocesi, Reggio Emilia (Italy), treating urban and industrial waste. The tests with the three disinfectants were performed on 4 different days during a period of 1 year from May 1996 to May 1997. In each test, samples of the final effluent were collected for both physico-chemical and bacteriological analyses. Then, samples were divided into 11 aliquots and treated with the relevant dose of disinfectant (NaClO, ClO_2, peracetic acid (PAA)) for 15 min under room temperature and moderate shaking. To stop any possible residual oxidizing activity sodium thiosulphate was added. A preliminary test was performed to determine the concentrations of haloforms produced during chlorination; this enabled us to choose the doses of NaClO and ClO_2 capable of reducing the number of coliforms with a low quantity of THM. The following doses of disinfectant were used on the basis of the preliminary tests: 20 mg/l NaClO, 20 mg/l ClO_2, 3 mg/l PAA. The corresponding doses of sodium thiosulphate able to stop any possible residual oxidizing activity were 42.5 mg/l, 47 mg/l and 12.3 mg/l in the tests with NaClO, ClO_2 and PAA, respectively. In each sampling event, bacteriological and physico-chemical parameters were determined following the Standard Methods (APHA 1992).

In order to study the effect of the final effluent on the microbial community inhabiting the receiving water body, the toxicological tests were performed using three common ciliate species such as *Dexiostoma campylum, Euplotes patella* and *Spirostomum teres*. In each test, it was registered the response of each species when treated with the same disinfectant (T) and then compared with results obtained treating protista with both untreated effluent + sodium thiosulphate (UT) and untreated effluent (U).

Tests with ciliates

Toxicity tests were performed using three species (*Dexiostoma campylum, Euplotes patella* and *Spirostomum teres*) that are both common in freshwater environments and suitable to be cultured in laboratory. The morphometry of the three ciliate species are showed in Table 1. For each species, individual organisms were picked from stream water samples with a micropipette, washed repeatedly in drops of sterile natural water and then put into a 60 mm diameter Petri dish for culturing. The culture medium consisted of one boiled rice grain and one boiled wheat grain in 10 ml of filtered natural water. The selected species were grown at 20 ± 1°C, oxygen saturation >45% and a photoperiod of 16 : 8 h light : dark. Only individuals from populations reaching log-phase growth were used in the experiments.

For each disinfectant and species, four tests were performed and for each of them three replicates were run. Costar® tissue culture plates with 24 wells were employed. For each replicate 12 ciliates were tested. The ciliates were picked from the culture with a micropipette, washed in natural water, and individually inoculated into each well (16 mm diameter containing 1 ml of treated effluent) (T). The same procedure was used inoculating ciliates in two sets of wells containing 1 ml of untreated effluent with (UT) and without (U) sodium thiosulphate. As a control, single ciliates were inoculated into 12 wells containing 1 ml of untreated natural water (C). Ciliates were not fed during the tests. The mortality, or survival, was checked 24 h after inoculation under a stereomicroscope at low magnification. Cells unable to swim or creep on the bottom of the well, together with disappeared cells, were regarded as dead.

RESULTS AND DISCUSSION

Physical and chemical parameters in both treated and untreated effluent samples are shown in Table 2. Production of THM - as expected - was high in the samples treated with NaClO, with a peak during test T4 in which the concentration of THM changed from 4.49 µg/l in the untreated effluent to 162 µg/l in the treated effluent. Conversely, the treatment with ClO_2 caused a slight increase of THM concentration only in two cases. In general, the reduction of both coliforms and streptococci was higher than 90% for each test with the three disinfectants.

Table 1. Morphometry of the three ciliate species used in the toxicity tests. All measurements are based on more than 20 cells

Ciliate	Order	Length (µm)	Width (µm)
Dexiostoma campylum	Hymenostomatida	38.6 ± 1.3	15.7 ± 0.9
Euplotes patella	Hypotrichida	121.6 ± 10.7	80.8 ± 6.2
Spirostomum teres	Heterotrichida	302.8 ± 12.0	35.0 ± 3.1

Table 2. Mean values of physical, chemical, and microbiological parameters measured in the activated sludge final effluent treated with the selected disinfectants. Four different tests (T1-T4) compared to untreated effluent (UT)

Parameter	NaClO					ClO_2					Peracetic acid				
	UT	T1	T2	T3	T4	UT	T1	T2	T3	T4	UT	T1	T2	T3	T4
pH	7.9	8.2	8.1	8.0	8.2	7.8	7.3	7.2	7.3	7.3	7.8	7.9	7.9	7.9	8.1
Conductivity (µS/cm)	1847	1613	1978	2593	2100	1850	2233	1615	2626	2150	2220	2220	2543	3093	2040
Water temperature (°C)	18.5	18.2	18.5	18.7	15.2	17.1	13.4	18.3	19.0	15.5	17.7	14.8	19.9	18.9	16.8
D.O. (mg/l)	5.3	5.5	5.5	5.4	7.0	5.8	6.9	5.7	5.5	6.8	6.0	7.0	5.5	7.9	8.0
$N\text{-}NH_4$ (mg/l)	0.9					<1					<1				
$N\text{-}NO_2$ (mg/l)	0.2					0.2					0.2				
$N\text{-}NO_3$ (mg/l)	7.2					7.8					9.7				
P (mg/l)	2.1					1.8					2.7				
BOD5 (mg/l)	10					10					11				
Residual disinfectant (mg/l)	-	0.4	5.0	5.4	0.2	-	0.2	2.4	0.2	0.1	-	0.5	1.7	2.5	1.9
THM (µg/l)	0.2	50.3	90.7	70.5	162	0.2	2.0	3.4	5.6	4.0	-	-	-	-	-
Total coliforms (UFC/100ml)	210,000	5	0	5	-	210,000	5	0	10	-	172,000	2,800	7,400	350	-
Total coliform abat. (%)	-	>99	100	>99	-	-	>99	100	>99	-	-	99	98	>99	-
Fecal streptococci abat. (%)	3,000	10	50	0		27,000	10	20	0		10,000	70	2,900	22	
Fecal streptococci abat. (%)	-	>99	98	100		-	>99	>99	100		-	>99	71	>99	

The toxicity tests with ciliates produced different results depending on species and disinfectant used (Fig. 1). In all experiments, no mortality was observed after 24 h in the control tests (C), and this allows us to exclude possible stress conditions in ciliate cultures. In no cases did addition of sodium thiosulphate to both treated and untreated effluent cause toxic effects. For this reason, we chose to compare the response of each species when treated with the same disinfectant (T) with results obtained treating protista with untreated effluent + sodium thiosulphate (TU).

In the samples of sewage treated with NaClO the percentage of surviving *Spirostomum teres* individuals observed after 24 h was high (> 80%). Also the small *Dexiostoma campylum,* in presence of sewage treated with NaClO, showed high rates of survival. Only in the test T3 the percentage of survival of this species was slightly lower than 80%. The ciliate *Euplotes patella* showed moderate sensitivity to the treated effluent. In fact, during test T1 and T2 mortality of these protists was 30% and 35%, respectively; however, the rate of survival was always lower than 100%.

The treatment with ClO_2 showed in all tests a remarkable toxic effect on *S. teres* with rates of mortality ranging from 55% to 100%. In one case (T2) the effect appears delayed as mortality was observed only after 48 h; probably this relates to the different characteristics of the sewage during the four tests. *D. campylum* showed in all tests a little sensitivity to the effluent treated with ClO_2. *E. patella* in three out of four tests showed a little sensitivity to this disinfectant, but in T4 test the mortality of this species was 100%.

The samples of sewage treated with PAA was no toxic for the ciliate *S. teres.* Also *D. campylum* in three out of four tests resulted to be indifferent to this disinfectant. Only in T1 test *D. campylum* showed an high mortality (72%) probably due in part to the toxicity of the sewage than of the disinfectant. The response of *E. patella* to the PAA treatment was different during the four tests. In T2 this hypotrich appeared insensible to the disinfectant while in T1 and T4 it showed an high toxic effect with mortality of 80% and 100%, respectively.

In general, the disinfected effluents produced a moderate toxic effect on ciliated protozoa populations. Nevertheless, it should be stressed that the results from each treatment differed according to the tested ciliate species. Taking into account the saprobity of each species, *D. campylum* is a poly-isosaprobic species (saprobic index SI = 3.9), *S. teres* a polysaprobic organism (SI = 3.6), and *E. patella* a b-mesosaprobic species

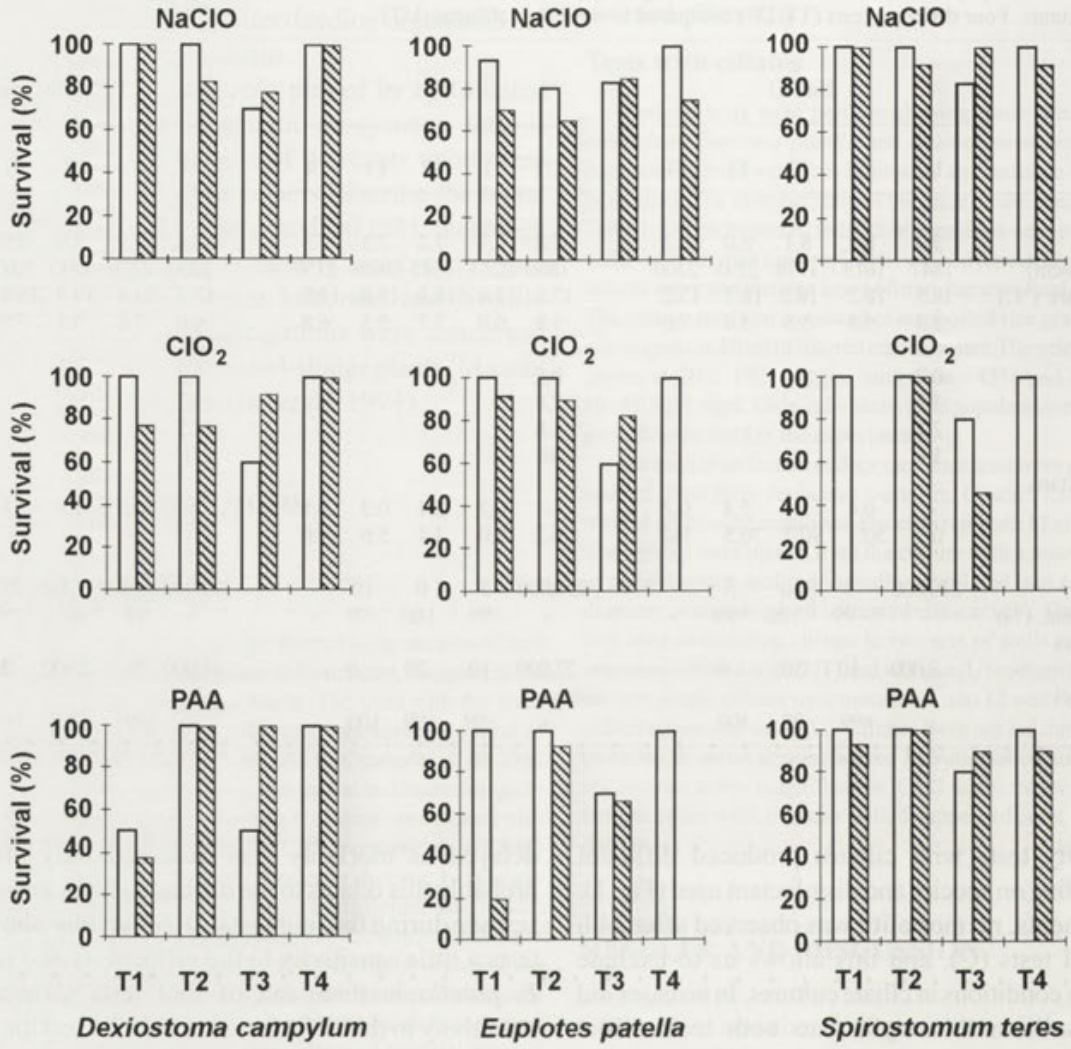

Fig. 1. The rate of survival of *Dexiostoma campylum, Euplotes patella* and *Spirostomum teres* in disinfected effluent from sewage treatment plant. Empty and dashed bars represent tests with untreated and treated effluent, respectively. Sample size - 36 ciliates

(SI = 2.3) as reported by Foissner *et al.* (1995). Polyisosaprobic ciliates can resist better than mesosaprobic or oligosaprobic ciliates to polluted waters, and this may be the reason of both the lowest sensitivity showed by *D. campylum* and the highest sensitivity showed by *E. patella.* Since *D. campylum* is the smallest among the tested ciliate species, this can lead to the hypothesis that the toxicity of the disinfected effluents may be also related to the size of cells and thus to the extent of their surface in contact with the toxicant. Moreover, the remarkable variability in the rates of survival (from 42% to 100%) observed in the tests with untreated sewage (UT), point out both the high variability in the physico-chemical characteristics of the sewage coming out from Roncocesi plant and the possibility that untreated sewage may in some cases be toxic in itself. It should be emphasized that in such a case, addition of the disinfectant buffered the toxic effect of the sewage, by producing rates of cell survival higher than in the untreated sewage.

The toxicological tests performed with the three chemicals used to disinfect the effluents from sewage treatment plants, enable us to draw the following conclusions: (i) the effluent treated with NaClO produced moderate toxic effects only on the ciliate *E. patella*; (ii) the effluent treated with ClO_2 caused toxic effects in all tested organisms but higher rates of mortality were observed only for *S. teres*; (iii) in the test with peracetic acid only *E. patella* showed an high sensitivity to this disinfectant; (iv) in

general, *E. patella* resulted to be the most sensitive ciliate in this study, whilst *D. campylum* was the less sensitive ciliate.

Acknowledgments. This research received financial support from the Italian Ministry for University and Scientific and Technologic Research (MURST 60%, P. Madoni). We thank Dr. Nadia Fontani (AGAC, Reggio Emilia) for providing advice and help with aspects of the chemistry.

REFERENCES

APHA (1992) Standard Methods for the Examination of Water and Wastewater, 18th Ed. American Public Health Association, Washington, D.C.

Cairns J. Jr., Hart K.M., Henebry M.S. (1980) The effects of a sublethal dose of copper sulfate on the colonization rate of freshwater protozoan communities. *Am. Midl. Nat.* **104:** 93-101

Carmineo D., Contini E., Di Marino R., Donadio F., Liberti L., Ranieri E. (1994) Wastewater disinfection by UV at Trani municipal plant. *Wat. Sci. Tech.* **30:** 125-132

Dini F. (1981) Relationship between breeding systems and resistance to mercury in *Euplotes crassus* (Ciliophora: Hypotrichida). *Mar. Ecol. Prog. Ser.* **41:** 195-202

Fernandez-Leborans G., Novillo A. (1996) Protozoan communities and contamination of several fluvial systems. *Wat. Envir. Res.* **68:** 311-319

Foissner W., Berger H., Blatterer H., Kohmann F. (1995) Taxonomische und ökologische revision der ciliaten des saprobiensystems. Band IV. Bayerisches Landesamt für Wasserwirtschaft, München

Gracia M.P., Salvado H., Rius M., Amigo J.M. (1994) Effects of copper on ciliate communities from activated sludge plants. *Acta Protozool.* **33:** 219-226

Le Du A., Dive D., Philippo A. (1990) Interaction between components of electroplating industry wastes. Influence of the receiving water on the toxicity of the effluent. *Envir. Pollut.* **65:** 251-267

Lykins B.W., Koffskey W.E., Miller R.G. (1986) Chemical products and toxicologic effects of disinfection. *J. Am. Wat. Wks. Ass.* **78:** 66-75

Madoni P., Davoli D., Gorbi G. (1994) Acute toxicity of lead, chromium, and other heavy metals to ciliates from activated sludge plants. *Bull. Envir. Contam. Toxicol.* **53:** 420-425

Madoni P., Esteban G., Gorbi G. (1992) Acute toxicity of cadmium, copper, mercury, and zinc to ciliates from activated sludge plants. *Bull. Envir. Contam. Toxicol.* **49:** 900-905

Madoni P., Davoli D., Gorbi G., Vescovi L. (1996) Toxic effect of heavy metals on the activated sludge protozoan community. *Wat. Res.* **30:** 135-141

Morris R. (1993) Reduction of microbial levels in sewage effluents using chlorine and peracetic acid disinfectants. *Wat. Sci. Tech.* **27:** 387-393

Stebbinga R.B., Soria S., Burt G.R., Cleary J.J. (1990) Water quality bioassays in two Bermudan harbours using the ciliate *Euplotes vannus*, in relation to tributyltin distribution. *J. Exp. Mar. Biol. Ecol.* **138:** 159-166

Received on 29th May, 1998; accepted on 27th July, 1998

Acta Protozoologica (1998) 37: 227 - 240

ACTA
PROTOZOOLOGICA

Systematic Position and Phylogenetic Relationships of the Genera *Bursaridium, Paracondylostoma, Thylakidium, Bryometopus,* and *Bursaria* (Ciliophora: Colpodea)

Wilhelm FOISSNER[1] and Martin KREUTZ[2]

[1] Universität Salzburg, Institut für Zoologie, Salzburg, Austria; [2] Private Laboratory, Constance, Germany

Summary. The morphology and infraciliature of *Paracondylostoma cavistoma oligostriatum* ssp. n. (differs from *P. cavistoma cavistoma* by non-overlapping morphometric characteristics), *P. setigerum chlorelligerum* ssp. n. (differs from *P. setigerum setigerum* by having symbiotic green algae), and *Bursaridium pseudobursaria* were studied in live and silver-impregnated specimens. *Paracondylostoma* and *Bursaridium* are sister groups due to a unique synapomorphy, namely, a circumoral ciliary ribbon produced by narrowly spaced somatic kinetids at the anterior end of the somatic kineties. *Bursaridium* differs from *Paracondylostoma* by the euplanktonic mode of life and the paroral membrane, the middle portion of which has very loosely spaced kinetids. Based on the morphological details discovered, a Hennigian phylogeny of the genera *Bursaridium*, *Paracondylostoma*, *Thylakidium*, *Bryometopus*, and *Bursaria* is proposed. These genera are linked by four synapomorphies, namely: (1) an apical oral opening secondarily lost in *Bryometopus*, which ventralized the oral apparatus; (2) a ventral vestibular cleft occupied by the ventralized oral structures in *Bryometopus*; (3) a conspicuous adoral zone of adoral organelles; and (4) a simple paroral membrane composed of a row of dikinetids secondarily amplified to a conspicuous field of short, dikinetidal kineties in *Bursaria*, which is thus derived.

Key words: Colpodea, Hennigian phylogeny, infraciliature, *Paracondylostoma cavistoma oligostriatum* ssp. n., *Paracondylostoma setigerum chlorelligerum* ssp. n.

INTRODUCTION

Colpodid ciliates have a fascinating morphological and ecological diversity, reviewed by Foissner (1993a). For instance, *Bursaria truncatella*, one of the largest (up to 1300 µm) ciliates known, is an omnivore living in astatic and permanent freshwater habitats, while *Nivaliella plana*, one of the smallest (10 - 25 µm) ciliates known, is a strict mycophage living exclusively in terrestrial biotopes. The phylogenetic relationships of the 60 genera and about 180 species presently assigned to the class (Foissner 1993a-c, 1994a, b, 1995) have been investigated with both classical morphological and modern molecular methods (Foissner 1993a, Lynn *et al.* 1998, Stechmann *et al.* 1998).

Lynn *et al.* (1998) used the small subunit rRNA gene sequences to test the Hennigian phylogeny of the colpodids suggested by Foissner (1993a), which makes three important predictions, namely: (1) that the kreyellid silverline

Address for correspondence: Wilhelm Foissner, Universität Salzburg, Institut für Zoologie, Hellbrunnerstrasse 34, A-5020 Salzburg, Austria; Fax: +43 (0) 662 8044-5698

system separates bryometopids, such as *Bryometopus*, from all other colpodeans; (2) that the macro-micronuclear complex of cyrtolophosids, such as *Platyophrya*, is the next major synapomorphy; and (3) that the merotelokinetal stomatogenesis of colpodids *s. str.*, such as *Colpoda*, *Bresslaua*, and *Pseudoplatyophrya* is highly derived. The molecular tree topologies confirmed the two last mentioned synapomorphies, while the silverline system failed.

In the present paper, we analyze the morphology and evolution of a small group of colpodids having an apical vestibular opening with a more or less distinct ventral cleft. The investigation was stimulated by the rediscovery of *Paracondylostoma*, a rare genus, not found again since the original description by Foissner (1980).

MATERIALS, METHODS AND TERMINOLOGY

Paracondylostoma cavistoma oligostriatum was discovered in the bottom material of a dry rock-pool near Puerto Ayacucho, Venezuela. *Paracondylostoma setigerum chlorelligerum* was found in the mud of a moorland pond near Constance, Germany. For site details, see ecology and occurrence section in species descriptions. *Bursaridium pseudobursaria* occurred in the plankton of a small lake (Högelwörther See, N47°49'/E12°50') in southern Bavaria.

Specimens were studied *in vivo* using a high-power oil immersion objective and differential interference contrast. The ciliary pattern (infraciliature) and other cytological details were revealed by scanning electron microscopy and various silver impregnation techniques, preferably silver carbonate, all described in Foissner (1991); protargol does not work well with this group of ciliates.

Counts and measurements on silvered specimens were performed at a magnification of x 1,000. Although these provide only rough estimates, it is worth giving such data as specimens usually shrink in preparations and contract during fixation. Illustrations of live specimens were based on free-hand sketches and micrographs, those of impregnated cells were made with a camera lucida. All figures are oriented with the anterior end of the organism directed to the top of the page. Terminology is according to Foissner (1993a).

RESULTS

Paracondylostoma cavistoma oligostriatum ssp. n. (Figs. 1-17; Table 1)

Diagnosis: *in vivo* about 35 x 20 µm. 20 ciliary rows and 11 adoral organelles on average.

Type location: soil and sediment from rock-pools on a Laja near the farm of Mr. Eisenberg, vicinity of Puerto Ayacucho (W68°/N5°), Venezuela.

Type slides: two slides (1 holotype and 1 paratype) with protargol-impregnated specimens have been deposited in the Oberösterreichische Landesmuseum in Linz (LI), Austria, accession numbers: 1998/45, 46. The slides contain several specimens, with relevant cells marked by a black ink circle on the cover glass. *Paracondylostoma cavistoma oligostriatum* is difficult to impregnate with protargol and thus the type slides are of mediocre quality. Accordingly, we declare Figures 12-17 in the present paper as additional holotype material.

Etymology: composite of the Greek adjective *oligos* (few) and the Latin noun *striatus* (striae), meaning a *Paracondylostoma* with few ciliary rows.

Description: very fragile and thus difficult to observe *in vivo*, usually disintegrates when taken up with fine pipettes and/or observed under slight coverglass pressure. Size *in vivo* 25-40 x 18-25 µm, usually about 35 x 20 µm. Broadly ellipsoidal (1.5:1, Fig. 1), ellipsoidal (2:1, Fig. 3) or slightly conical (Fig. 2); anterior end slightly to distinctly broader than evenly rounded posterior, transverse truncate with dorsal side slightly longer than ventral, thus oblique when viewed laterally (Figs. 4, 10). Macronucleus usually in posterior body half, broadly ellipsoidal, contains many minute (about 0.3 µm) nucleoli. Two to three globular micronuclei (1.2 - 2µm, x 1.7, n 13, protargol impregnation) attached to macronucleus, impregnate only faintly with protargol (Figs. 1, 8, 10, 15, 17). Contractile vacuole subterminal on ventral side. Cortex flexible and very fragile (see above), rather distinctly furrowed by ciliary rows, contains a stripe of minute (about 0.2 µm), colourless granules (mucocysts ?) between each two ciliary rows (Figs. 5, 6). Cytoplasm colourless, contains some bright fat globules and food vacuoles 4 - 8µm across with bacteria and granular material, very likely bacterial remnants. Swims rather fast by rotation about main body axis.

Somatic cilia about 8 µm long and rather evenly spaced, except for anterior end, where each row commences with three narrowly spaced cilia, forming rather distinct ribbon in live specimens. Ciliary rows distinctly separate from paroral membrane, equidistant and very slightly spiral, composed of dikinetids having only the posterior basal body ciliated (Figs. 1, 7-9, 12-17).

Oral (vestibular) opening on anterior end of cell, margin opaque and slightly indented in midline of ventral side by minute vestibular cleft. Vestibulum fragile, occupies circa 35% of body length, oblique conical, that is, straight ventrally and obliquely extending dorsally. Adoral zone of organelles (left polykinetid) on left wall of vestibulum, inconspicuous because short, narrow and oriented with the smaller side to the observer when the cell is viewed ventrally or dorsally (Figs. 1, 8, 13). Individual organelles

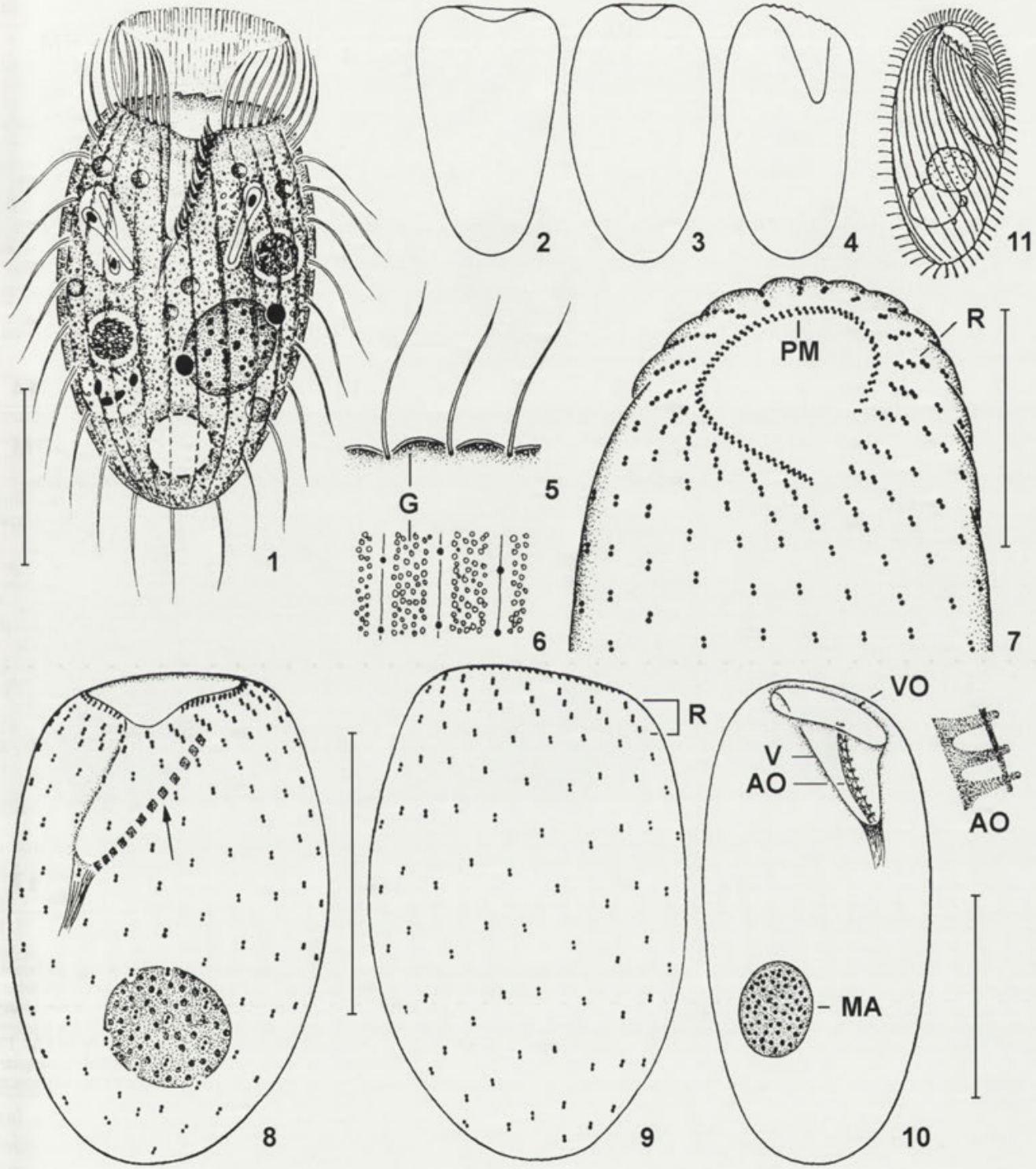

Figs. 1-11. *Paracondylostoma cavistoma oligostriatum* (1 - 10) and *P. cavistoma cavistoma* (11, from Gelei 1954) from life (1 - 6, 11) and after protargol impregnation (7 - 10). 1 - ventral view of a representative specimen containing sporulating bacteria; 2, 3 - funnel-shaped and obovate shape variants; 4 - ventrolateral view; 5, 6 - optical section and surface view of cortex, which contains stripes of minute granules; 7 - infraciliature of anterior ventral side; 8, 9 - infraciliature of ventral and dorsal side. Arrow marks zone of adoral organelles; 10 - lateral view showing location of main cell organelles, 11 - *P. cavistoma cavistoma*. Ventro-lateral view of a mercuric chlorid fixed specimen, length 60 µm. AO - adoral organelles, MA - macronucleus, PM - paroral membrane, R - ribbon of three narrowly spaced dikinetids, V - vestibulum, VO - vestibular opening. Scale bars - 15 µm (Figs. 1, 8-10) and 10 µm (Fig. 7)

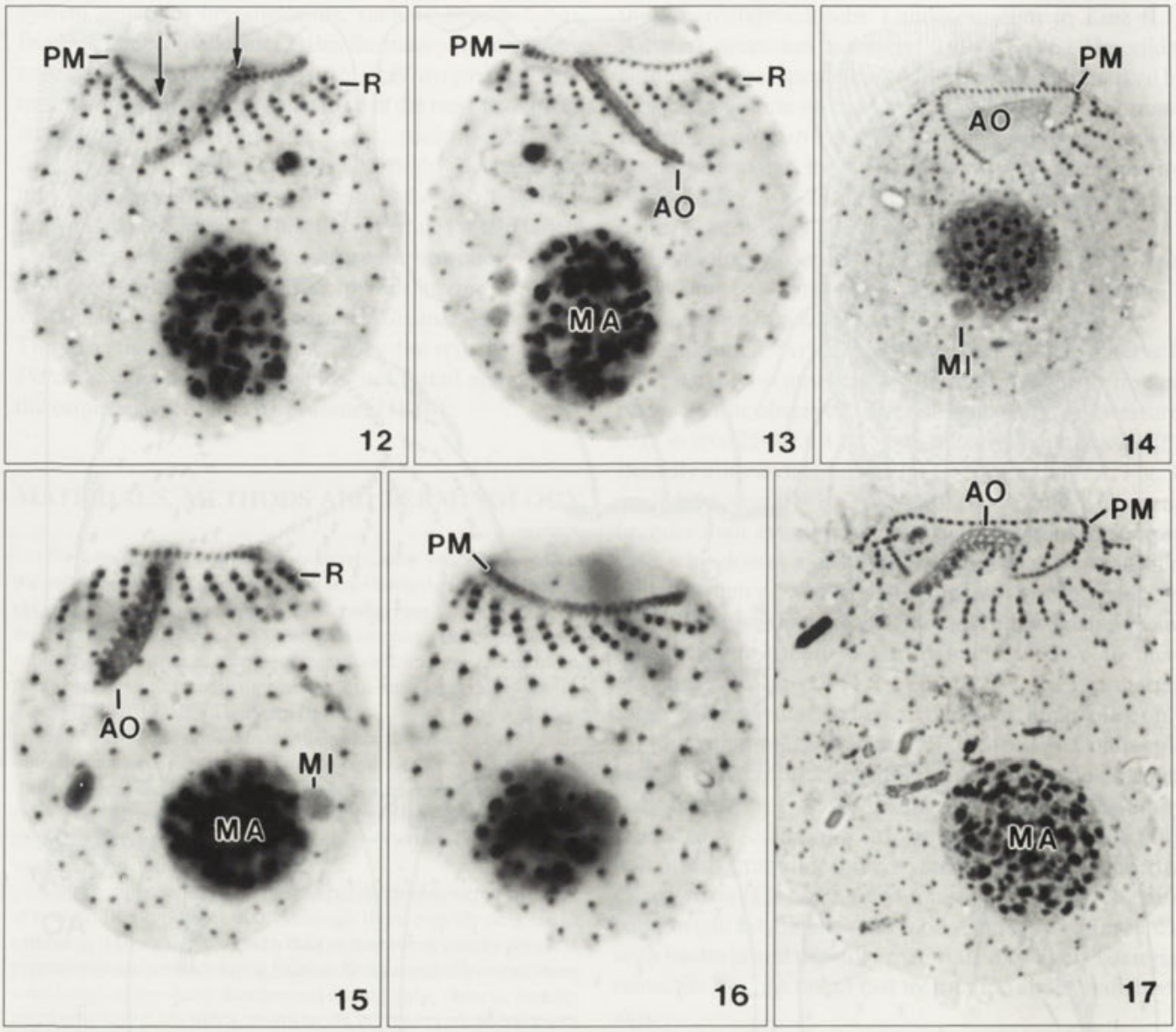

Figs. 12-17. *Paracondylostoma cavistoma oligostriatum*, oral and somatic infraciliature and nuclear apparatus after silver carbonate impregnation. To reveal details, specimens were strongly flattened by the cover glass. 12, 13 - ventral and dorsal view of same specimen, where the adoral zone of organelles is directed toward the observer with the smaller side and thus appears as narrow band (cp. Fig. 15, 17). Arrows mark ends of paroral membrane. Note the distinct ciliary ribbon formed by three narrowly spaced dikinetids each at the anterior end of the somatic kineties; 14, 17 - oblique ventral anterior polar views. Twelve adoral organelles, which form a reticulate structure, are recognizable in Fig. 17; 15, 16 - dorsolateral view of same specimen, where the adoral zone of organelles is directed toward the observer with the wider side and thus appears as broad band. AO - adoral zone of organelles, MA - macronucleus, MI - micronucleus, PM - paroral membrane, R - ribbon of three narrowly spaced dikinetids

slightly cuneate, touch each other proximally, connected by fine line distally, forming reticulate pattern (Figs. 10, 15, 17). Paroral membrane encircles anterior body end, except for ventral cleft, where about 10 dikinetids are lacking; consists of dikinetids, whose cilia form, together with the ciliary ribbon produced by the narrowly spaced cilia at the anterior end of the somatic kineties, a conspicuous corona (Figs. 1, 7, 12 - 17).

Ecology and occurrence: as yet found only at type location, that is, a large granitic rock (Laja) with many dry pools containing up to 5 cm thick layers of greybrown, sandy soil and sediment with many roots from plants of

Table 1. Morphometric data from *Paracondylostoma cavistoma oligostriatum* (PC) and *P. setigerum chlorelligerum* (PS)

Character*	Species	Method**	$\bar{x}$	M	SD	SE	CV	Min	Max	n
Body, length	PC	P	29.0	28	4.2	1.2	14.5	20	36	13
	PS	V	74.2	73	6.2	1.4	8.4	65	88	21
Body, maximum width	PC	P	17.5	17	1.3	0.4	7.2	16	20	13
	PS	V	31.8	30	3.6	0.8	11.3	28	43	21
Anterior end to proximal end of adoral zone, distance	PC	P	10.0	10	1.9	0.5	18.7	6	13	13
	PS	V	35.8	36	3.8	0.8	10.6	28	42	21
Anterior end to macronucleus, distance	PC	P	16.2	16	3.1	0.9	19.1	10	22	13
	PS	V	39.5	40	6.5	1.4	16.5	25	50	21
Anterior end to contractile vacuole, distance	PS	V	51.6	52	7.7	1.7	14.9	35	73	21
Macronucleus, length	PC	P	7.5	8	1.5	0.4	19.3	5	10	13
	PS	V	13.3	13	1.1	0.2	8.3	11	15	21
Macronucleus, width	PC	P	6.5	6	1.1	0.3	16.2	5	8	13
	PS	V	11.2	10	1.8	0.4	16.1	9	15	21
Normal somatic cilia, length	PS	V	5.1	5	-	-	-	5	6	21
Tactile cilia, length	PS	V	19.9	20	2.7	0.6	13.6	15	25	20
Symbiotic algae, length	PS	V	5.1	5	-	-	-	5	6	21
Symbiotic algae, width	PS	V	4.1	4	-	-	-	4	5	21
Symbiotic algae, number	PS	V	31.3	29	12.6	2.7	40.3	18	64	21
Macronuclei, number	PC	P	1.0	1	0.0	0.0	0.0	1	1	13
	PS	V	1.0	1	0.0	0.0	0.0	1	1	21
Micronuclei, number	PS	V	2.3	3	-	-	-	1	3	21
Somatic kineties, number	PC	P	19.5	20	0.8	0.2	4.0	18	21	13
	PS	SC	46.7	47	1.7	0.6	3.6	45	49	7
Dikinetids in a somatic kinety, number	PC	P	12.8	12	1.5	0.4	11.6	11	17	13
	PS	SC	34.7	35	2.6	1.0	7.9	33	38	7
Adoral organelles, number	PC	P	11.5	11	0.9	0.3	7.9	10	13	13

* CV - coefficient of variation in %, M - median, Max - maximum, Min - minimum, n - number of individuals investigated, SD - standard deviation, SE - standard error of mean, $\bar{x}$ - arithmetic mean

** P - protargol impregnation (Foissner's protocol), mounted specimens; SC - silver carbonate impregnation; V - *in vivo*

the endemic Velloziaceae family. The rock-pools were dry and the bottom partially covered by minute mosses when the sample was taken. In the Petri dish, most specimens of *P. cavistoma oligostriatum* were found in a mossy patch, indicating that it prefers this habitat.

Comparison with related species: *Paracondylostoma cavistoma oligostriatum* is very likely closely related to *Cyrtolophosis cavistoma*, discovered by Gelei (1954) in a temporary pool in Hungary (Fig. 11). Gelei (1954) mentioned that he did not study the species, especially its oral structures, in detail. Our investigations confirm Foissner (1993a), who transferred Gelei's species to *Paracondylostoma*.

Gelei's species (Fig. 11) and the Venezuelan population (Figs. 1, 8, 9) differ mainly in some morphometric characteristics: size about 60x30 µm vs. about 35x20 µm, 30-34 distinctly spiral ciliary rows vs. 18-21 almost straight rows. Thus, we separate the Venezuelan population only at subspecies level. A more distinct character would be the dwelling tube *P. cavistoma cavistoma* inhabitats. However, we cannot exclude that *P. cavistoma oligostriatum* also produces a dwelling tube, although we did not find any, because it was rare and fragile and thus could not be studied in great detail.

Paracondylostoma setigerum setigerum and *P. setigerum chlorelligerum* have a length of 65-90 µm, 45-50 ciliary rows, and 30-40 adoral organelles, whereas *P. cavistoma oligostriatum* is 25-40 µm long and has 18-21 ciliary rows and 10-13 adoral organelles. These differences are large enough to classify both types as distinct species.

***Paracondylostoma setigerum chlorelligerum* ssp. n. (Figs. 18-30; Table 1)**

Diagnosis: as *P. setigerum setigerum* Foissner, 1980, but with symbiotic green algae.

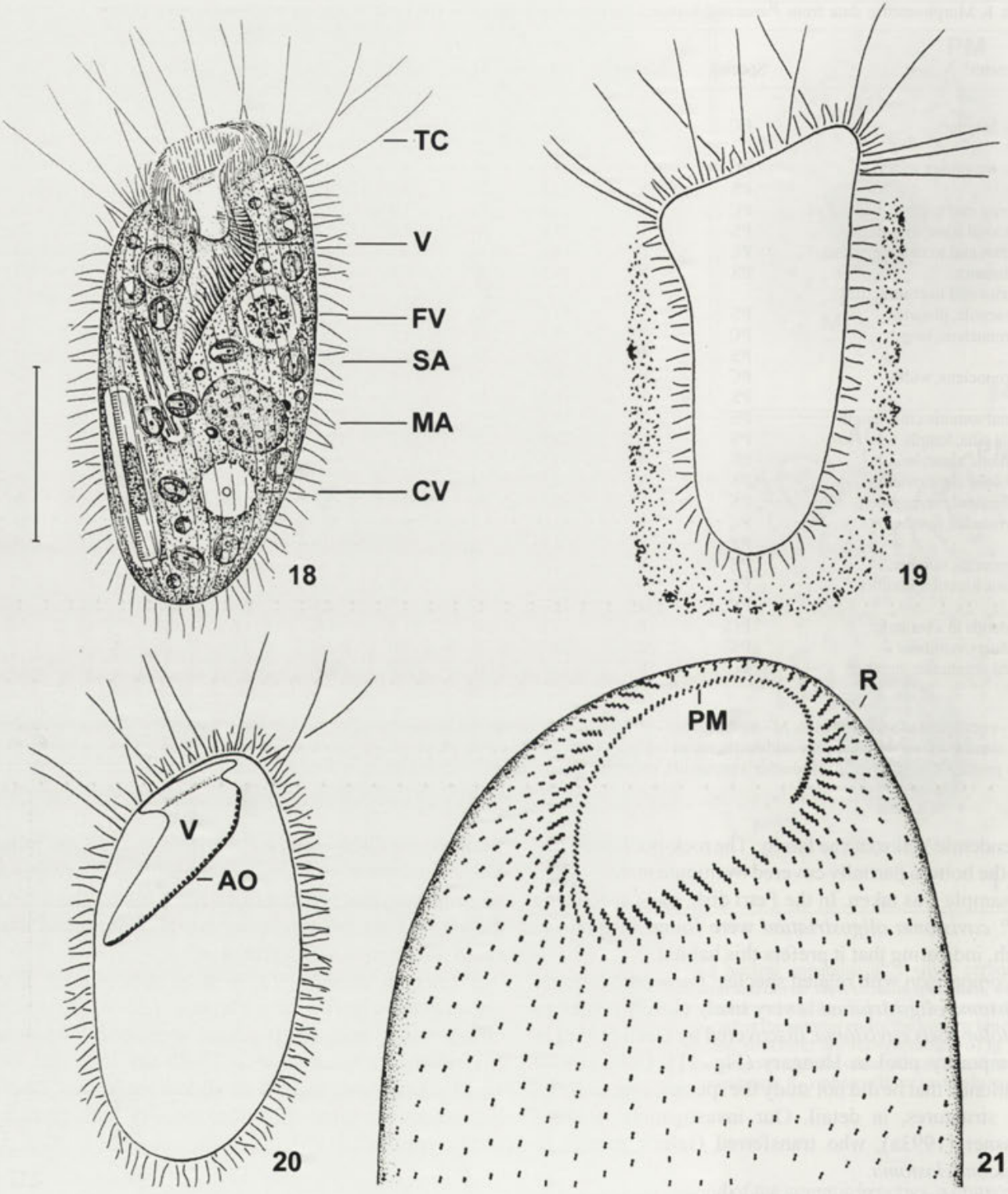

Figs. 18 - 21. *Paracondylostoma setigerum chlorelligerum* from life (18 - 20) and after silver carbonate impregnation (21). 18, 20 - ventral and lateral view of representative specimens with slightly contracted vestibular opening; 19 - specimen with fully extended anterior portion and very hyaline dwelling tube (cp. Fig. 24); 21 - infraciliature of ventral anterior portion (redrawn from squashed specimen). AO - adoral zone of organelles, CV - contractile vacuole, FV - food vacuole, MA - macronucleus, PM - paroral membrane, R - ribbon of narrowly spaced dikinetids, SA - symbiotic algae; TC - tactile cilia, V - vestibulum. Scale bar - 30 µm

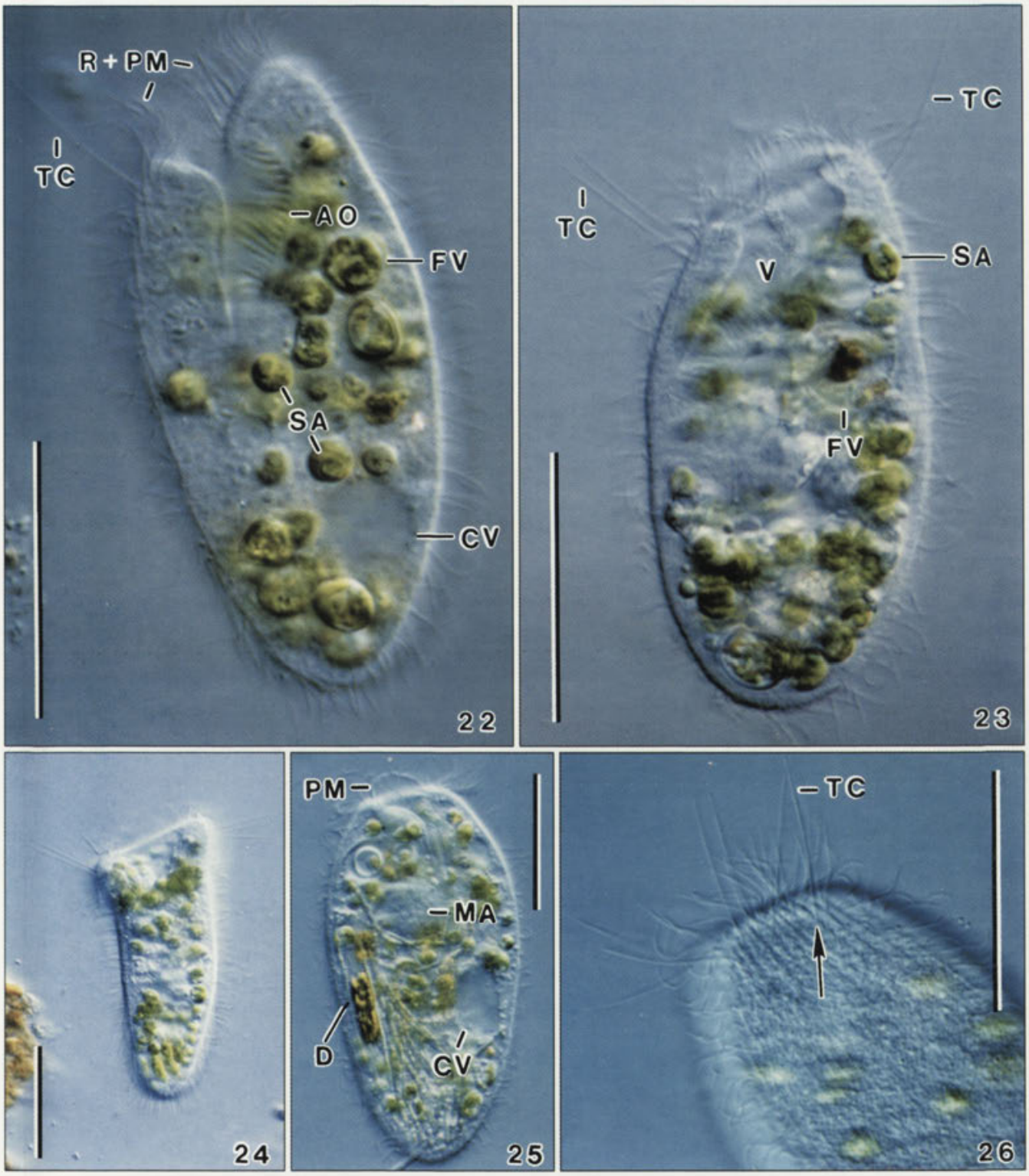

Figs. 22 - 26. *Paracondylostoma setigerum chlorelligerum*, electronic flash micrographs of live specimens. 22, 23 - ventral and lateral view of specimens with slightly contracted anterior end; 24 - fully extended specimen within very hyaline, mucous dwelling tube; 25 - specimen packed with food items and distinct paroral membrane (kindly supplied by P. Mayer, Germany); 26 - dorsal anterior end showing tactile cilia (arrow) originating at the posterior border of the ciliary ribbon surrounding the oral opening. AO - adoral zone of organelles, CV - contractile vacuole, D - diatom, FV - food vacuoles, MA - macronucleus, R + PM - cilia of somatic ribbon and paroral membrane, SA - symbiotic algae, TC - tactile cilia, V - vestibulum. Scale bars - 30 μm

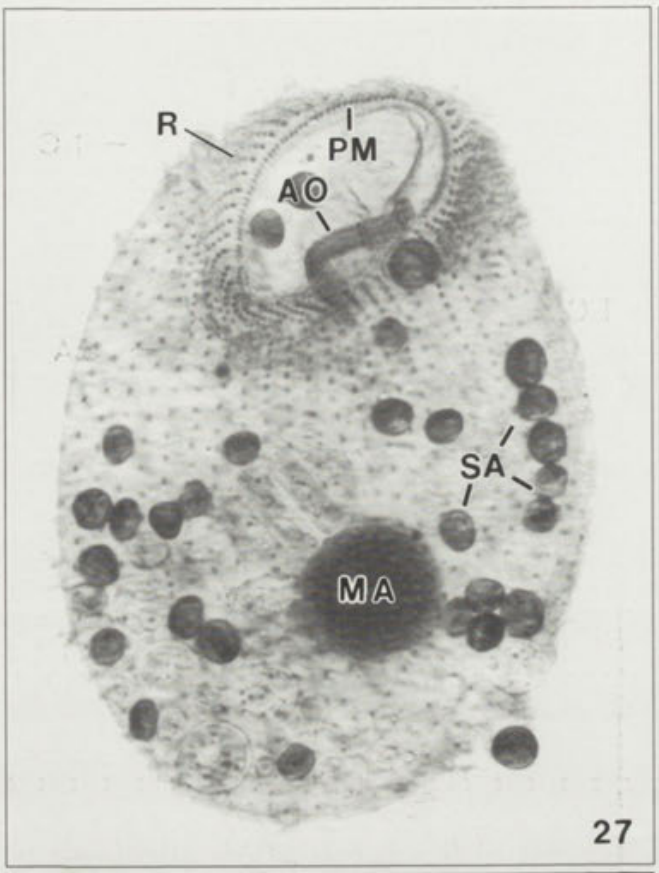

27

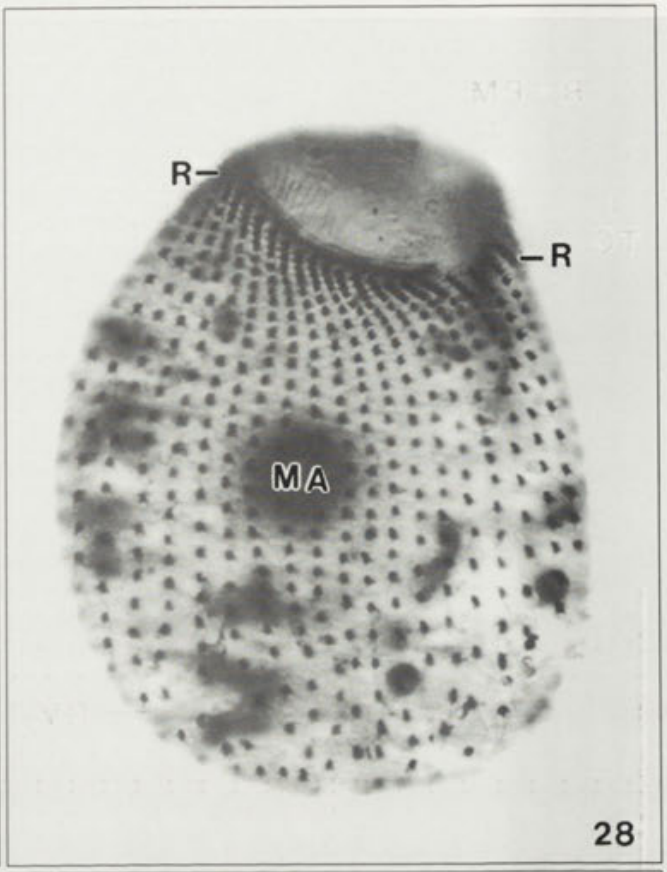

28

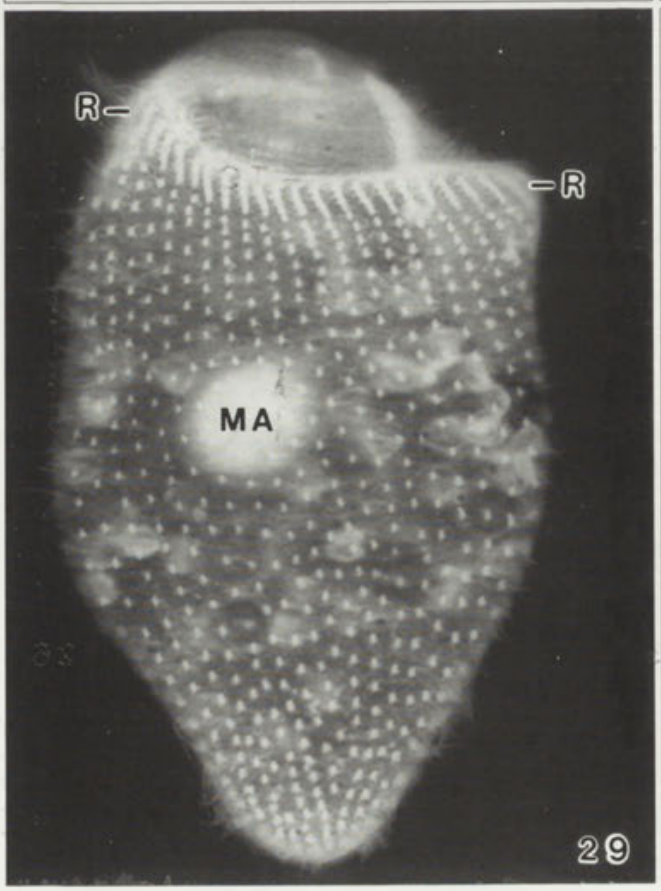

29

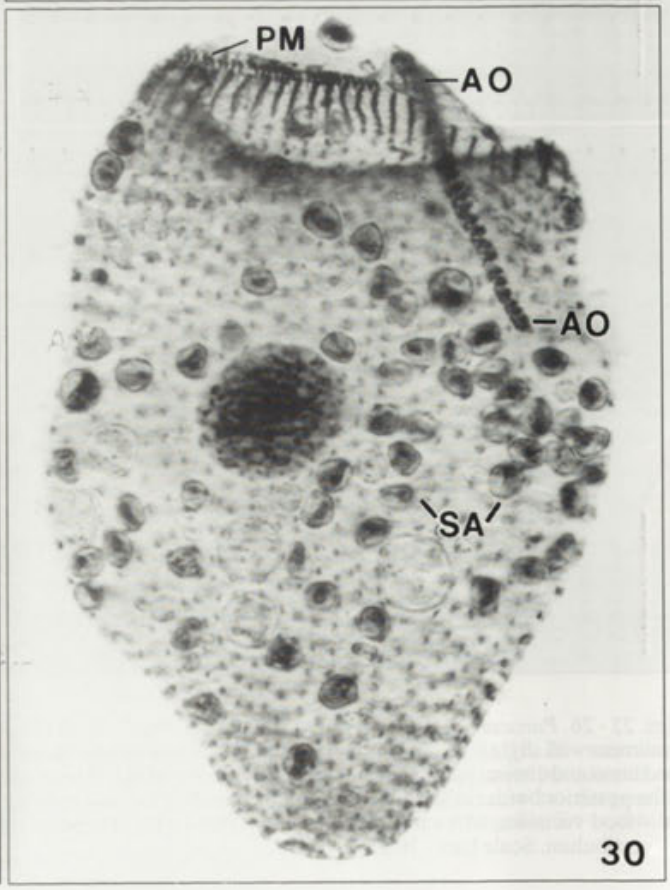

30

Type location: pond mud near Hegne, a suburb of Constance, Germany (E9°10'/ N47°40').

Type slides: no permanent slides were made. Thus, the figures in this paper must serve as type material.

Etymology: *chlorelligerum* (bearing chlorellae) refers to the main subspecies character, that is, the symbiotic green algae.

Description: size *in vivo* 65 - 88 x 28 - 43 µm, on average 73 x 30 µm (Table 1). On slides usually elongate ellipsoidal to slightly conical (Figs. 18, 20, 22, 23, 25), natural shape, however, like that shown in Figs. 19 and 24, that is, cylindroidal with distinctly broadened anterior region, which can be contracted, providing cells with obconical appearance; anterior end obliquely truncate to right and ventral side, posterior rounded. Macronucleus slightly underneath mid-body on average, globular to slightly ellipsoidal, contains many minute (< 1 µm) nucleoli; 1 - 3, usually 3, micronuclei attached to macronucleus (Figs. 18, 25, 29, 30; Table 1). Contractile vacuole in fourth fifth of body, with single excretory pore in midline of ventral side (Figs. 18, 22, 25). Cortex flexible, rather distinctly furrowed by ciliary rows, contains many tightly spaced, minute (< 0.5 µm), colourless granules (mucocysts? Fig. 26). Cytoplasm colourless, cells, however, appear greenish due to 18 - 64, on average 29 (Table 1), symbiotic algae (Fig. 24); symbionts irregularly distributed, about 5 x 4 µm, with cup-shaped chloroplast and without eyespot (Figs. 18, 22, 23, 27, 30). Feeds on bacteria and algae (globular green algae, Scenedesmus, diatoms; Figs. 18, 22, 23, 25).

Paracondylostoma setigerum chlorelligerum lives in a mucous dwelling tube, which is very hyaline and thus difficult to recognize when not covered by organic particles (Fig. 24). The dwelling tube is left when the cell is transferred from the natural sample to the slide, and rebuilt within 12 h. When the cell is slightly disturbed and/or the elongated (tactile) cilia (see below) touch certain objects, it draws back into the tube, soon extending and assuming the obconical shape typical of the sessile, swirling organism (Fig. 24).

Normal somatic cilia *in vivo ca* 5 µm long and rather evenly spaced, except of anterior end, where each row commences with 4-8 narrowly spaced cilia, forming distinct ribbon. About 20-30 distinctly elongated (20 µm, Table 1) tactile cilia around anterior end, very likely originate from first and/or second dikinetid underneath circumoral ribbon (Figs. 18 - 20, 22 - 24, 26). Ciliary rows distinctly separate from paroral membrane, equidistant and rather distinctly spiralling, composed of dikinetids with, probably, only the posterior basal body ciliated (Figs. 18, 21, 22, 27-30).

Oral apparatus more conspicuous, but of same fine structure, than in *P. cavistoma oligostriatum* because occupying almost 50% of body length. Adoral zone composed of about 30-35 organelles. Paroral widely open ventrally, that is, surrounds vestibular opening by about 300° (Figs. 18, 20-23, 27-30).

Ecology and occurrence: as yet found only at type location, that is, a small (about 5 x 3 m, max. depth 1 m), acidic (pH 5.5- 6.0) brownwater pond at the grassy margin of a 100 m broad *Sphagnum* stripe with dwarfed pines (*Pinus* sp.). The pond surface was covered with water lilies (*Nymphaea* sp.), while on the bottom was a thick layer of mud, the upper zone of which contained a rich and diverse community of bacteria, algae, and protozoans, including *P. setigerum chlorelligerum*.

Comparison with related species: *P. setigerum chlorelligerum* is very similar, if not identical, to *P. setigerum setigerum* Foissner, 1980, except for the symbiotic algae, whose taxonomical value is controversial (for detailed discussion, see Foissner & Wölfl 1994). We find it appropriate to separate such populations at subspecies level, considering the distinctiveness of the character and the physiological and ecological differences they show.

Bursaridium pseudobursaria (Fauré-Fremiet, 1924) Kahl, 1927 (Figs. 31-37)

This species has been reinvestigated by Foissner (1993a) and is well-known, except for the paroral membrane, whose identity remained doubtful. Our investigations show that its location (close above the circumoral ribbon formed by the anterior end of the somatic kineties) and structure (single row of dikinetids) are very similar to that

Figs. 27 - 30. *Paracondylostoma setigerum chlorelligerum*, somatic and oral infraciliature after silver carbonate impregnation. Specimens were strongly squashed to reveal as many details as possible in the same focal plane. 27 - ventral view; 28 - lateral view; 29, 30 - lateral view of same specimen focused to surface and body centre. AO - adoral zone of organelles, MA - macronucleus, PM - paroral membrane, R - ciliary ribbon at anterior end of somatic kineties, SA - symbiotic algae

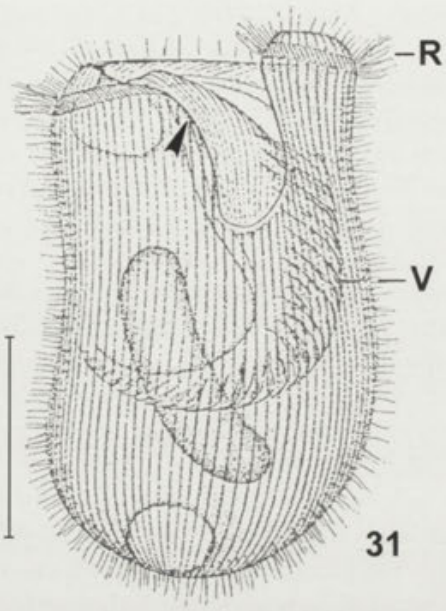

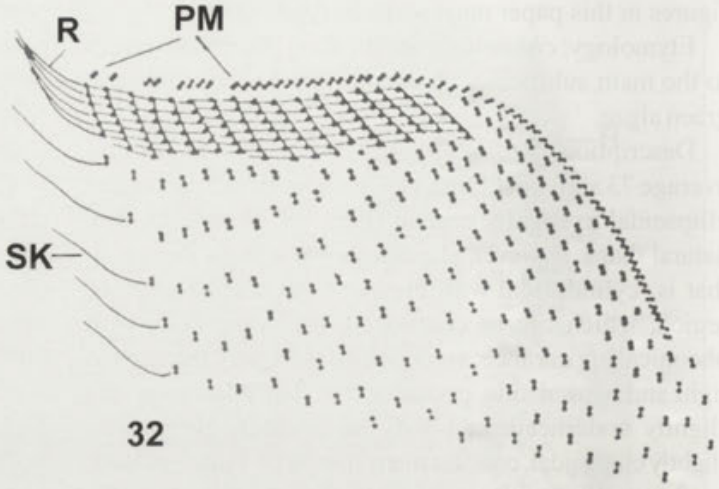

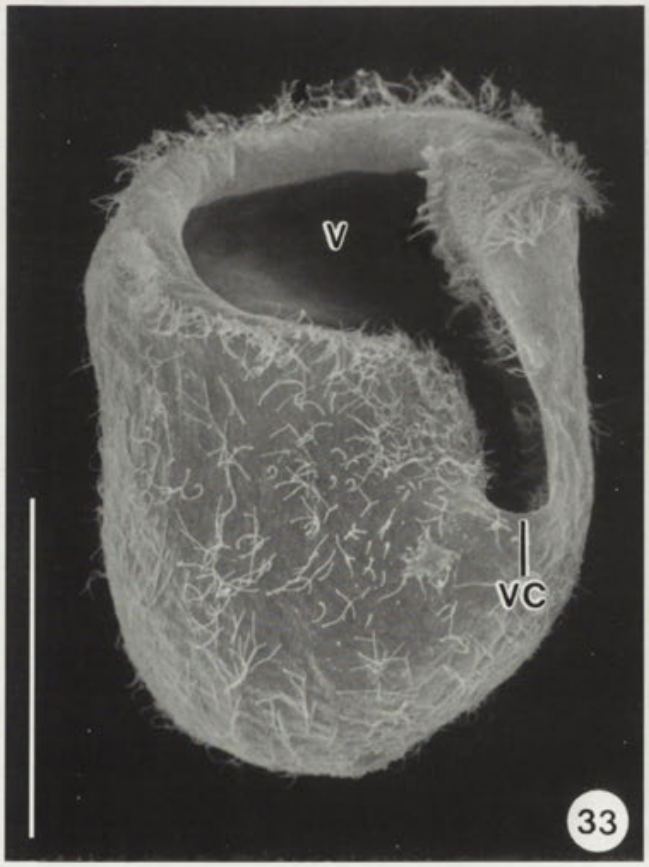

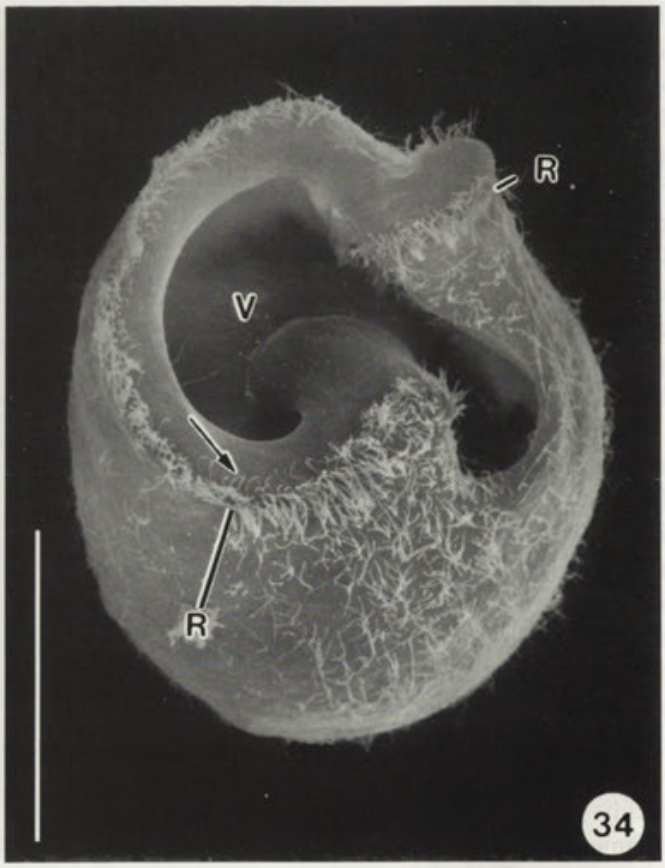

Figs. 31 - 34. *Bursaridium pseudobursaria* from life (31, from Fauré-Fremiet 1924), after silver carbonate impregnation (32, from Foissner 1993a), and in the scanning electron microscope (33, 34). 31 - ventral view of representative specimen, with arrowhead marking area shown in Fig. 32 after silver impregnation; 32 - infraciliature of outer surface of right vestibular wall, marked by arrowhead in Fig. 31; 33, 34 - ventrolateral and oblique frontal view showing general organization and huge vestibulum, which has a distinct ventral cleft. Arrow marks loosely ciliated paroral, shown at higher magnification in Fig. 37. PM - paroral membrane, R - circumoral ciliary ribbon formed by the anterior end of the somatic kineties, SK - somatic kineties, V - vestibulum, VC - vestibular cleft. Scale bars - 50 μm

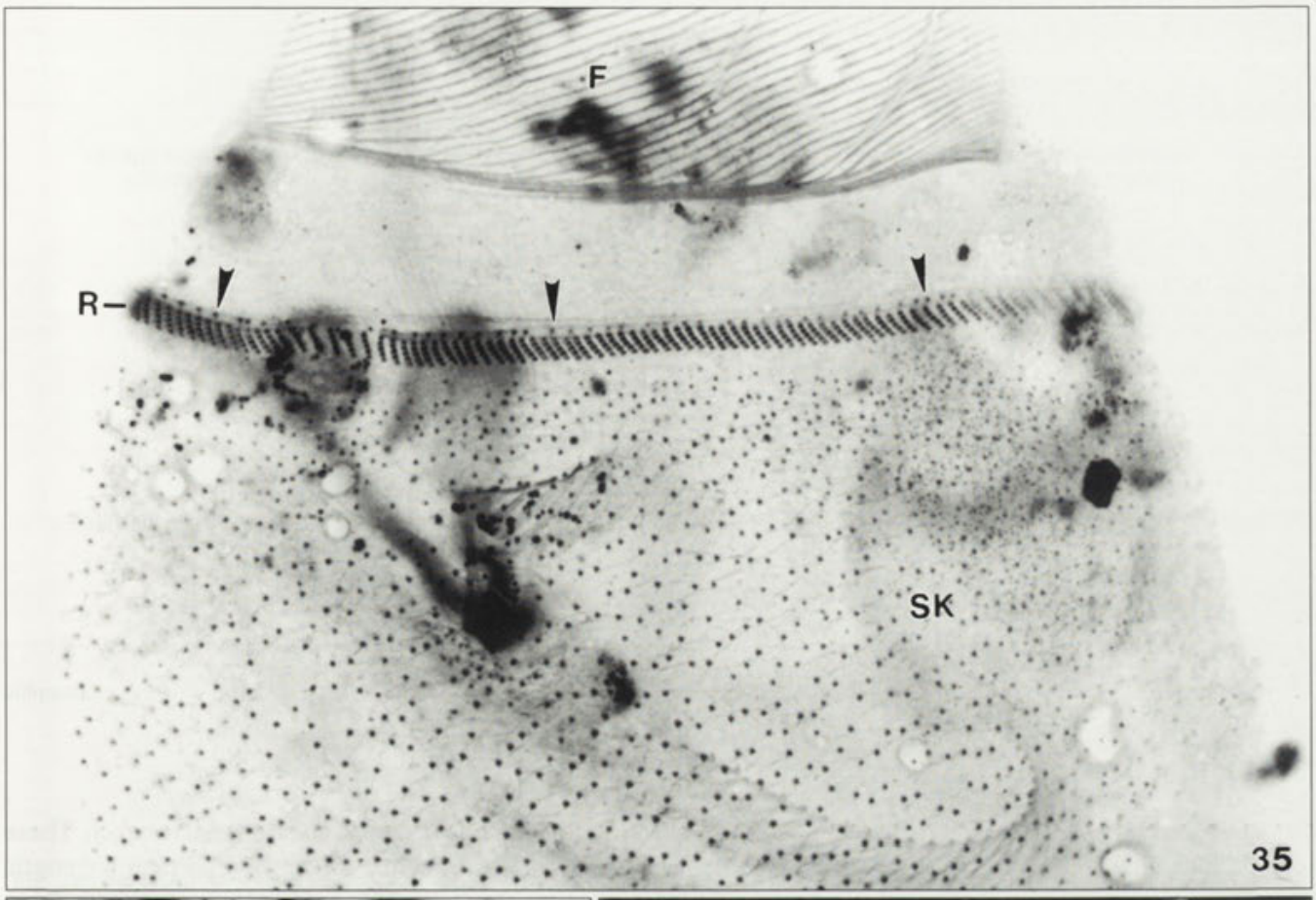

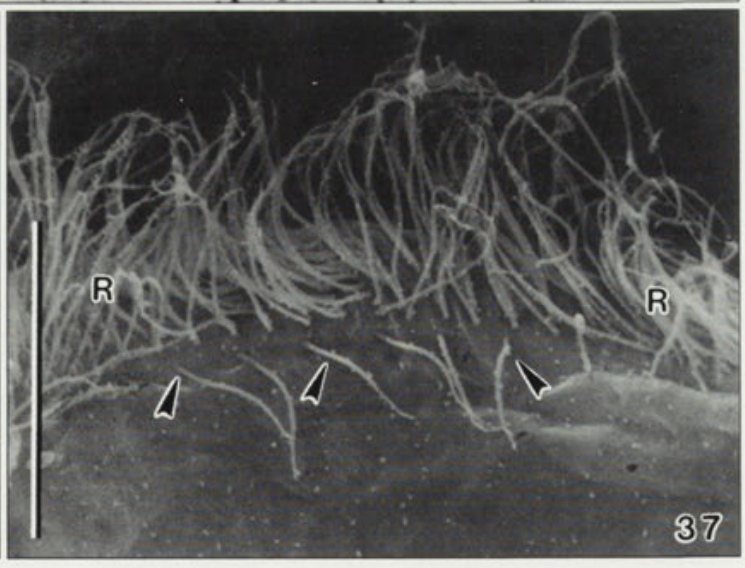

Figs. 35 - 37. *Bursaridium pseudobursaria*, somatic and oral infraciliature after silver carbonate impregnation (35, 36) and in the scanning electron microscope (37). The silver carbonate impregnated specimens were strongly squashed to reveal as many details as possible in the same focal plane. 35, 37 - anterior dorsal portion showing fibres lining the vestibular wall and the paroral membrane (arrowheads), which is composed of very loosely spaced kinetids, close above the conspicuous circumoral ciliary ribbon, which is distinctly separate from the somatic kineties; 36 - left end of paroral membrane (arrowheads) and circumoral ciliary ribbon. F - fibres, R - ciliary ribbon at anterior end of somatic kineties, SK - somatic kineties. Scalle bar - 10 μm

Table 2. State for the characters shown in Figure 38. See Foissner (1993a) for detailed explanation of characters.

No.	Apomorphic ●	Plesiomorphic ○
1	micronucleus in perinuclear space of macronucleus	macronucleus and micronucleus separate
2	conspicuous zone of adoral organelles	small, brick-shaped adoral organelles
3	ventral cleft	without ventral cleft
4	apical oral opening	ventral oral opening
5	paroral composed of many dikinetidal rows	paroral a single row of dikinetids
6	with conjugation (sex)	without sex
7	resting cyst with emergence pore	resting cyst without emergence pore
8	vestibulum obconical or cornute and curved to right. Adoral organelles each composed of two long rows and one short row of basal bodies in zigzag pattern*	vestibulum cornute and curved to left. Adoral organelles each composed of three rows of same length with basal bodies not in zigzag pattern*
9	LKM fibre reduced (V-shaped pattern)	LKM fibre typical
10	supraepiplasmic microtubules	no supraepiplasmic microtubules
11	circumoral somatic ciliary ribbon	without ciliary ribbon
12	loss of ventral cleft and ventralization of oral apparatus	with ventral cleft and apical oral opening
13	paroral within vestibulum	paroral at margin of oral opening
14	vestibulum obconical	vestibulum cornute
15	paroral kinetids loosen	paroral kinetids evenly spaced
16	euplanktonic	benthic, semi-sessile

* For details, see Foissner (1993a), Perez-Paniagua *et al.* (1980), and Wirnsberger *et al.* (1985). Generally, the adoral ciliature of bursariomorphid and bryometopid ciliates is insufficiently known.

of *Paracondylostoma*. The sole difference is that the paroral dikinetids, which have only one basal body ciliated (Fig. 37), are more loosely spaced laterally and dorsally than ventrally (Figs. 32, 35, 36).

DISCUSSION

Recent molecular data showed that *Bursaria* and *Bryometopus* are rather closely related (Lynn *et al.* 1998), that is, did not confirm Foissner (1993a), who assigned *Bursaria*/*Bursaridium*/*Paracondylostoma* and *Bryometopus*/*Thylakidium* to different subclasses, viz. the Colpodia and Bryometopia. Foissner (1993a) over-interpreted details of the silverline system and somatic cortical microtubular pattern; furthermore, the detailed structure of the oral apparatus was not known in *Bursaridium* and *Paracondylostoma*.

The present investigation shows some new aspects, which will be discussed in the following paragraphs using a Hennigian scheme of argumentation (Fig. 38; Table 2). We shall demonstrate that the relationships of the genera in question are now fairly clear. The scheme is based on the new molecular data mentioned above, which show a rather close relationship of *Bursaria* and *Bryometopus* and indicate that cyrtolophosids are the sister taxon. These data agree with the morphological and morphogenetic evidences available (Foissner 1993a). Accordingly, a pleurotelokinetal stomatogenesis and a "simple" paroral composed of a single row of dikinetids, are the apomorphies for the whole group.

(1) *Bursaridium*, *Paracondylostoma*, *Thylakidium*, *Bryometopus*, and *Bursaria* have a unique character constellation not found in any other colpodid, viz. an apical oral opening, a ventral cleft, and a conspicuous "heterotrich" zone of adoral organelles. Thus, they are very likely monophyletic.

(2) *Bursaria* is separated from the other genera by the paroral ciliature (many short rows), the structure of the resting cyst (with emergence pore; lacking in all other colpodids), and the occurrence of sex (conjugation; unknown in other colpodids). This suggests not only a rather separate (derived) position of *Bursaria* within the group, but also maintenance of the ordinal rank (Foissner 1993a, Lynn and Small 1997).

(3) We were unsuccessful in finding a strong synapomorphy uniting the genera *Bursaridium*, *Paracondylostoma*, *Thylakidium*, and *Bryometopus*, indicating underinvestigation and /or misclassification. The details of the oral apparatus mentioned in Table 2 are

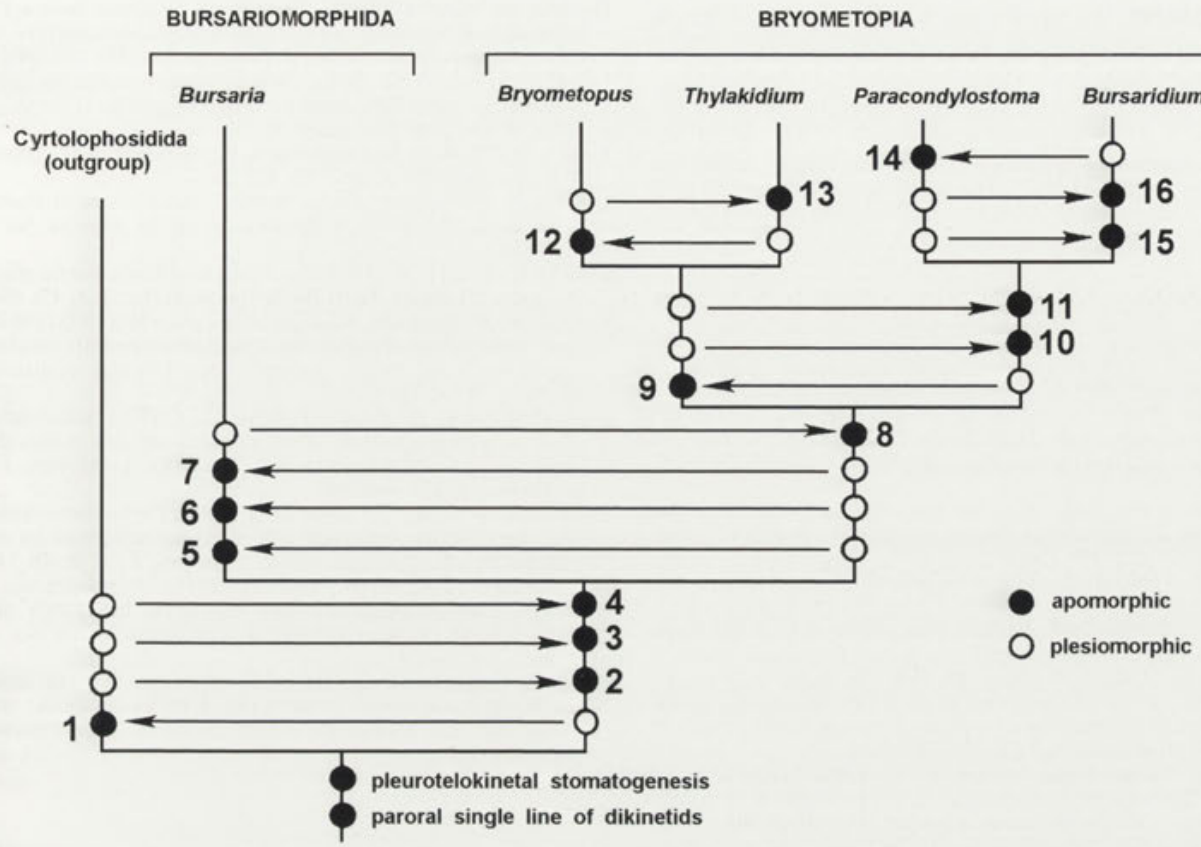

Fig. 38. Hennigian phylogeny of the genera *Bursaria*, *Bryometopus*, *Thylakidium*, *Paracondylostoma*, and *Bursaridium*. For character states, see Table 2

weak. However, the general appearance of these genera is more similar to each other than to *Bursaria*. Furthermore, several ultrastructural details argue against considering any of these genera to be very closely related to *Bursaria*: *Bursaridium* (and very likely also *Paracondylostoma*) has supraepiplasmic microtubules (Foissner 1993a), which are lacking in *Bursaria* (Lynn 1980, Perez-Paniagua *et al.* 1980) and *Bryometopus* (Wirnsberger *et al.* 1985; re-checked in the original material); and *Bryometopus* (very likely also *Thylakidium*) has short, non-overlapping transverse microtubule ribbons (Wirnsberger *et al.* 1985), while those of *Bursaria* are very long and overlapping (Lynn 1980, Perez-Paniagua *et al.* 1980).

(4) *Paracondylostoma* and *Bursaridium* have two strong synapomorphies, namely, the supraepiplasmic microtubules (as yet, definitely shown only in *Bursaridium*; Foissner 1993a) and the circumoral ciliary ribbon, which is composed of narrowly spaced somatic kinetids having a particular fine structure (Foissner 1993a), at the anterior end of the somatic kineties (Figs. 7, 13, 21, 29, 32, 35). No other colpodid has such a pattern. Thus, even the generic separation could be questioned. However, the slightly different structure of the paroral membrane (kinetids loosen in mid-portion of *Bursaridium*; Figs. 27, 32, 35-37), the large, cornute vestibulum (Figs. 31, 33, 34), and the euplanktonic mode of life of *Bursaridium* are rather different from the simple, obconical vestibulum (Figs. 1, 12, 18, 20, 23) and the semi-sessile life strategy of *Paracondylostoma*. Thus, generic separation still seems appropriate.

(5) *Bryometopus* and *Thylakidium* are linked by the short transverse microtubule ribbons forming a V-shaped pattern (Wirnsberger *et al.* 1985, Foissner 1993a). *Bryometopus* differs from the other genera in the argumentation scheme by the ventralization of the oral appa-

ratus. Possibly, the vestibulum has flattened and driven the oral structures into the ventral cleft during the evolution of the genus.

Acknowledgements. Supported by the Austrian Science Foundation (FWF Project P-12367-BIO). The technical assistance of Brigitte Moser, Dr. Eva Herzog, and Mag. Eric Strobl is greatly acknowledged.

REFERENCES

Fauré-Fremiet E. (1924) Contribution a la connaissance des infusoires planktoniques. *Bull. biol. Fr. Belg. Suppl.* **6:** 1-171

Foissner W. (1980) Taxonomische Studien über die Ciliaten des Grossglocknergebietes (Hohe Tauern, Österreich). IX. Ordnungen Heterotrichida und Hypotrichida. *Ber. Nat.-Med. Ver. Salzburg* **5:** 71-117

Foissner W. (1991) Basic light and scanning electron microscopic methods for taxonomic studies of ciliated protozoa. *Europ. J. Protistol.* **27:** 313-330

Foissner W. (1993a) Colpodea (Ciliophora). *Protozoenfauna* **4/1**: I-X, 1-798

Foissner W. (1993b) *Corticocolpoda kaneshiroae* n. g., n. sp., a new colpodid ciliate (Protozoa, Ciliophora) from the bark of Ohia trees in Hawaii. *J. Euk. Microbiol.* **40:** 764-775

Foissner W. (1993c) *Idiocolpoda pelobia* gen. n., sp. n., a new colpodid ciliate (Protozoa, Ciliophora) from an ephemeral stream in Hawaii. *Acta Protozool.* **32:** 175-182

Foissner W. (1994a) *Bryometopus hawaiiensis* sp. n., a new colpodid ciliate from a terrestrial biotope of the Hawaiian Archipelago (Protozoa: Ciliophora). *Annln naturhist. Mus. Wien* **96B:** 19-27

Foissner W. (1994b) *Pentahymena corticicola* nov. gen., nov. spec., a new colpodid ciliate (Protozoa, Ciliophora) from bark of *Acacia* trees in Costa Rica. *Arch. Protistenk.* **144:** 289-295

Foissner W. (1995) Tropical protozoan diversity: 80 ciliate species (Protozoa, Ciliophora) in a soil sample from a tropical dry forest of Costa Rica, with descriptions of four new genera and seven new species. *Arch. Protistenk.* **145:** 37-79

Foissner W., Wölfl S. (1994) Revision of the genus *Stentor* Oken (Protozoa, Ciliophora) and description of *S. araucanus* nov. spec. from South American lakes. *J. Plankton Res.* **16:** 255-289

Gelei J. von (1954) Über die Lebensgemeinschaft einiger temporärer Tümpel auf einer Bergwiese im Börzsönygebirge (Oberungarn) III. Ciliaten. *Acta biol. hung.* **5:** 259-343

Kahl A. (1927) Neue und ergänzende Beobachtungen heterotricher Ciliaten. *Arch. Protistenk.* **57:** 121-203

Lynn D. H. (1980) The somatic cortical ultrastructure of *Bursaria truncatella* (Ciliophora, Colpodida) *Trans. Am. microsc. Soc.* **99:** 349-359.

Lynn D. H., Small E. B. (1997) A revised classification of the phylum Ciliophora Doflein, 1901. *Revta Soc. mex. Hist. nat.* **47:** 65-78

Lynn D. H., Wright A.-D., Schlegel M., Foissner W. (1998) Phylogenetic relationships of orders within the class Colpodea (Ciliophora), inferred from small subunit rRNA gene sequences. *J. Molec. Evol.* (in press)

Perez-Paniagua F., Puytorac de P., Savoie A. (1980) Caractéristiques de la stomatogenèse et des ultrastructures corticale et buccale du cilié Colpodidea *Bursaria truncatella* O. F. Müller, 1773. *J. Protozool.* **27:** 300-308

Stechmann A., Schlegel M., Lynn D. H. (1998) Phylogenetic relationship between prostome and colpodean ciliates tested by small subunit rRNA sequences. *Molec. Phylogen. Evol.* **9:** 48-54

Wirnsberger E., Foissner W., Adam H. (1985) Morphogenesis, fine structure, and phylogenetic relationships of the "heterotrich" ciliate *Bryometopus atypicus* (Protozoa, Colpodea). *Annls Sci. nat. (Zool.)* **7:** 113-128

Wright A.-D. G., Lynn D. H. (1997) Maximum ages of ciliate lineages estimated using a small subunit rRNA molecular clock: crown eukaryotes date back to the paleoproterozoic. *Arch. Protistenk.* **148:** 329-341

Received on 2nd July, 1998: accepted on 12th August, 1998

Acta Protozoologica (1998) 37: 241 - 245

ACTA
PROTOZOOLOGICA

Myxobolus macroplasmodialis sp. n. (Myxozoa: Myxosporea), a Parasite of the Abdominal Cavity of the Characid Teleost, *Salminus maxillosus*, in Brazil

Kálmán MOLNÁR[1], Maria Jose RANZANI-PAIVA[2], Jorge Costa EIRAS[3] and Edson Lara RODRIGUES[4]

[1]Veterinary Medical Research Institute, Hungarian Academy of Sciences, Budapest, Hungary; [2]Instituto de Pesca de Sao Paulo, Sao Paulo, Brazil; [3]Departamento de Zoologia e Antropologia, Faculdade de Ciencias, Universidade do Porto, Porto, Portugal; [4]Laboratorio de Impacte Ambiental e Histopatologia, Instituto Adventista de Ensino, Sao Paulo, Brazil

Summary. A new myxosporean species, *Myxobolus macroplasmodialis* sp. n., infecting the Brazilian freshwater fish *Salminus maxillosus*, is described. The species forms large plasmodia in the abdominal cavity, which are filled with spores differing from all known *Myxobolus* species by their anteriorly diverging and anteriolaterally opening polar capsules. In this respect the species resembles members of the genus *Triangula* but in all other features it shows the characteristics of the genus *Myxobolus*.

Key words: Brazil, *Myxobolus*, Myxosporea, new species, pisces, *Salminus*.

INTRODUCTION

Few myxosporean parasites have been reported from South America. Of these, members of the genus *Henneguya* Thélohan are most studied (Pinto 1928; Guimaraes and Bergamin 1933, 1934; Cordeiro *et al.* 1984; Azevedo and Matos 1989, 1995; Azevedo *et al.* 1990; Rocha *et al.* 1992). Compared to the number of *Myxobolus* species known from other parts of the world (Donets and Shulman 1984, Landsberg and Lom 1991) the number of *Myxobolus* species recorded from South American fishes is relatively low. The results of myxosporean research in South America were summarised by Walliker (1969), who reported eleven known species and described a new species, *M. serrassalmi*. The occurrence of some other *Myxobolus* spp. has been mentioned by Thatcher (1981) and Molnár and Békési (1993).

The present paper reports on the occurrence of a *Myxobolus* species which forms unusually large plasmodia in the abdominal cavity of dourado (*Salminus maxillosus*), a common economically important fish in Southern Brazil. The species is described as *M. macroplasmodialis*.

Address for correspondence: Kálmán Molnár, Veterinary Medical Research Institute, Hungarian Academy of Sciences, POB 18, H-1581 Budapest, Hungary; Fax: 252 1069; E-mail: kalman@novell.vmri.hu

MATERIALS AND METHODS

Salminus maxillosus (Pisces, Characidae) was collected from the River Mogi-Guacu, near Cachoeira de Emas (Pirassununga). A total of

247 fish (36–87 cm long) were examined for the presence of myxosporean plasmodia between August 1996 and June 1997. Some plasmodia located free in the abdominal cavity were fixed in 70% ethyl alcohol, while others were preserved in 10% formalin. Dimensions of the plasmodia (cysts) were measured during necropsy of freshly killed fish. Spores obtained from the plasmodia (cysts) were measured after fixation. Measurements were taken from 25 alcohol fixed and 25 formalin fixed spores. Drawings were made of both formalin- and alcohol-fixed material. For photomicrography, spores were freed from alcohol-fixed cysts, laid on top of a thin agar layer, and covered with a coverslip according to the method of Lom (1969). Permanent preparations were made by placing a portion of spores into glycerol-gelatine and mounting them under a coverslip. The spores were checked for the presence of an iodinophilous vacuole after adding a drop of Lugol's solution. The measurements of spores were determined by comparing images of spores projected from an Olympus microscope to the screen of a video recorder with a computer-calibrated scale of measurements.

For histology, cysts, a part of the intestine and the inner organs, were fixed in 10% buffered formalin, embedded in paraffin wax and cut into 4 µm thick sections, which were stained with histological Giemsa stain and with haematoxylin and eosin (H & E). Plasmodial structure was studied on a well-developed plasmodium filled with fully developed spores. Photographs of alcohol-fixed spores and of the histological sections were taken with a camera attached to a Jenaval microscope.

RESULTS

Twenty-four of 247 fish had plasmodia (cysts) located free in the abdominal cavity. The majority of the fish had one plasmodium. One fish, however, harboured 28 specimens. Plasmodia were elliptical in shape, 7–24 mm long and 3–13 mm in wide. All plasmodia found contained thousands of spores. The plasmodial wall was composed of a thin (30–42 µm) layer of host origin, which contained cytoplasm-deficient cells with large nuclei. The layer of host origin was connected to the ectoplasm of the plasmodium with a structureless layer staining blue in Giemsa-stained histological sections (Fig. 1). This structureless part of the cyst wall continued in the thin layer of the ectoplasm containing vegetative stages and developing sporoblasts of the parasite. The endoplasm contained mature spores (Fig. 2).

Description of the species:

Type host: dourado *Salminus maxillosus* Valenciennes, 1840.

Locality: river Mogi-Guacu, near Cachoeira de Emas (Pirassununga, Sao Paulo State).

Site of infection: abdominal cavity.

Type material: spores have been deposited in the protozoological collection of the Hungarian Natural History Museum.

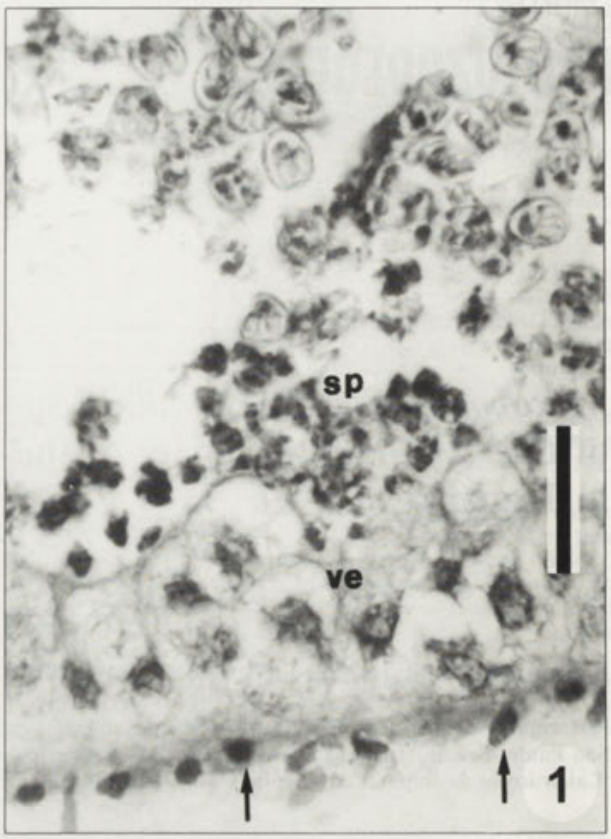

Fig. 1. Histological section of a plasmodium of *Myxobolus macroplasmodialis*, located close to the periphery of the „cyst". Layer of host origin with cytoplasm-deficient cells (arrows). Vegetative stages in the ectoplasm (ve). Young sporogonic stages (sp) consisting of sporoblasts and immature spores. Giemsa stain. Scale bar - 30 µm

Description of spores: spores (Figs. 3, 4) variable in shape, being ovoid or trapezoid in character, narrower at the posterior end in frontal view, and lemon-shaped in lateral view. Anterior end impressed in most spores, particularly in those fixed in formalin. Other spores (most notifiably specimens preserved in glycerol-gelatine) the end is rounded. Some spores with impressed end show a triangular shape (Figs. 4a-d). Spore valves relatively thin, symmetrical and smooth. Sutural line indistinct, sutural edge less protruding. Spores 11 (10.5–12) µm in length, 8.5 (8–9) µm in width, and 5.2 (5–5.5) µm in thickness. Two polar capsules pyriform in shape, equal in size, 4.5 (4–5) µm long and 2.8 (2-3) µm wide. Polar capsules diverge toward the anterior end and open anteriolaterally in a small thickening in the sutural line. The divergence of polar openings is more distinct in spores with an impressed anterior end (Figs. 4c, d). Polar filaments closely coiled, with 6 turns in the polar capsule, aligned perpendicularly

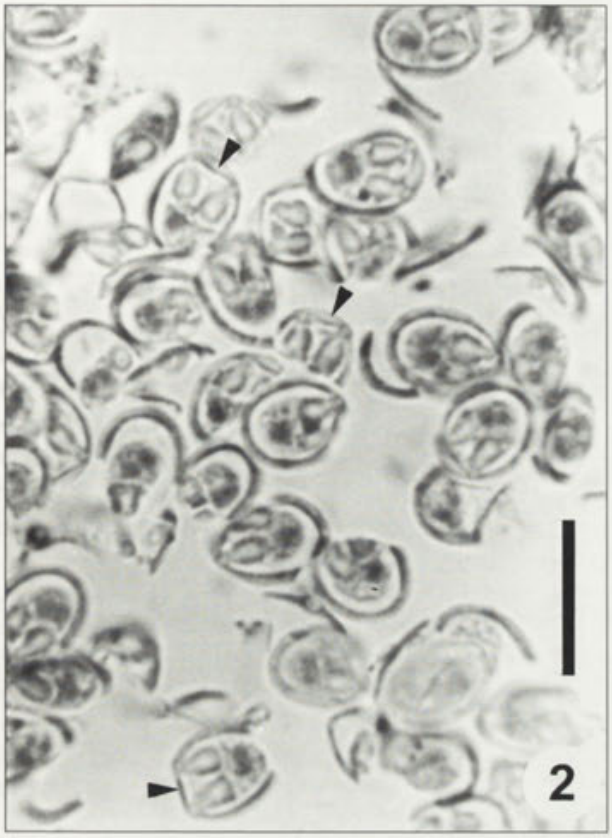

Fig. 2. Cross-sectioned spores in the endoplasm of *Myxobolus macroplasmodialis*. See the impressed anterior part and the diverging polar capsules of the spores (arrowhead). H & E. Scale bar - 15 μm

Fig. 3. *M. macroplasmodialis* spores from an alcohol-fixed plasmodium. H & E . Scale bar - 10 μm

to the longitudinal axis of the capsule. A large, triangular intercapsular appendix is located anterioraly. Due to the impression of the spore wall only a loose contact is observable between the wall and the appendix. Iodinophilous vacuole absent. Two nuclei of the sporoplasm are well discernible also in unstained preparations.

DISCUSSION

The taxonomic position of this species is uncertain. It bears the characteristics of both the genus *Myxobolus* Buetschli and the genus *Triangula* Chen & Hsieh. In its large plasmodia, in the oval shape of polar capsules in spores preserved in glycerol-gelatine, and in the well-developed intercapsular appendix, *M. macroplasmodialis* resembles other species of the genus *Myxobolus* and differs from the two known histozoic *Triangula* spp. (*T. yangkiangensis* and *T. percae*), which develop with small plasmodia in the epithelium and in the brain, respectively (Chen and Hsieh 1984, Langdon 1989). As regards the position of the openings of polar capsules, however, this species fits well into the genus *Triangula*. The polar capsule openings of the majority of *Myxobolus* species lie very close to each other at the anterior pole of the spores; therefore, polar capsules usually converge towards the anterior pole. Nevertheless, at present this is the only major difference between our species and other *Myxobolus* species and we do not have enough arguments to relate *M. macroplasmodialis* to the already known species of the genus *Triangula*. Of species of the latter genus, *T. percae* resembles *M. macroplasmodialis* in its structure, but *T. yangkiangensis* seems to have characters rather distinct from those of the latter species.

Myxobolus spp. are common parasites of freshwater fishes. Most of the fish species whose parasite fauna has

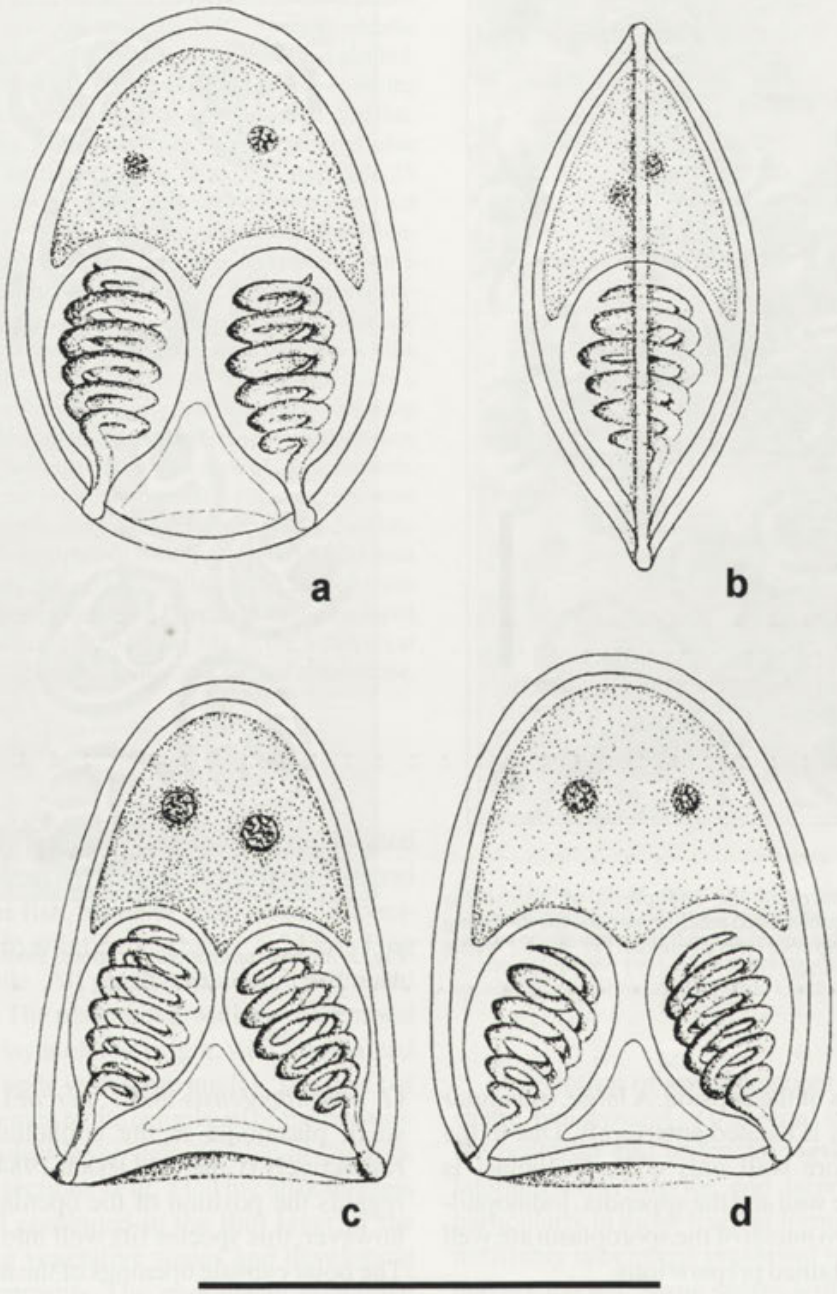

Fig. 4. Schematic illustration of *M. macroplasmodialis*. a - alcohol-fixed spores in frontal view; b - alcohol-fixed spores in lateral view; c,d - formalin-fixed spores. Scale bar - 10 μm

been studied has one or more *Myxobolus* species. Little is known about the host specificity of *Myxobolus* spp. but new data indicate that the number of species with a wide host range is low and most species appear to be strictly host specific or capable of developing only in closely related fishes. From characid fishes only a single *Myxobolus* species, *M. colossomatis* has been described (Molnár and Békési 1993) and the occurrence of two other *Myxobolus* spp. mentioned (Walliker 1969). *M. macroplasmodialis* is distinct in that it develops in unique, large cysts. The plasmodia of the majority of *Myxobolus* species measure 0.5–3 mm, whereas those in *M. macroplasmodialis* exceed 1 cm. Furthermore, the plasmodium of *M. macroplasmodialis* is composed of a single unit, in

contrast with some other species with large amalgamated plasmodia such as *M. nodulointestinalis* (Massoumian *et al.* 1996). In addition to its cyst size, *M. macroplasmodialis* differs from other species in spore morphology. For lack of fresh material it cannot be determined whether the impression on the anterior end is only a consequence of fixation or a genetic characteristic of the species. As in glycerol-gelatine preparations the majority of spores regain their oval shape, this species differs from other *Myxobolus* spp. only in its diverging polar capsules. No information is available on the tissue specificity of this species, but the location of mature cysts suggests that this species starts its development in the serous membranes of the abdominal wall or abdominal organs, and becomes detached from those sites only at an advanced stage of development.

Acknowledgements. The authors are indebted to FAPESP (Fundo de Amparo á Pesquisa do Estado de Sao Paulo), to the staff of the "Laboratorio de Peixes Fluviais Dr. Pedro Azevedo", from the Instituto de Pesca at Pirassununga, and to Mr. José Plaza and Mr. Hélio S. Mariscal. This paper was partially supported by CIMAR (Centro de Investigacao Marinha e Ambiental).

REFERENCES

Azevedo C., Matos E. (1989) Some ultrastructural data on the spore development in a *Henneguya* sp. parasite of the gill of a Brazilian fish. *Parasitol. Res.* **76:** 131–134

Azevedo C., Matos E. (1995) *Henneguya adherens* n. sp. (Myxozoa, Myxosporea), parasite of the Amazonian fish, *Acestrorhynchus falcatus*. *J. Euk. Microbiol.* **42:** 515-518

Azevedo C., Corral L., Matos E., Gusmao S. (1990) Some ultrastructural aspects of the life cycle of *Henneguya* sp. (Myxozoa), a parasite of an estuarine fish of the Amazon River. Pathology in Marine Science. Academic Press, New York, 175-180

Chen Ch-L, Hsieh S-R (1984) New myxosporidians (Protozoa) from the freshwater fishes of China. In: Parasitic Organisms of Freshwater Fish of China (Ed. by Institute of Hydrobiology, Academia Sinica), Agricultural Publishing House, Beijing, China, 69-104 (in Chinese edition) and 13-14 (in abstracted English edition)

Cordeiro N. S., Artigas P. T., Gióia I., Lima R. S. (1984) *Henneguya pisciforme* n. sp. mixosporideo parasito de branquias do Lambari *Hyphessobrycon anisitsi* (Pisces, Characidae). *Mem. Inst. Butantan* **47/48:** 61-69

Donets Z .S., Shulman S. S. (1984) Parasitic Protozoa. In: Key to the Parasites of Freshwater Fish of the USSR (Ed. O. N. Bauer) Nauka, Leningrad, **1:** 1-426 (in Russian)

Guimaraes J. R. A., Bergamin F. (1933) Consideracoes sobre as ictioepizootias produzidas pelos mixosporideos do genero „*Henneguya*" Thélohan, 1892 *Henneguya travassosi* sp. n. *Rev. Indust. Animal.* **10:** 1151-1156

Guimaraes J. R A., Bergamin F. (1934) *Henneguya santae* sp. n.-um novo mixosporideo parasito de *Tretragnopterus* sp. *Rev. Indust. Animal.* **12:** 110-113

Landsberg J. H., Lom J. (1991) Taxonomy of the genera of the *Myxobolus/Myxosoma* group (Myxobolidae: Myxosporea), current listing of species and revision of synonyms. *Syst. Parasitol.* **18:** 165-186

Langdon J. S. (1989) Spinal curvatures and an encephalotropic myxosporean, *Triangula percae* sp. nov. (Myxozoa: Ortholineidae), enzootic in redfin perch, *Perca fluviatilis* L., in Australia. *J. Fish Dis.* **10:** 425-434

Lom J. (1969) On a new taxonomic character in Myxosporidia, as demonstrated in description of two new species of *Myxobolus*. *Folia Parasitol.* **16:** 97-103

Massoumian M., Baska F., Molnár K. (1996) *Myxobolus nodulointestinalis* sp. n. (Myxosporea, Myxobolidae), a parasite of the intestine of *Barbus sharpeyi*. *Dis. aquat. Org.* **24:** 35-39

Molnár K., Békési L. (1993) Description of a new *Myxobolus* species, *M. colossomatis* n. sp. from the teleost *Colossoma macropomum* of the Amazon River basin. *J. Appl. Ichthyol.* **9:** 57-63

Pinto C. (1928) Myxosporideos e outros protozoarios intestinaes de peixes observados na America do sul. *Arch. Inst. Biol. S. Paulo* **1:** 101-136

Rocha E., Matos E., Azevedo C. (1992) *Henneguya amazonica* n. sp. (Myxozoa, Myxobolidae), parasitising the gills of *Crenicichla lepidota* Heckel, 1840 (Teleostei, Cichlidae) from Amazon river. *Eur. J. Protistol.* **28:** 273-278

Thatcher V. E. (1981) Patologia de peixes da Amazonia Brasileira, 1. Aspectos gerais. *Acta Amazonica* **11:** 125-140

Walliker D. (1969) Myxosporidia of some Brazilian freshwater fishes. *J. Parasitol.* **55:** 942-948

Received on 18th May, 1998; accepted on 30th July, 1998

Acta Protozoologica (1998) 37: 247 - 258

ACTA
PROTOZOOLOGICA

Life History and Description of *Leidyana subramanii* sp. n. (Apicomplexa: Eugregarinida). A New Cephaline Gregarine Parasite of a Grasshopper (Insecta: Orthoptera) in Tamil Nadu, India

Kasinathan PUSHKALA* and Madabushi C. MURALIRANGAN

G. S. Gill Research Institute, Guru Nanak College, Chennai, India

Summary: The morphology and life history of a new species of septate gregarine (Apicomplexa: Eugregarinida) from the digestive tract of *Eyprepocnemis alacris alacris* (Serville) (Insecta: Orthoptera) is described. The gregarine belong to the genus *Leidyana.* The characteristic features of the gregarine are: globular epimerite; 657 µm (maximum) long solitary sporadin; gametocyst spherical with anisogamous gametes; sporulation through 1-13 sporoducts; barrel-shaped sporocyst or oocysts of 6.6 x 3.5 µm in dimension; LP:TL = 1:3-11 and WP:WD = 1:1.3 -2.1. The gregarine is compared with other species in the genus *Leidyana* reported from different hosts to establish its distinctiveness.

Key words: Cephaline gregarine, *Leidyana, Leidyana subramanii* sp. n.

INTRODUCTION

The genus *Leidyana* was established by Watson (1915) to contain those gregarine species possessing a simple epimerite, solitary sporont, gametocyst dehiscing through sporoducts and dolioform oocyst or sporocyst (Keilin 1918, Bhatia and Setna 1924, Lipa and Martignoni 1984, Roy 1989, Clopton 1995). Reproductive associations are formed only by mature gamonts just before syzygy and gametocyst formation begins (Clopton 1995).

Address for correspondence: M.C. Muralirangan, G. S. Gill Research Institute, Guru Nanak College, Chennai, India; E-mail: grignc@gias.md01.vsnl.net.in

* Present address: S.D.N.B. Vashnav College for Women, Chromepet, Chennai-600 044, India

Complete life histories for 19 of the 27 recorded species belonging to the genus *Leidyana* have been traced (Clopton 1995). Nine species reported from different grillid (Gryllidae: Orthoptera) hosts (Sarkar 1988) and one from a Madagascar hissing cockroach (Blattidae: Orthoptera) (Clopton 1995) were also found to infect other orthopterans (Dufour 1837; Watson 1915; Geus 1966; Corbel 1967a; Issi and Lipa 1968; Hoshide 1973a, b, 1978; Haldar and Sarkar 1979; Hooger and Amoji 1986; Sarkar 1988; Clopton 1995). The species described in the present study represents the first record of *Leidyana* from a grasshopper (Orthoptera: Acrididae).

A small population of *Eyprepocnemis alacris alacris* (Insecta: Orthoptera: Acrididae) was observed to be

infected with gregarine parasites. A study of the life cycle of the parasite revealed characters diagnostic of the genus *Leidyana*. The species under investigation is morphologically and morphometrically distinct from all known species of *Leidyana* and thus is described as a new species.

MATERIALS AND METHODS

Fifty grasshoppers were collected on 15th June, 1991 from a grass field in and around Chennai (Chengleput district, Tamil Nadu, India) and their digestive tracts dissected in 0.5% saline solution. One hundred percent infection was observed in the field population. A small slit was made in the midgut to release the gut contents which contained the free gregarines. Permanent smears of the gut contents and 5-6 µm thick sections of the midgut were prepared. Smears were fixed in Bouin's fluid and were subsequently stained in Hiedenhain's iron haematoxylin. Gametocysts, collected from the hindgut of the infected hosts, were washed in distilled water and kept in a moist chamber in order to observe sporulation.

Additional gregarines were placed in 4% (v/v) glutaraldehyde in 1% phosphate buffer, rinsed in buffer and post-fixed in 1% phosphate buffered osmium tetroxide. For scanning electron microscopy (SEM), free gregarines were dehydrated through an alcohol series, dried overnight in a critical point drier on a coverslip, coated with gold for 5-10 min, and scanned using a Leica Stereoscan electron microscope. Similarly, cysts from the moist chamber, after different hours of incubation, were mechanically ruptured directly onto a slide and prepared as before for SEM studies.

Repeated observations indicated that placing faecal pellets from infected hosts in parasite-free cultures was sufficient to infect fresh, healthy insects. Faecal pellets of infected *Eyprepocnemis alacris alacris* were collected and stored at 18-20°C and used as a stock for infection. Because the spore concentrations could not be calculated, 10 ml alloquots of faecal pellets from the stock culture were used and introduced into cages containing 30 third instar nymphal stages and these insects were used for further studies. In laboratory cultures, the mortality rate was negligible after the 3rd instar. One hundred percent infection was confirmed in the laboratory populations by sacrificing all the individuals (30 third instars) maintained simultaneously with same infected faecal pellets (stock).

In order to study the life history, observations were made every 24 h following the initial infection. Parameters such as the number of days required to complete intracellular development, detachment of sporonts, formation of syzygy and gametocysts were recorded.

Morphometric measurement of 20 free gregarines and 20 conjugants (syzygy) were taken.

OBSERVATION

Taxonomic account

Order: Eugregarinida Leger 1892 *sensu stricto* Levine *et al.* 1980

Family: Leidyanidea Kudo 1954

Genus: *Leidyana* Watson 1915

Diagnosis: associations late; epimerite simple, globular, sessile; gametocysts dehiscing through sporoducts; oocysts dolioform, released in long chains.

Leidyana subramanii sp. n.

Life history

The parasite life cycle begins in the grasshopper with the penetration of sporozoites into the epithelial cells of the midgut. The earliest stage observed in a newly infected host is a spherical body measuring 9 µm in diameter, enclosed in a vacuole (Fig. 1). This spherical body develops a knob-like epimerite or holdfast from which a post epimerite is formed. Following growth of the parasite, the post epimerite enlarges and differentiates into an anterior protomerite and a posterior deutomerite (Fig. 2). A constriction exists between the two segments and is now recognised as the neck region (Figs. 19, 20). Eventually the nucleus is pushed into the deutomerite. At this stage, the protomerite and the deutomerite are thrust out of the epithelial cells and the parasite remains attached to the host cell by the epimerite. Due to this attachment an indendation in the host cell is noticed (Fig. 3). Even in a heavily infected host, none of the free gregarines have an epimerite, confirming the inability of the sporozoite to develop in the gut lumen. Detachment of the trophozoite from the gut epithelium is a random process and is in no way related to the final stage of development. The gut lumen has free sporadins of different ages, even 4 days after the initiation of a fresh infection. During detachment the epimerite is left behind in the host cell and it leaves a scar on the protomerite of the sporadin. Gregarines found free in the gut lumen are termed sporonts (Canning 1956).

During conjugation, two matured sporonts (conjugants) come closer and the protomerite of the satellite, (termed the collar) becomes flattend, before attachment. Mature conjugants (gamonts) normally are seen in the gut 6 days after infection and conjugation takes place 8-10 days after infection. During conjugation, the protomerite of the satellite is attached to the deutomerite of the primite (Fig. 7). There was no specificity among the conjugants with regard to their size. Both conjugants normally have opaque cytoplasm, or one may have a hyaline cytoplasm, indicating that accumulation of food materials is not an essential criteria for the gregarine to undergo conjugation.

The primite and satellite bend into a "v"- shaped body and then fuse to form a round, ball-shaped gametocysts

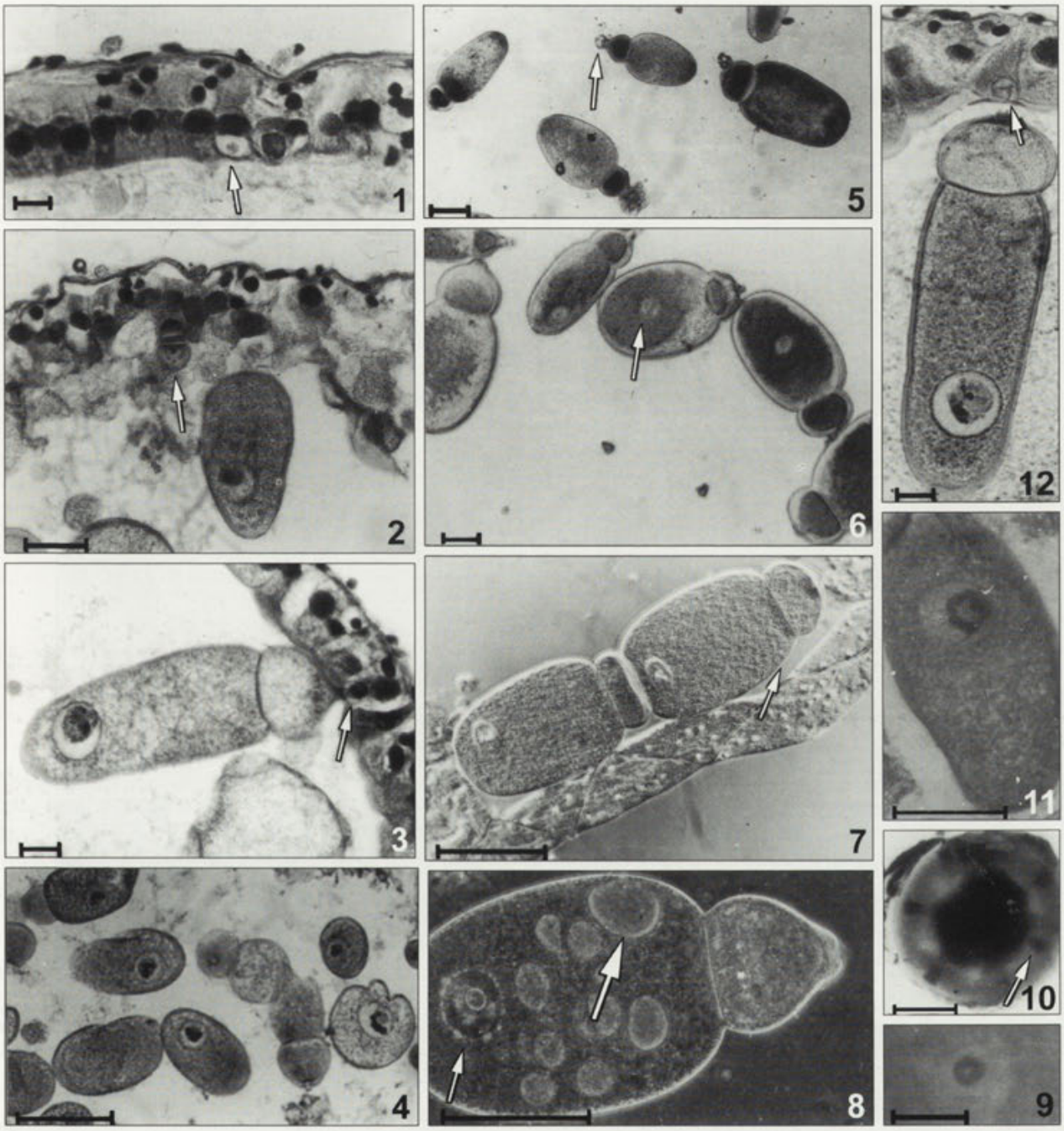

Figs. 1-12. *Leidyana subramanii* sp.n. 1- midgut epithelium, arrow indicates the sporozoites enclosed in a vacuole; 2- midgut epithelium with developing trophozoite with three segments (arrow); 3- trophozoite; 4- sporonts showing different endosome pattern; 5, 6- fresh smear showing free sporonts, arrows mark the epimerite (5) and nucleus (6).7- syzygy, arrow marks primite. 8- sporeduct sporonts with liquid filled vacuoles (big arrow); nucleus (small arrow); 9- sporeduct - polar view; 10- gametocyst with ectocyst and sporeduct, arrow; 11-sporont showing endosome pattern; 12- midgut epithelium showing the epimerite (arrow) and free sporont. Scale bars - 30 μm (Fig. 1); 1000 μm (Figs. 2, 7-11); 15 μm (Fig. 3); 10 μm (Fig. 4); 107 μm (Fig. 5); 90 μm (Fig.6); 17,2 μm (Fig.12)

(cysts), 196-468 μm in diameter. A protective ectocyst of mucus is secreted which swells, on absorption of water. This aids lodging the cyst either onto the wall of the epithelium or to the faecal pellet (Fig. 11). Before formation of the polar tube, the ectocyst has a slightly opaque periphery with residual cytoplasm in the centre. Normally, the cysts from the adult host grasshoppers are smaller but more in numerous than those collected from nymphal

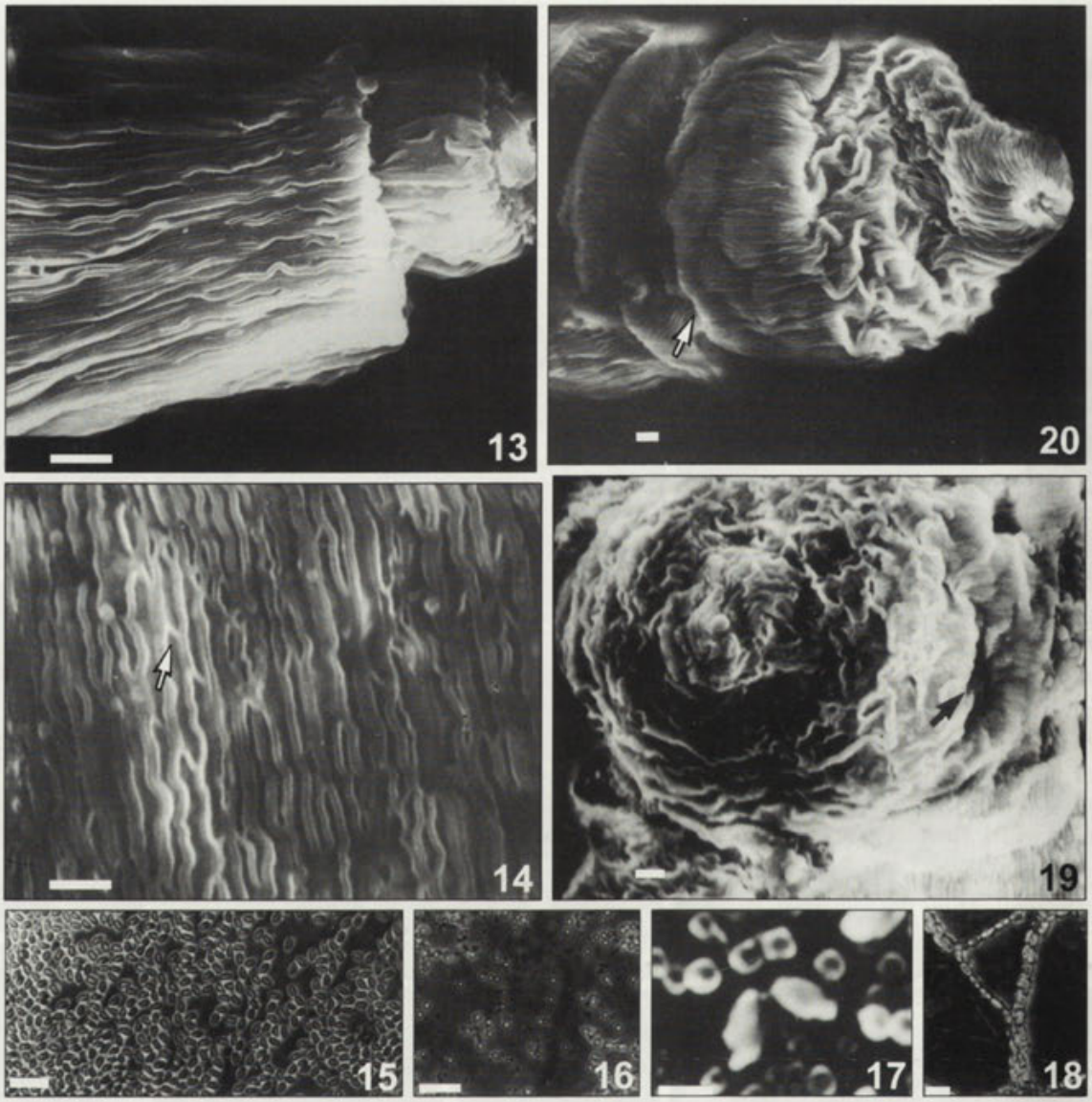

Figs. 13-20. *Leidyana subramanii* sp.n. 13- trophozoite with epimerite and protomerite, SEM; 14- portion of the epicyte fold; SEM. Arrow marks connection between the epicyte fold, 15- spore fresh smear. 16- gametocyst burst to show the anisogamous gametes, 17- smear of the cyst with gametes and barrel shaped spores; SEM, 18-spore chain, 19,20- protomerite showing the arrangement of the epicyte fold; SEM. Scale bars - 2 μm (Figs. 13, 20); 3 μm (Figs. 14, 19); 16,5 μm (Fig. 15); 30 μm (Fig. 16); 7,7 μm (Fig. 17); 2,8 μm (Fig. 18)

stages. The cysts are voided with the faeces. The conjugants take 7-8 days to form the cysts. Cysts were collected only 16-18 days after infection. The cyst has round anisogamous gametes (Fig. 16). The resulting zygote produces sporozoites that are accomodated in barrel-shaped spores (Figs. 15, 17, 18). Gametogenesis and spore formation takes place simultaneously in the cyst (Fig. 17). Spores have been noticed in cysts 8 h after incubation. After 48-52 h of incubation, the cyst less opaque areas appear which eventually form a ring around the centre (Figs. 9, 10). This area turns yellow or orangish-yellow indicating the beginning of development of the polar tube. The polar tube is formed either on the exposed area of the cyst or on all sides. Spores come out only through the polar tube of the exposed region. The number of polar tubes (2-13) depends on the cyst size. A maximum of 13 polar tubes were observed in the largest cyst that measured 415 μm in diameter. The polar tube is very short and does not project outside the cyst (Fig. 10).

Spores are released through the polar tube. Long threads or chains are formed by the end to end attachment of the individual spores (Fig. 18). Cysts incubated in the

Table 1. *Leidyana subramanii* sp.n. Morphometrical measurements of sporadins from midgut of the 2nd instar *E.alacris alacris*, 20 days after infection

No	LP (μm)	WP (μm)	LD (μm)	WD (μm)	TL (μm)	Ratios				
						LP:LD	LP:TL	WP:WD	WP:TL	WD:TL
1	18	27	36	36	54	1:2	1:3	1:1.3	1:2	1:1.9
2	18	27	45	36	63	1:2.5	1:3	1:1.3	1:2	1:1.5
3	18	27	54	36	72	1:3	1:4	1:1.3	1:2.7	1:1.5
4	63	81	207	150	270	1:3.3	1:4.3	1:1.9	1:3.3	1:1.8
5	63	81	225	117	288	1:3.6	1:4.6	1:1.4	1:3.6	1:1.8
6	72	90	225	162	297	1:3.1	1:4.1	1:1.8	1:3.3	1:1.9
7	54	108	306	189	360	1:5.7	1:6.6	1:1.7	1:3.3	1:2
8	72	108	333	216	405	1:4.6	1:5.6	1:4.3	1:3.7	1:1.8
9	72	117	342	216	414	1:4.8	1:5.8	1:2	1:3.5	1:2
10	81	126	333	207	414	1:4.1	1:5.1	1:1.8	1:3.3	1:1.9
11	90	135	360	234	450	1:4	1:5	1:1.6	1:3.3	1:2.3
12	90	135	360	243	450	1:4	1:5	1:1.7	1:3.3	1:1.5
13	90	126	387	234	477	1:4.3	1:5.3	1:1.8	1:3.8	1:1.8
14	108	135	405	243	513	1:3.8	1:4.7	1:1.8	1:3.8	1:1.9
15	117	153	405	216	522	1:3.5	1:4.5	1:1.8	1:3.4	1:2.4
16	90	144	432	270	522	1:4.8	1:5.8	1:1.4	1:3.6	1:1.9
17	108	162	432	306	540	1:4	1:5	1:1.8	1:3.3	1:2
18	135	135	450	252	585	1:3.3	1:4.3	1:1.9	1:4.3	1:1.5
19	54	153	540	324	594	1:10	1:11	1:2.1	1:3.9	1:2.4
20	54	153	540	324	594	1:10	1:11	1:2.1	1:3.9	1:2.4

D-deutomerite, P-protomerite, TL-total length, L-length, W-width, N-20, SB-389.85±17

laboratory in a moist chamber show silvery-white coils of spore chains, formed after 5 h from the time a clear area appears on the surface of the cyst. The spore chain is very delicate and breaks very easily by loosing the contact with each other.

Description

Trophozoite

Trophozoites not free in lumen of host digestive system. Spherical bodies (Fig. 1) in newly infected host 9 μm in diameter, and is encircled by vacuole. Each free trophozoite consisted of three segments: a spherical epimerite, a hemispherical protomerite (Fig. 13), and a cylindrical deutomerite with rounded end. Nucleus in deutomerite spherical in shape (Fig. 2).

Sporadin

Fully mature sporonts macroscopic, free, elongated, yellowish and opaque (Figs. 5, 6, 12). Protomerite stout, wider at the neck, 27-153 μm in diameter, tapering anteriorly. Anterior end with funnel-shaped depression representing the location of epimerite. Ratio of length of protomerite to total body length ranges from 1:3 to 11 (Table 1). In fresh smear (unstained) preparations (Figs. 5, 6) both protomerites and deutomerites have hyaline homogenous ectoplasm and granular opaque endoplasm. Young gregarines typically not opaque, unlike fully mature ones. Deutomerite widest in middle, length 36- 540 μm (Table 1). Average ratio of longer individuals ranged from 3:4.8. Ratio of length of the protomerite to total body length varied between 3.0 to 11 (Table 2), though most were between 4.0 to 5.8. Ratio of width of protomerite to width of deutomerite ranged between 1.3 to 2.1.

Nucleus of deutomerite (Figs. 6, 8) located either centrally or placed in posterior half of body. Karyosomes arranged in threads (Figs. 4, 11). Single liquid filled vacuole present at apex of protomerite in younger sporonts where epimerite had detached.

Deutomerite of young sporonts with many membrane bound vesicles attributed to dehydration process (Fig. 8). Epicyte folds, as observed in electron micrographs (Figs. 19, 20) numerous, arranged like rose petals at tip of protomerite, extend longitudinally from neck to end

Table 2. *Leidyana subramanii* sp.n. Morphometric measurement of syzygy or conjugants from midgut of the 2nd instar *E. alacris alacris* 20 dyas after infection

No	Primite (μm)	Satellite (μm)	Difference
1	423 F	441 F	18
2	459	504 F	45
3	369	468	99
4	459	540	81
5	468	360	108
6	504	405	99
7	477	576	99
8	450	405	45
9	450	487	37
10	396 F	324 P	72
11	387 F	378 F	9
12	378 F	324 P	54
13	396 F	405 F	09
14	378 F	306 P	72
15	387 F	378 F	9
16	360 F	405 F	45
17	378 P	319 P	59
18	387 F	468 F	81
19	396 F	306 P	90
20	387 F	504 F	117
21	540 H	441 F	99
22	441 P	423 H	18
23	477 H	387 F	90
24	441 P	333 P	108
25	450 F	396 F	54
26	450 F	504 F	54
27	468 F	573 F	45
28	477 H	387 F	90
29	387 F	468 F	81
30	378 F	324 P	54

F-fully opaque, H-hyaline, P-partially opaque

of deutomerite (Fig. 14). Folds with cross connections to adjacent folds, appear fork-like and wavy (Fig. 14). Constriction between protomerite and deutomerite is deep (Figs. 19, 20) and clearly distinct. Free gregarines collected from gut move very slowly with no change in general body shape.

Conjugants

Two matured sporonts (conjugants) come closer and form a syzygy (Fig. 7). An analysis of the conjugants (Table 2) showed that the difference in the total length between the primite and satellite varied between 9-117 μm.

Gametocysts

Ball shaped, 196-468 μm in diameter with a protective ectocyst of mucus, measuring 26-52 μm in thickness. The cyst with anisogamous gametes (Fig. 16), with 2-13 polar tubes to release spores.

Sporocyst

Barrel-shaped, measuring 6.6x3.5 μm in diameter.

TAXONOMIC SUMMARY

Host: *Eyprepocnemis alacris alacris* (Serville 1839) (Insects: Orthoptera).

Types: syntypes- Gregarines on three slides, numbers GRI/*Leidyana*-I, GRI/*Leidyana*-II and GRI/*Leidyana*-III are deposited at Zoological Survey of India, Southern Regional Station, 100, Santhome High Road, Chennai, India-600 028.

Type locality: Chennai, Chengleput district, Tamil Nadu, India.

Etymology: the species has been errected in rememberance of the husband of the first author Professor (Late) Mr. V. Subramanian who has been a great source of inspiration.

DISCUSSION

The species described above possess: (1) a simple globular epimerite; (2) solitary sporont; (3) dehiscing of the gametocyst through sporoducts; and (4) barrel-shaped spores (sporocysts) that are characteristics of the genus *Leidyana.* The digestive tract, especially the midgut and midgut caeca of insects, proves to be a viable environment for *Leidyana* species to meet its nutritional requirement. The comparative study of different species of *Leidyana* (Table 3) gives a clear indication that inspite of possessing common generic diagnostic features, morphometrically the different stages of the gregarine differ in more then one distintive feature for taxonomic consideration.

The *Leidyana* species with similar morphological characters namely *L. erratica* (Crawley 1903), *L. gryllorum* (Cuénot 1897), *L. oblongata* (Dufour 1837), *L. suzumushi* (Hoshide 1973a), *L. oviformis* (Hoshide 1978), *L. gnyanagangai* (Patil and Amoji 1979) have spherical gametocyst and barrel shaped sporocyst similar to *L. subramanii* but differ in: (1) the morphometry of the sporadins; (2) size of the gametocyst; (3) size of the spores; and (4) number of sporoducts. The shape and size of protomerite, constriction between protomerite and

Table 3. The comparison of the different *Leidyana* spp.

Leidyana Species	Host	Epimerite	Sporadin (Max. TL) (LP: TL) (WP:WD)	Gametocyst shape diameter	Sporocyst	Type locality	Additional characters compared to other representive spp.	Additional characters compared to *L. subramanii*
Leidyana berkeleyi Martignoni 1984)	*Phryganidia californica* (Oak worm) (Lepidoptera)	globular 8 µm (dia)	422 µm 1:4.6-11.2 1:0.9-2.1	111-142 µm	spindle shape gamete no spore	USA California	one karyosome	* 2-3 karyosome
Leidyana gnyanagangai (Patil & Amoji 1979)	*Rhytinota impolita* (Coleoptera)	sessile knob like 5 x 5 µm	350 µm 1:3-10 1:1-2-5	350 µm ectocyst 10 µm	dolioform 6.25 x 3.75 µm 19-21 sporeduct holes 20 µm (dia)	India	no intracellular stage; max size before detachment is 50 µm; pro.of sporont is 40 x 60µm	intracellular stage present; max size before detachment is 45 µm; pro. of sporont is 9-90 µm
Leidyana latifola (Braune & Geus 1969)	*Niptus hololeucus* (Lepidoptera)	button like	200 µm	–	–	–	sporont ovdial; deu. tapering; end septum between pro. & deu. indistinct	sporont cylindrical; deu. not tapering septum; between pro. & deu. distinct
Leidyana oryzeaphilus (Roy 1989)	*Oryzeaphilus mercator* (Coleopteria)	not button like 4-13 x 22-26 µm	116 µm 1:2.4-12 1:1-5.8	spherical 55-75 µm	barrel shape 6 x 4 µm 5 sporeduct	India	sporont ovidal shape; deu. triangular; rounded or oval nucleus; indistinct constriction between pro. & deu.	* sporont cylindrical; deu. cyryndried; nucleus always rounded; distinct constriction between pro. & deu.

Table 3. (con.)

Leidyana peregrinata (Ormieres 1967)	*Aglosa pinguinalis Asopiafarinatis* (Lepidoptera)	10.5-16.1 x 11.5 -18.1	–	–	–	–	the sporont passes through the epithelial cells & form coelomic cyst	* no such coelomic cyst
Leidyana phryganidae (Lipa & Martignoni 1984)	*Phryganidia californica* (Lepidoptera)	globular 10 µm (dia)	633 µm 1:6.6-9.06 1:1.3-2.2	118-149 µm (dia)	Oval 2.1-4.3 µm 6 sporeduct	USA	–	–
Leidyana subramanii sp.n.	*Eyprepocnemis alacris alacris* (Orthoptera)	globular	657 µm 1:3-11 1:1.3:2.1	spherical 195-468 µm ectocyst- 26-52 µm width	barrel shape 6.6 x 3.5 µm 1-13 sporeduct	India	–	–
Leidyana tinei (Keilin 1918)	*Endrosis fenestrelia* (Lepidoptera)	–	300 µm	spherical 90-110 µm (dia)	barrel shape 7 µm 2-5 sporeduct	England Cambridge Tonbridge	no boundary between pro. & deu. of young cephalont; max size before detachment is 30-200 µm pro. of the sporont 40 µm long; epicyst 8-10 µm thick sporulation takes place between 12-20 days	cephalant always seen with pro. & deu.; max size before detachment 45 µm; pro. 9-90 µm; epicyst wall 26 µm; sporulation takes place between 48-52 h.
Leidyana xylocopae (Bhatia & Setna 1924)	*Xylocopa* (Hymenoptera)	sessile glob like knob 13 µm (dia)	174 µm 1:4.6-7 1:1.3-1.8	no cyst	no spore	India	sporont 23-174 µm long	* sporont 45-657 µm long
Unident. spp. (Rabindra & Ayaraj 1980)	*Nephantis serinopa* (Lepidoptera)	–	–	no gametocyst	no spore	India	the sporont passes through the epithelial cells & form coelomic cyst	* no such coelomic cyst

deu.-deutomerite, pro.-protomerite, LP-length of the protomerite, TL-total length , WD-width of the deutomerite, WP-width of the protomerite, * *Leidyana subramanii*

Table 4. Comparison of *Leidyana* spp. reported from orthopteran hosts

Leidyana Species	Host	Epimerite	Sporadin (Max. TL) (LP: TL) (WP:WD)	Gametocyst	Sporocyst	Locality	Additional characters compared to other representative spp.	Additional characters compared to *L. subramanii*
Leidyana bimaculata (Hooger & Amoji 1986)	*Gryllus bimaculatus*	spherical to papilla like 3-7x2.5 µm	315 µm 1:3-7 1:3-2	oval 330-350 µm	dolioform shaped 3.5x5 µm; 10 sporeduct	India	–	–
Leidyana erratica (Crawley 1903)	*Gryllus obreviatus* *Gryllus pensilvanicus* (Gryllidae)	spherical knob	500 µm 1:5.7 1:1.3-1.7	Spherical 260-350 µm (dia); ectocyst-30µm thick	barrel shape 6x3 µm 1-12 sporeduct	North America	conical pro. never rounded. 80 µm long. constriction between pro. & deu. not deep	* hemispherical pro. 9-90 µm long; constriction deep
Leidyana gryllorum (Cuenot 1897)	*Gryllus assimilis* *Gryllus campestris* *Acheta domesticus* (Gryllidae)	–	420 µm 1:5 1:1.1	spherical or oval 190-240 µm (dia)	barrel shape 7 µm 3-8 sporeduct	France	subspherical or round pro. 84 µm long. deu. cylindrical & tapering end	* hemispherical pro. 9-90 µm long; deu cylindrical & rounded end
Leidyana guttiventrisa (Sarkar 1988)	*Plebeiogryllus guttiventris* (Gryllidae)	conical to lance shape 8.7x7.5 µm	206.5 µm 1:4.2-5 1:0.69-1.12	ovoidal to egg shaped 231x196 µm	barrel shape 8.8x6.4 µm	India		
Leidyana linguata (Haldar & Sarkar 1979)	*Pteronemobius concolor* (Gryllidae)	tongue-like 15.7x7 µm	415.8 µm 1:5.5 1:1.3	spherical 75-15 4 µm	cylindrical 9.8x4.1 µm	India		
Leidyana migrator (Clopton 1995)	*Gromphadorhina portentosa* (Blattiodea)	globular obovoid to broadly obovoid 37*45 µm	352 µm 1:0.12-0.22 1:0.66	elliptoid 1.066 µm (dia)	dolioform 8x4 µm 4-8 sporeduct	USA Texas		

Table 4. (con.)

Leidyana oblongata (Dufour 1837)	*Gryllus compestris Nemobius silvestris* (Gryllidae)	spherical knob 18-24 µm (dia)	210 µm 1:4.8-8.6	–	–	France		
Leidyana oviformis (Hoshide 1978)	*Pteronemobius fascipes & Pteronemobius taprobanensis* (Gryllidae)	spatulate shape 3x18 µm (dia)	350 µm 1:5.6 1:1.7	spherical 155 µm (dia)	barrel-shaped 6x3 µm	Japan	–	–
Leidyana saigonensis (Corbel 1967)	*Gryllus bimaculatus Gryllodes sigillatus* (Gryllidae)	–	350 µm	–	dolioform 7.5x3.5 µm	Vietnam	–	–
Leidyana subramanii sp.n.	*Eyprepocnemis alacris alacris* (Eyprepocnemidae)	globular 13 µm (dia)	657 µm 1:3-11 1:1.3-2.1	spherical 195-468 µm (dia); ectocyst- 26-52 µm width	barrel shape 6.6 x 3.5 µm; 1-13 sporeduct	India	–	–
Leidyana suzumushi (Hoshide 1973a)	*Homoeogryllus japonicus*	sessile knob	348 µm 1:6.1 1:1.4	spherical 200 µm (dia)	barrel 3x5.5 µm 4-6 sporeduct	Japan	–	–

deu.-deutomerite, pro.-protomerite, LP-length of the protomerite, TL-total length , WD-width of the deutomerite, WP-width of the protomerite, * *Leidyana subramanii*

deutomerite of *L. erratica* and deutomerite shape of *L. gryllorum*, spatula-shaped epimerite of *L. oviformis* are additional dissimilar characters observed in *L. subramanii*.

The Indian species recorded from orthopteran hosts namely *L. lingouta* (Haldar and Sarkar 1979), *L. bimaculata* (Hooger and Amoji 1986) and *L. guttiventrisa* (Sarkar 1988) differ from *L. subramanii* in the following characters: (1) host; (2) shape and size range of epimerite; (3) morphometry of sporadins; (4) size range of gametocyst; (5) size of sporocyst (Table 4). Similarly *L. erratica, L. gryllorum, L. oblongata, L. suzumushi, L. oviformis* from orthopteran host also have spherical gametocyst and barrel shaped spores similar to *L. subramanii*, but differ in: (1) morphometry of the sporadins; (2) size of gametocyst; (3) size of the spores; and (4) number of sporeducts. The Indian species from non-orthopteran hosts namely *L. gnyanagangi* (Patil and Amoji 1979) (host: Coleoptera), *L. oryzeaphils* (Roy 1989) (host: Coleoptera), *L. xylocopae* (Bhatia and Setna 1924) (host: Hymenoptera) and *Leidyana* spp. (Rabindra and Jayaraj 1980) (host: Leipdoptera) also showed differences like: (1) shape and size of epimerite; (2) morphometry of sporadins; (3) diameter of the gametocyst; (4) size of sporocyst; (5) number of spore duct as well as few additional characters compared with the repersentative species (Table 3).

Ten *Leidyana* species are specifically recorded from orthoperan hosts namely *L. erratica, L. gryllorum, L. saigonensis* (Corbel 1967 a, b), *L. oblongata, L. suzumushi, L. oviformis, L. linguota, L. bimaculata, L. guttiventrisa, L. migrator* (Clopton 1995), and *L. gnyanagangai.* All the species of *Leidyana* examined (Table 4) have hosts other than grasshoppers except for this putative cephaline gregarine *L. subramanii* under consideration in addition to dissimilarities discussed earlier. While revising the genus *Leidyana* Corbel (1967b) stressed the host specificity of gregarines, as all attempts to infect tettigonids and acridids by *L. gryllorum* had failed. *L. subramanii* is the 20th species of the genus *Leidyana* whose complete life cycle has been studied so far.

Acknowledgements, We thank Dr. K.P. Sanjayan, Associate Director, G.S. Gill Research Institute, Guru Nanak College, Chennai, India, for his helpful suggestions and critical reading of the manuscript and also to Dr. V. Mahalingam, of the same Institution for helping with microphotography. Thanks are due to Dr. A. Sundaram, Department of Pathology, Madras Medical College, India, and Dr. Tamilvel, Crystal Growth Center, Anna University, Chennai, India, for their assistance with scanning electron microscopy.

REFERENCES

Bhatia B. L., Setna S. (1924) On some new cephaline gregarines. *Parasitology* **16:** 279-288

Canning E. U. (1956) A new eugregarine of locusts, *Gregarina garnhami* n.sp., parasitic in *Schistocerca gregaria* Forsk. *J. Protozool.* **3:** 50-62

Chakravarty M. M. (1960) Systematic position of some genera and classification of the suborder Cephalina Delage and Herouard. *Proc. Zool. Soc. Calcutta* **12:** 71-81

Clopton R. E. (1995) *Leidyana migrator* sp. nov (Apicomplexa: Eugregarinida: Leidyanidae) from the Madagascar hissing cockroach, *Gromphadorhina portentosa* (Insecta: Blattiodea) *Invert. Biol.* **114:** 271-278

Corbel J. C. (1967a) Gregarines nouvelles parasites d'Orthopteres. *Bull. Mus. Natl. Hist. Nat.* **39:** 992-996

Corbel J. C. (1967b) Revision du genre *Leidyana* Watson 1915 (Eugregarines, Gregarinidae). *Bull. Mus. Natl. Hist. Nat.* **39:** 997-1000

Crawley H. (1907) The polycystid gregarines of the United States (Third Contribution). *Proc. Acad. Nat. Sci. Philadelphia* **59:** 220-228

Cuénot L. (1897) C. R. *Acad. Sci. Paris*, **125:** 52-54

Dufour L. (1837) Recherches sur quelques entozoaires et larves parasites des insects Orthopteres et Hymenopteres. *Ann. Sci. Nat.* **7:** 5-20

Geus A. (1966) *Leidyana stejskali* n. sp., eine neue Gregarine aus Larven von *Achroea grisella* FBR. *Zool Anz.* **177:** 442-446

Haldar D. P., Sarkar N. K. (1979) Cephaline gregarine *Leidyana linguata* sp. n. parasite of a gryllid *Pteronemobius concolor* Walker from India. *Acta Protozool.* **18:** 435-440

Hoogar V. N., Amoji S. D. (1986) *Leidyana bimaculata* sp nov. a new cephaline gregarine parasite of a cricket *Gryllus bimaculatus* De Geer. *Acta Protozool.* **25:** 465-470

Hoshide K. (1973a) Notes on the gregarines of Japan. 5. A new eugregarine *Leidyana suzumushi* n. sp. from *Homoeogryllus japonicus* De Haan. *Bull. Fac. Ed. Yamaguchi Univ.* **23:** 69-75

Hoshide K. (1973b) Notes on the gregarines in Japan. 6. Two cephaline gregarines from *Gryllus yemma* Ohamachi et Matsuura. *Bull. Fac. Ed. Yamaguchi Univ.* **23:** 77-85

Hoshide K. (1978) Notes on the gregarinein Japan new eugregarines and nine other gregarines from Orthoptera and Dictyoptera. *Bull. Fac. Ed. Yamaguchi Univ.* **28:** 91-126

Issi I.V., Lipa J. J. (1968) Report on identification of protozoa pathogenic for insects in the Soviet Union (1961-1966), with some descriptions of new species. *Acta Protozool.* **6:** 281-219

Keilin D. (1918) On the occurrence of a cephaline gregarine, *Leidyana tinei* n. sp., in lepidopteruslarvae. *Parasitology* **10:** 406-410

Kudo R. R. (1954) Protozoology (4th edition). Charles C. Thomas, Springfield, Illinois

Levine N. D. (1971) Uniform terminology for the protozoan subphylum Apicomplexa. *J. Protozool.* **18:** 352-355

Levine N. D., Corliss J. O., Cox F. E. G., Deroux G., Grain J., Honigberg B. M., Leedale G. F., Loeblich III JR., Lom J., Lynn D., Merinfeld E. G., Page F. C., Poljansky G., Sprague V., Vavra J., Wallace F. G. (1980) A newly revised classification of the protozoa. *J. Protozool.* **27:** 37-58

Lipa J. J., Martignoni M. E. (1984) *Leidyana phryganidiae* and *Leidyana berkeleyi*: two new species of gregarines from *Phryganidia californica*. *J. Invert. Path.* **43:** 69-76

Ormieres R. (1967) *Leidyana peregrinata* n. sp., eugregarine parasite de lepidopteres Pyralidae: cycle normal et cycle coelomique. *Protistologica* **3:** 295-300

Patil C. C., Amoji S. D. (1979) Eugregarine parasites of Coleoptera from north-east region of Karnataka. II. *Leidyana gnyanagangai*

n.sp., found in the gut of *Rhytinota impolita* Fairm. *Curr. Sci.* **48:** 736-737

Rabindra R. J., Jayaraj S. (1980) On the occurrence of a cephaline gregarine Leidyana sp. in the gut of the coconut black head caterpillar, *Nephantis serinopa Meyer. Sci. Cult.* **47:** 363

Roy K. (1989) Some gregarines (Sporozoa, Apicomplexa) from the stored fruit beetle, *Oryzaephilus mercator* Fauv.(Coleoptera) from India. *J. Protozool.* **36:** 20-23

Sarkar N. K. (1988) *Leidyana guttiventrisa* sp. n. a new cephaline gregarine (Apicomplexa: Eugregarinida) parasite of a gryllid of West Bengal, India. *Acta Protozool.* **27:** 67-73

Watson M. E. (1915) Some new gregarines from arthropods. *J. Parasitol.* **2:** 25-36

Received on 20th March, 1998; accepted on 20th August, 1998

Acknowledgement

The editors wish to acknowledge the help of the following colleagues who have served as reviewers for one or more manuscripts submitted for publication in our journal in 1998.

Alex D.W. Acholonu
Richard J. Arthur
Kurt Augsten
Christian F. Bardele
Linda Basson
Louis Bayens
Elizabeth U. Canning-Wilson
John Clamp
Guliano Colombetti
D. Cone
John O. Corliss
Isabelle Desportes-Livage
Iva Dyková
Genoveva Esteban
Ronald Fayer
Wilhelm Foissner
Michael A. Gates
Francesco Ghetti
Maria P. Gracia Royo
Jean Grain
Lucyna Grębecka
Norman Grim
Manfred Hauser
Klaus Hausmann
Ronald P. Hedrick
Fred G. Hochberg
Eggehard Holler
Norbert Hülsmann
Shosuke Ito
Jake Jacobson
Kwang W. Jeon
Stanisław Kazubski
Włodzimierz Korohoda
W. Korting
Katarzyna Kwiatkowska
John J. Lee
Vagn Leick
Jiří Lom
Piero Luporini
Miles Markus
William C. Marquard
Geoffrey McFadden
Ralf Meisterfeld
Jean-Pierre Mignot
W.H. Moolenaar
Kálmán Molnár
Helga Müller
Jytte Nilsson
Klaus Odening
David. J. Patterson
Przemysław M. Płonka
James Pratt
Terry Preston
Pierre de Puytorac
S. Scherer
Michael Schweikert
Inacio D. da Silva Neto
Ariadna Sitja-Bobadilla
Michael Sleigh
H. G. Smith
Judith E. Smith
Eugene B. Small
Andrzej Sobota
Steve J. Upton
Alessandro Valbonesi
Jerzy Warchoł
Krzysztof Wiąckowski
R.J.M. Wilson

Author Index: Acta Protozoologica 37 (1-4) 1998

Subject Index: Acta Protozoologica 37 (1-4) 1998

ACTA PROTOZOOLOGICA

NENCKI INSTITUTE OF EXPERIMENTAL BIOLOGY
WARSAW, POLAND
1998
VOLUME 37
ISSN 0065-1583

Polish Academy of Sciences
Nencki Institute of Experimental Biology
and
Polish Society of Cell Biology

ACTA PROTOZOOLOGICA

International Journal on Protistology

ACTA PROTOZOOLOGICA appears quarterly.

The price (including Air Mail postage) of subscription to ACTA PROTOZOOLOGICA at 1999 is: US $ 180.- by institutions and US $ 120.- by individual subscribers. Limited number of back volumes at reduced rate are available. TERMS OF PAYMENT: Cheque, money oder or payment to be made to the Nencki Institute of Experimental Biology. Account Number: 11101053-3522-2700-1-34 at Państwowy Bank Kredytowy XIII Oddz. Warszawa, Poland. WITH NOTE: ACTA PROTOZOOLOGICA! For matters regarding ACTA PROTOZOOLOGICA, contact Managing Editor, Nencki Institute of Experimental Biology, ul. Pasteura 3, 02-093 Warszawa, Poland; Fax: (4822) 8225342; E-mail: jurek@ameba.nencki.gov.pl (for more information see web page **http://www.nencki.gov.pl/public.htm**).

Front cover: *Polychaos dubium*. In: A. A. Schaeffer (1916) Notes on the specific and other characters of *Amoeba proteus* Pallas (Leidy), *A. discoides* spec. nov. and *A. dubia* spec. nov. *Arch. Protistenk.* **37:** 204 - 228

This publication is supported by the State Committee for Scientific Research

Desktop processing: Justyna Osmulska, Data Processing Laboratory of the Nencki Institute
Printed at the MARBIS, ul. Kombatantów 60, 05-070 Sulejówek, Poland

Contents of Volume 37 (1-4) 1998

Number 4

INSTRUCTIONS FOR AUTHORS

ACTA PROTOZOOLOGICA publishes original papers on experimental or theoretical research in all fields of protistology with the exception of faunistic notices of local character and purely clinical reports. Short communications, as well as longer review articles may also be submitted. Contributions should be written in English. Submission of a manuscript to ACTA PROTOZOOLOGICA implies that the contents are original and have not been published previously, and are not under consideration or accepted for publication elsewhere. There are no page charges except colour illustration. Names and addresses of suggested reviewers (four to six) will be appreciated. In case of any question please do not hesitate to contact Editor. Authors should submit papers to:

Miss Małgorzata Woronowicz
Managing Editor of ACTA PROTOZOOLOGICA
Nencki Institute of Experimental Biology,
ul. Pasteura 3
02-093 Warszawa, Poland
Fax: (4822) 8225342
E-mail: jurek@ameba.nencki.gov.pl

Extensive information on ACTA PROTOZOOLOGICA is now available *via* internet. The address is: **http://www.nencki.gov.pl/public.htm**

Organization of Manuscripts

Submissions

Please enclose three copies of the text, one set of original of line drawings (without lettering!) and three sets of copies with lettering, four sets of photographs (one without lettering). In case of photographs arranged in the form of plate, please submit one set of original photographs unmounted and without lettering, and three sets of plates with lettering.

The ACTA PROTOZOOLOGICA prefers to use the author's word-processor disks (3.5" and 5.25" format IBM or IBM compatible, and MacIntosh 6 or 7 system on 3.5" 1.44 MB disk only) of the manuscripts instead of rekeying articles. If available, please send a copy of the disk with your manuscript. Preferable programs are Word or WordPerfect for Windows and DOS WordPerfect 5.1. Disks will be returned with galley proof of accepted article at the same time. Please observe the following instructions:

1. Label the disk with your name: the word processor/computer used, e.g. IBM; the printer used, e.g. Laserwriter; the name of the program, e.g. Word for Windows or WordPerfect 5.1.
2. Send the manuscript as a single file; do not split it into smaller files.
3. Give the file a name which is no longer than 8 characters.
4. If necessary, use only italic, bold, underline, subscript and superscript. Multiple font, style or ruler changes, or graphics inserted the text, reduce the usefulness of the disc.
5. Do not right-justify and use of hyphen at the end of line.
6. Avoid the use of footnotes.
7. Distinguish the numerals 0 and 1 from the letters O and l.

Text (three copies)

The text must be typewritten, double-spaced, with numbered pages. The manuscript should be organized into Summary, Key words, Abbreviations used, Introduction, Materials and Methods, Results, Discussion, Acknowledgements, References, Tables and Figure Legends. The Title Page should include the full title of the article, first name(s) in full and surname(s) of author(s), the address(es) where the work was carried out, page heading of up to 40 characters. The present address for correspondence, Fax, and E-mail should also be given.

Each table must be on a separate page. Figure legends must be in a single series at the end of the manuscript. References must be listed alphabetically, abbreviated according to the World List of Scientific Periodicals, 4th ed. (1963). Nomenclature of genera and species names must agree with the International Code of Zoological Nomenclature, third edition, London (1985) or International Code of Botanical Nomenclature, adopted by XIV International Botanical Congress, Berlin, 1987. SI units are preferred.

Examples for bibliographic arrangement of references:

Journals:

Häder D-P., Reinecke E. (1991) Phototactic and polarotactic responses of the photosynthetic flagellate, *Euglena gracilis*. *Acta Protozool.* **30:** 13-18

Books:

Wichterman R. (1986) The Biology of *Paramecium*. 2 ed. Plenum Press, New York

Articles from books:

Allen R. D. (1988) Cytology. In: *Paramecium*, (Ed. H.-D. Görtz). Springer-Verlag, Berlin, Heidelberg, 4-40

Zeuthen E., Rasmussen L. (1972) Synchronized cell division in protozoa. In: Research in Protozoology, (Ed. T. T. Chen). Pergamon Press, Oxford, **4:** 9-145

Illustrations

All line drawings and photographs should be labelled, with the first author's name written on the back. The figures should be numbered in the text as Arabic numerals (e.g. Fig. 1). Illustrations must fit within either one column (86 x 231 mm) or the full width and length of the page (177 x 231 mm). Figures and legends should fit on the same page. Lettering will be inserted by the printers and should be indicated on a tracing-paper overlay or a duplicate copy.

Line drawings (three copies + one copy without lettering)

Line drawings should preferably be drawn about twice in size, suitable for reproduction in the form of well-defined line drawings and should have a white background. Avoid fine stippling or shading. Computer printouts of laser printer quality may be accepted, however *.TIF, *.PCX, *.BMP graphic formats on disk are preferred.

Photographs (three copies + one copy without lettering)

Photographs at final size should be sharp, with a glossy finish, bromide prints. Photographs grouped as plates (in size not exceeding 177 x 231 including legend) must be trimmed at right angles accurately mounted and with edges touching and mounted on firm board. The engraver will then cut a fine line of separation between figures. Magnification should be indicated. Colour illustration on transparent positive media (slides 60 x 45 mm, 60 x 60 mm or transparency) are preferred.

Proof sheets and offprints

Authors will receive one set of page proofs for correction and are asked to return these to the Editor within 48-hours. Fifty reprints will be furnished free of charge. Orders for additional reprints have to be submitted with the proofs.

Indexed in Chemical Abstracts Service, Current Contents (Agriculture, Biology and Environmental Sciences), Elsevier BIOBASE/Current Awareness in Biological Sciences, LIBREX-AGEN, Protozoological Abstracts. POLISH SCIENTIFIC JOURNALS CONTENTS - AGRIC. & BIOL. SCI. data base is available in INTERNET under URL (UNIFORM RESOURCE LOCATOR) address: http://ciuw.warman.net.pl/alf/psjc/ any WWW browser; in graphical operating systems: MS Windows, Mac OS, X Windows - mosaic and Netscape programs and OS/2 - Web Explorer program; in text operating systems: DOS, UNIX, VM - Lynx and WWW programs.

ACTA
PROTOZOOLOGICA

ORIGINAL ARTICLES

1998 NOVEMBER
VOLUME 37 NUMBER 4